



Urban Planning: from GIS and BIM straight to CIM. Practical application in the urban area of Porto

TANYA ANGELOVA SIRAKOVA

Dissertação submetida para satisfação parcial dos requisitos do grau de
MESTRE EM ENGENHARIA CIVIL — ESPECIALIZAÇÃO EM PLANEAMENTO

Orientador: Professora Doutora Cecília Alexandra Abreu Coelho da Rocha

Coorientador: Professor Doutor João Pedro da Silva Poças Martins

JULHO DE 2018

MESTRADO INTEGRADO EM ENGENHARIA CIVIL 2017/2018

DEPARTAMENTO DE ENGENHARIA CIVIL

Tel. +351-22-508 1901

Fax +351-22-508 1446

✉ miec@fe.up.pt

Editado por

FACULDADE DE ENGENHARIA DA UNIVERSIDADE DO PORTO

Rua Dr. Roberto Frias

4200-465 PORTO

Portugal

Tel. +351-22-508 1400

Fax +351-22-508 1440

✉ feup@fe.up.pt

 <http://www.fe.up.pt>

Reproduções parciais deste documento serão autorizadas na condição que seja mencionado o Autor e feita referência a *Mestrado Integrado em Engenharia Civil - 2017/2018 - Departamento de Engenharia Civil, Faculdade de Engenharia da Universidade do Porto, Porto, Portugal, 2018.*

As opiniões e informações incluídas neste documento representam unicamente o ponto de vista do respetivo Autor, não podendo o Editor aceitar qualquer responsabilidade legal ou outra em relação a erros ou omissões que possam existir.

Este documento foi produzido a partir de versão eletrónica fornecida pelo respetivo Autor.

To all people that will read this work,

*Simulated disorder postulates perfect discipline. Simulated fear postulates courage.
Simulated weakness postulates strength.*

Lao Tzu

ACKNOWLEDGMENTS

Бих искала преди всичко да благодаря на родителите ми за това, че винаги са ме подкрепяли във всички мои начинания и най-вече, когато реших да замина на Португалия. Искам да благодаря също така на моя най-добър приятел и бъдещ съпруг Христо, за това че винаги беше до мен дори и в най-трудните моменти не спря да ме буца напред и да вярва в мен.

Queria agradecer à minha orientadora Professora Cecília Rocha e coorientador Professor João Poças-Martins pela toda ajuda e disponibilidade e que aceitaram uma proposta de dissertação que será interessante para mim. Obrigada pelo tudo!

Queria agradecer também ao Laboratório de Física das Construções, ao Prof. Vasco Freitas, à Professora Eva Barreira e ao Eng. António Costa pela disponibilidade e pelo empréstimo do equipamento necessário para validação da ferramenta desenvolvida nesta dissertação.

I would also like to thank all my friends Rita, Zornitsa e David, Ekaterina, Viktoria, Gergana e Sabri for been there when I needed them most.

Special thanks to my friend Viktoriya Hristova who helped me with the revision of the English gramer in this work.

Tanya Angelova Sirakova

ABSTRACT

It is difficult to predict how a city will respond to climate changes. Temperature variations during the different seasons, the rain and other similar weather conditions put a strain on the urban environment. To produce a viable analysis and estimation it is imperative to collect data, while taking into consideration the budget required to do so. The best approach will demand to estimate possible negative effects of those extreme weather conditions and to take into consideration scarcity of resources. With the advance of technology, it is possible to a replication of the urban environment such as with 3D analytical models or even with virtual reality. With that option, it is possible to simulate real life catastrophes or extreme episodes and their consequences, to study how changes in the urban configuration and in the built environment can influence the microclimate, avoid expected damages and to draw the most adequate strategies.

This dissertation is devoted to this challenge. The development and implementation of a decision-making tool that will allow municipalities to anticipate the results of their decisions and avoid unnecessary costs.

With that purpose, City Information Modelling (CIM) is a new subject that grows in popularity in Urban Planning and Architecture, Engineering and Construction (AEC) community. It has the potential to become an integrated multi-platform model that allows representation of the smallest details in an urban area.

In the present case, CIM will be achieved with the use of Geographical Information Systems (GIS) and Building Information Modelling for creating a software tool analysing the thermal comfort conditions for public space and aid in the decision-making process of urban planning. It will take into consideration the geometry of the urban area and the interaction between weather conditions and built environment to simulate the consequences the new intervention will have on the public space.

The validation of this tool used Trindade Metro Station as Case Study. The choice of this location relates with its insertion in the city centre, the surrounding built environment, the function of the area and the geometry, with two levels with different materials. The upper level is mainly a large green area with the insertion of other materials on the elevator, crossing path and end walls, and the lower level, which includes granite, concrete and glass. The case study will permit to study the tool response to estimate different surface temperatures and in consequence to predict mean radiant temperature for citizens. On the course of the validation process, were conducted surface temperature measurements, later compared with the tool output. The differences found were on average in the interval between ± 2 and ± 3 which is small enough to consider that one can use this tool in real projects.

Later were also performed simulations for alternative scenarios to study how different materials will affect surface temperature and urban comfort. The results showed that the tool represent correctly the expected increase or decrease of surface temperature.

This model was designed to serve as a bridge between traditional and the foreseen digital urban planning in order to create conditions for more sustainable urban environment and enhancing quality of life, as it provides valuable information for the decision process by municipalities.

Key words: CIM, BIM, GIS, urban microclimate, thermal comfort, 3D model, simulation

RESUMO

Mudanças climáticas é sempre um desafio para a cidade se adaptar. As altas temperaturas durante o verão, os frios durante o inverno e inundações durante a primavera e o outono sobrecarregam a capacidade de adaptação do ambiente urbano. A resposta das cidades às diferentes condições climáticas é difícil de prever, devido a muitas variáveis nas considerações. A melhor abordagem exigirá estimar possíveis efeitos negativos dessas condições climáticas extremas e levar em consideração a escassez de recursos. Para isso, é aconselhável criar uma replicação do ambiente urbano, com modelos analíticos 3D ou mesmo com realidade virtual. Com essa opção, é possível simular catástrofes da vida real ou episódios extremos e suas consequências, essencialmente para conhecer os possíveis resultados, evitar danos esperados e traçar as estratégias mais adequadas.

Esta dissertação é dedicada a este desafio. O desenvolvimento e implementação de uma ferramenta de apoio de decisão que permitirá aos municípios antecipar os resultados de suas decisões e evitar custos desnecessários.

Com esse propósito, City Information Modeling (CIM) é um novo assunto que cresce em popularidade dentro da comunidade de planeamento urbano e Arquitetura, Engenharia e Construção (AEC). CIM tem o potencial de se tornar um modelo multiplataforma integrado que permite representar os menores detalhes de uma área urbana, fornecendo base para registo de dados, extração de informações, análise espacial e comunicação com outras plataformas de informação.

No presente caso, CIM será alcançada com o uso de Sistemas de Informações Geográficas (GIS) e Building Information Modeling (BIM) para criar uma ferramenta de software analisando as condições de conforto térmico para o espaço público e apoiando no processo de tomada de decisão do planeamento urbano. A ferramenta levará em consideração a geometria da área urbana e a interação entre as condições e o ambiente de construção para simular quais consequências a nova intervenção terá no espaço público.

O conforto na cidade não depende apenas das condições geográficas e meteorológicas, mas também está sujeito a como o ambiente de construção afeta seu microclima. Há pouca ou nenhuma preocupação sobre como o edifício único altera a temperatura do espaço aberto. Construção densa aprisiona mais calor e produz as chamadas ilhas de calor urbanas.

Neste trabalho, uma ferramenta será desenvolvida com a ajuda da metodologia e software BIM para estudar como o ambiente de construção afetará a temperatura da superfície e a temperatura radiante média de um espaço, dois parâmetros que desempenham um papel importante no conforto térmico de um espaço aberto. Ele usa dados de geometria de um modelo 3D, propriedades térmicas de materiais e leis físicas para simular cenários da vida real. Esta ferramenta pode ser usada como instrumento na tomada de decisões para planejar o projeto e as mudanças futuras para um espaço público e conhecer as consequências antes de implementar o projeto.

A ferramenta será desenvolvida usando a Estação de Metrô Trindade como Caso de Estudo. O local foi escolhido porque tem dois níveis com diferentes materiais. O nível superior é feito principalmente de espaço verde e o nível inferior é feito de granito. Isso permitirá estudar como a ferramenta responderá às diferentes temperaturas da superfície e, conseqüentemente, à temperatura radiante média.

A validação do componente da temperatura da superfície foi realizada e a comparação entre os resultados da ferramenta e a temperatura medida foi feita. A diferença encontrada é pequena o suficiente para concluir que a ferramenta desenvolvida pode ser usada em projetos reais. Alguns cenários alternativos foram criados para estudar como diferentes materiais afetarão a temperatura da superfície. Os resultados obtidos demonstraram que a ferramenta representa corretamente o aumento ou a diminuição esperada da temperatura da superfície.

Este modelo foi projetado para servir como uma ponte entre o planeamento urbano tradicional e o novo digital, a fim de criar condições para um ambiente urbano mais sustentável e melhorar a qualidade de vida.

Palavras-chave: CIM, BIM, GIS, microclima urbano, conforto térmico, modelo 3D, simulação

GENERAL INDEX

| | |
|---|-----------|
| ACKNOWLEDGMENTS | V |
| ABSTRACT | VII |
| RESUMO | IX |
| GENERAL INDEX | XI |
| TABLE OF FIGURES | XV |
| TABLE INDEX | XX |
| TABLE OF EQUATION | SXXI |
| SYMBOLS AND ACRONYMS | XXII |
| | |
| 1 INTRODUCTION | 1 |
| 1.1 FRAMEWORK | 1 |
| 1.2 OBJECTIVE | 2 |
| 1.3 OVERVIEW | 3 |
| | |
| 2 GIS, BIM AND CIM | 5 |
| 2.1 INTRODUCTION | 5 |
| 2.2 TECHNOLOGIES AND URBAN PLANNING | 7 |
| 2.2.1 GENERAL FRAMEWORK | 7 |
| 2.2.2 GEOGRAPHICAL INFORMATION SYSTEM (GIS) | 8 |
| 2.2.3 BUILDING INFORMATION MODELLING (BIM) | 11 |
| 2.2.4 CITY INFORMATION MODELLING (CIM) | 16 |
| | |
| 3 URBAN COMFORT | 27 |
| 3.1 CLIMATE CHANGE AND THE CITY | 27 |
| 3.2 URBAN MICROCLIMATE | 29 |
| 3.2.1 URBAN HEAT ISLAND | 30 |
| 3.2.2 UHI SCALES | 31 |
| 3.2.3 URBAN HEAT ISLAND MEASUREMENT | 32 |
| 3.2.4 FACTORS THAT INFLUENCE THE URBAN MICROCLIMATE | 33 |
| 3.3 OUTDOOR THERMAL COMFORT | 37 |
| 3.3.1 FACTORS THAT INFLUENCE THERMAL COMFORT | 38 |
| 3.3.2 OUTDOOR THERMAL COMFORT CALCULATION/INDICES | 41 |
| 3.4 MEAN RADIANT TEMPERATURE | 43 |
| 3.4.1 DEFINITION: | 43 |
| 3.4.2 CALCULATION OF T_{MRT} | 44 |

| | |
|--|------------|
| 3.4.3 METHODS FOR CALCULATING T_{MRT} | 51 |
| 3.5 SUSTAINABILITY, ADAPTATION AND MITIGATION | 52 |
| 4 CASE STUDY | 55 |
| 4.1 INTRODUCTION | 55 |
| 4.2 NEED FOR THE TOOL | 56 |
| 4.3 DYNAMO METHODOLOGY | 57 |
| 4.3.1 INSIGHT SOLAR ANALYSIS | 57 |
| 4.3.2 INITIAL DATA | 62 |
| 4.3.3 VIEW FACTORS | 64 |
| 4.3.4 SURFACE TEMPERATURE | 66 |
| 4.3.5 MEAN RADIANT TEMPERATURE | 67 |
| 4.4 MODEL VALIDATION | 67 |
| 4.4.1 BUILDING MATERIALS | 68 |
| 4.4.2 EQUIPMENT | 71 |
| 4.4.3 METEOROLOGICAL CONDITIONS | 71 |
| 4.4.4 MEASURED POINTS | 72 |
| 4.4.5 ESTIMATED RESULTS | 73 |
| 4.4.6 MEAN RADIANT TEMPERATURE | 76 |
| 4.4.7 CONCLUSIONS | 79 |
| 4.5 CHANGES IN PHYSICAL ENVIRONMENT | 79 |
| 4.5.1 CHANGE IN MATERIALS AND COLOURS | 80 |
| 5 CONCLUSIONS | 85 |
| 5.1 FINAL REFLECTION | 85 |
| 5.2 FUTURE DEVELOPMENTS | 86 |
| ANNEXES | 97 |
| ANNEX A DYNAMO CODE | 99 |
| A.1 INITIAL DATA | 99 |
| A.1.1 IMPORTING SOLAR ANALYSIS RESULTS | 100 |
| A.1.2 PARAMETERS EXTRACTION FROM INITIAL DATA | 103 |
| A.1.3 SEPARATION OF WALL AND FLOOR ELEMENTS | 103 |
| A.2 SKY VIEW FACTOR | 104 |
| A.2.1 GENERATING DOME AROUND EACH ANALYTICAL POINT | 104 |
| A.2.2 DEFINING ANGLE BETWEEN VECTORS | 105 |

| | |
|--|------------|
| A.2.3 CHECK IF VECTORS INTERSECT GEOMETRY | 105 |
| A.2.4 FINDING MAXIMUM VALUE OF ANGLE | 106 |
| A.2.5 CALCULATION OF SKY VIEW FACTOR | 106 |
| A.2.6 RESULT EXPORT | 106 |
| A.3 SURFACE TEMPERATURE | 107 |
| A.3.1 ENVIRONMENTAL PARAMETERS | 107 |
| A.3.2 INTERNAL TEMPERATURE | 108 |
| A.3.3 INITIAL TEMPERATURE | 108 |
| A.3.4 IMPORTING SVF | 109 |
| A.3.5 CALCULATING SURFACE TEMPERATURE | 109 |
| A.3.6 RESULTS OUTPUT | 111 |
| A.4 VIEW FACTOR SURFACE TO PERSON | 111 |
| A.4.1 DEFINING STARTING POINT | 112 |
| A.4.2 CALCULATING VIEW FACTOR IN 4 MAIN DIRECTIONS | 113 |
| A.4.3 RESULT | 114 |
| A.5 MEAN RADIANT TEMPERATURE | 115 |
| A.5.1 FINDING TEMPERATURE OF CLOSEST POINT | 115 |
| A.5.2 THERMAL PARAMETERS FROM FLOORS ONLY | 116 |
| A.5.3 FINDING THE ELEMENT CORRESPONDING TO THE CLOSEST POINT | 116 |
| A.5.4 CALCULATING MEAN RADIANT TEMPERATURE | 117 |

ANNEX B 133

| | |
|---|------------|
| B.1 AROUND THE ELEVATOR ON THE UPPER FLOOR OF TRINDADE METRO STATION | 120 |
| B.2 UPPER LEVEL FLOOR OF TRINDADE METRO STATION | 121 |
| B.3 SURROUNDING WALLS ON THE UPPER LEVEL OF TRINDADE METRO STATION | 123 |
| B.4 LOWER LEVEL FLOOR OF TRINDADE METRO STATION | 124 |
| B.5 SIDEWALL NEAR THE ELEVATOR OF TRINDADE METRO STATION | 125 |
| B.6 SIDEWALL OF TRINDADE METRO STATION FACING RUA DE CAMÕES | 126 |
| B.7 SIDEWALL NEAR THE STAIRS IN TRINDADE METRO STATION | 126 |
| B.8 SIDEWALL PERPENDICULAR TO THE METRO LINE IN TRINDADE METRO STATION | 128 |
| B.9 CENTRAL WALL IN TRINDADE METRO STATION | 130 |

TABLE OF FIGURES

| | |
|---|----|
| Figure 1. GIS and Urban Planning [14]. | 9 |
| Figure 2. BIM Dimensions [22]. | 12 |
| Figure 3. LOD levels and project stages. Source:[22] | 14 |
| Figure 4. a) Sub-models of BIM [31]. b) Sub-modules of CIM, Adapted after [30]. | 17 |
| Figure 5. Methodology of CIM [33]. | 19 |
| Figure 6. GIS and BIM integration for creating CIM [30] | 19 |
| Figure 7. CityEngine Data Flow [37]. | 21 |
| Figure 8. 3D model of Singapore created using Bentley's CIM products [41]. | 23 |
| Figure 9. Generation of Urban Heat Island [55]. | 31 |
| Figure 10. Schematic section of the urban atmosphere, showing the development of the urban boundary-layer (UBL) relative to the urban canopy-layer (UCL), which reaches the average building height (top), and the distinction between the homogeneous surface layer above the city and the heterogeneous urban canopy (bottom). The mixed layer and the roughness sub-layer are transition zones above and below the surface layer, respectively [57]. | 31 |
| Figure 11. Representation of urban surface energy budget by Oke 1988 [58]. | 33 |
| Figure 12. Three types of solar radiation: direct, diffuse and reflected [74]. | 34 |
| Figure 13. Radiation reflected and emitted from: a) a surface in an open environment, b) surface within urban canyon [75]. | 35 |
| Figure 14. Airflow within a city: a) Straight and parallel streets improve airflow. b) Narrow and winding streets make airflow slow [76]. | 36 |
| Figure 15. Albedo and surface temperature for different surface materials and colours [14]. | 37 |
| Figure 16. Factors that affect thermal sensation. Adapted from [75]. | 38 |
| Figure 17. PMV and Thermal Sensation [108]. | 42 |
| Figure 18. Components of T_{MRT} in urban environment [116]. | 44 |
| Figure 19. Illustration supporting the understanding of the definition and calculation of the T_{MRT} [118]. | 45 |
| Figure 20. Heat transfer equation for urban surfaces [116]. | 47 |
| Figure 21. View Factors from patch to rectangular plate [120]. | 49 |
| Figure 22. Sky View Factor is the ratio between the area of open-space and the total area of the hemisphere. Source:[121] | 50 |
| Figure 23. (a) Polygon $g(x)$ as a border of the visible sky and dividing the hemisphere under $g(x)$ equally into slices by angle α (heights are equal to the $g(x)$ values in the middle points of the intervals) and (b) a slice of a 'width' of α (S) of a basin with an elevation angle β [122]. | 50 |
| Figure 24. Standard Globe Thermometer | 51 |
| Figure 25. Proposed tool vs different existing methods for estimating/simulating T_{MRT} [116, 124]. | 52 |
| Figure 26. Metro Station Trindade: Real life scenario (Google Maps) vs. simplified 3D model | 55 |
| Figure 27. Workflow of the software tool. | 56 |
| Figure 28. Dynamo methodology. | 57 |
| Figure 29. Location of the case study. | 58 |

| | |
|--|-----|
| Figure 30. Case Study Time Frames for Solar Analysis. | 59 |
| Figure 31. Revit Sun Settings Panel. | 59 |
| Figure 32. Configuring Solar Analysis Menu. | 60 |
| Figure 33. Exported Excel Data | 61 |
| Figure 34. Dynamo node alternative for Solar Analysis. | 62 |
| Figure 35. Initial Data | 63 |
| Figure 36. Parameters extracted from Initial Data | 63 |
| Figure 37. Separation of the Floors | 64 |
| Figure 37. SFV calculation process | 65 |
| Figure 38. Ray Tracing methodology used to determine the View Factor. | 65 |
| Figure 39. View Factor from person to surface at high 1.5m. | 66 |
| Figure 40. Process of calculating surface temperature. | 67 |
| Figure 41. Process of calculating Mean Radiant Temperature. | 67 |
| Figure 42. Metro Station Trindade: Real life scenario (Google Maps) vs. simplified 3D model | 68 |
| Figure 43. Thermal properties of the materials in Revit. | 69 |
| Figure 44. Revit Project Parameters Menu | 70 |
| Figure 45. Protimeter MMS2 | 71 |
| Figure 46. Weather Station 126071. | 72 |
| Figure 47. Difference between calculated by the tool and measured in reality from 9:00 to 11:00. | 73 |
| Figure 48. Difference between calculated by the tool and measured from 11:00 to 12:00. | 74 |
| Figure 49. Difference between calculated by the tool and measured from 12:00 to 13:00. | 74 |
| Figure 50. Difference between calculated by the tool and measured from 13:00 to 14:00. | 75 |
| Figure 51. Difference between calculated by the tool and measured from 14:00 to 15:00. | 75 |
| Figure 52. Difference between calculated by the tool and measured from 15:00 to 17:00. | 76 |
| Figure 53. Influence of Longwave component over Mean Radian Temperature. | 77 |
| Figure 54. Influence of the Shortwave component over Mean Radian Temperature | 78 |
| Figure 55. Total Mean Radian Temperature. | 78 |
| Figure 56. Increase in surface temperature as result of asphalt pavement. | 81 |
| Figure 57. All pavement "painted" white. | 82 |
| Figure 58. Surface Temperature when introducing more green space and trees. | 83 |
| | |
| Figure A. 1. Initial Data structure. | 99 |
| Figure A. 2. Node group for importing Solar Analysis Results. | 100 |
| Figure A. 3. Extraction of data from excel file. | 100 |
| Figure A. 4. Excel file produced by Solar Analysis. | 101 |
| Figure A. 5. Attributing element ID to analytical points | 101 |

| | |
|---|---------------|
| Figure A. 6. Separating information of analytical point into solar radiation with corresponding X, Y, Z values. | 102 |
| Figure A. 7. End result of the data extraction from the excel file. | 102 |
| Figure A. 8. Getting the thermal parameters for each analytical point. | 103 |
| Figure A. 9. Separation of the Floors and Walls elements. | 104 |
| Figure A. 10. Node groups for SVF. | 104 |
| Figure A. 11. Generating dome's points. | 105 |
| Figure A. 12. Finding the angle between vectors. | 105 |
| Figure A. 13. Check if vectors intersects with geometry. | 106 |
| Figure A. 14. Finding maximum angle for SVF calculation. | 106 |
| Figure A. 15. Calculation of the Sky View Factor. | 106 |
| Figure A. 16. Exporting the results of the SVF calculation to excel file. | 107 |
| Figure A. 17. Node group for extracting air temperature humidity and other basic meteorological parameters. | 108 |
| Figure A. 18. Internal Temperature node group | 108 |
| Figure A. 19. Initial temperature node group. | 109 |
| Figure A. 20. Importing SVF from excel file. | 109 |
| Figure A. 21. Calculations of Surface Temperature. | 109 |
| Figure A. 22. Calculating constants for quadratic function. | 110 |
| Figure A. 23. Calculation of the quadratic function. | 111 |
| Figure A. 24. Surface Temperature result output. | 111 |
| Figure A. 25. Node groups for calculating View Factors between Person and Surface. | 112 |
| Figure A. 26. Defining the starting points. | 112 |
| Figure A. 27. Finding if vectors intersect with any geometry. | 113 |
| Figure A. 28. Calculating minimum distance between analytical and intersection points. | 113 |
| Figure A. 29. Extraction of wall height. | 114 |
| Figure A. 30. Calculating the View Factor. | 114 |
| Figure A. 31. Results of the View Factor calculation. | 115 |
| Figure A. 32. Node group for calculating Mean Radiant Temperature. | 115 |
| Figure A. 33. Finding the temperature of the closes wall analytical point. | 116 |
| Figure A. 34. Separating thermal parameter for floors only. | 116 |
| Figure A. 35. Removing information about the element of the corresponding intersection point. | 117 |
| Figure A. 36. Calculation of the Mean Radiant Temperature. | 117 |
| | |
| Figure B. 1 Walls around the elevator of Trindade Station in Porto, Portugal.. | 120 |
| Figure B. 2. Upper level floor of Trindade Station in Porto, Portugal. | 121 |
| Figure B. 3. Upper level surrounding walls of Trindade Station in Porto, Portugal. | Error! |
| Bookmark not defined. | |

| | |
|--|-----|
| Figure B. 4. Lower level floor of Trindade Station in Porto, Portugal. | 124 |
| Figure B. 5. Sidewall near the elevator of Trindade Station in Porto, Portugal. | 125 |
| Figure B. 6. Sidewall of Trindade Station facing Rua de Camões, Porto, Portugal | 126 |
| Figure B. 7. Sidewall near the stairs in Trindade Station, Porto, Portugal. | 127 |
| Figure B. 8. Sidewall perpendicular to the metro line in Trindade Station, Porto, Portugal | 128 |
| Figure B. 9. Central wall of Trindade Station, in Porto, Portugal | 130 |

TABLE INDEX

| | |
|--|-----|
| Table 1. Projected impacts upon urban areas of changes in extreme weather and climate events [46]. | 28 |
| Table 2. Variation of PET in different scenarios [113]. | 42 |
| Table 3. Absorption coefficient for short and longwave radiation [118]. | 44 |
| Table 4. Thermal properties of the materials [133-136]. | 70 |
| Table 5. Hourly measured air temperature and relative humidity. | 71 |
| Table 6. Thermal properties of the new materials [3-6]. | 80 |
| | |
| Table A. 1 Measured Air Temperature and Humidity recorded at the case study location. | 107 |
| | |
| Table B. 1. Measured values of the surface temperature (°C) in the walls around the elevator of Trindade Station in Porto, Portugal: 15 th July 2018 | 120 |
| Table B. 2. Measured values of the surface temperature (°C) on the floor of the upper level of Trindade Station in Porto, Portugal: 15 th July 2018 | 121 |
| Table B. 3. Measured values of the surface temperature (°C) on the walls of the upper level of Trindade Station in Porto, Portugal: 15 th July 2018. | 123 |
| Table B. 4. Measured values of the surface temperature (°C) on the floor of the lower level of Trindade Station in Porto, Portugal: 15 th July 2018. | 124 |
| Table B. 5. Measured values of the surface temperature (°C) on the sidewall of the elevator on the lower level of Trindade Station in Porto, Portugal: 15 th July 2018. | 125 |
| Table B. 6. Measured values of the surface temperature (°C) on the sidewall of Trindade Station in Porto facing Rua da Camões, Portugal: 15 th July 2018. | 126 |
| Table B. 7. Measured values of the surface temperature (°C) on the sidewall near the stairs of Trindade Station in Porto, Portugal: 15 th July 2018. | 127 |
| Table B. 8. Measured values of the surface temperature (°C) on the sidewall perpendicular to the metroline in Trindade Station, Porto, Portugal: 15 th July 2018. | 128 |
| Table B. 9. Measured values of the surface temperature (°C) on the central wall in Trindade Station, Porto, Portugal: 15 th July 2018. | 130 |

TABLE OF EQUATIONS

| | |
|---|----|
| Equation 1. Urban energy balance. | 32 |
| Equation 2. Components of net all-wave radiation. | 33 |
| Equation 3. Energy balance for the human body. | 42 |
| Equation 4. Stefan-Boltzmann's law for long wave radiation. | 45 |
| Equation 5. Radiation flux density. | 45 |
| Equation 6. Relation between radiation flux density and mean radiant temperature. | 46 |
| Equation 7. Mean radiant temperature. | 46 |
| Equation 8. Stefan- Boltzmann's law for multiple surfaces. | 47 |
| Equation 9. View Factor between different surfaces. | 48 |
| Equation 10. Summary of all view factors to a plane. | 48 |
| Equation 11. Incident solar radiation in Revit. | 58 |

SYMBOLS AND ACRONYMS

ΔQ_A – Net heat advection flux

ΔQ_S – Heat storage

ΔT – Surface temperature change

2D – Two Dimensional

3D – Three Dimensional

4D – Four Dimensional

5D – Five Dimensional

6D – Six Dimensional

7D – Seven Dimensional

AEC – Architecture, Engineering and Construction

AIA – American Institute of Architects

A_j – Arbitrary oriented surface

α – Albedo of surface material

ASHRAE – American Society of Heating, Refrigerating, and Air-Conditioning Engineers

BIM – Building Information Modelling

C – Convective heat flow

C – Heat capacity

CAD – Computer Aided Design

CIM – City Information Modelling

D – Diffuse shortwave energy

E_D – The latent heat flow

E_{dir} – Direct normal solar radiation

E_i – Long wave radiation

E_{ind} – Indirect solar radiance

E_{sw} – Heat flow due to evaporation of sweat

F_i – View factors from surface to its surroundings

FM – Facility Management

GIS – Geographical Information System

GML – Geographical Markup Language

GPS – Global Positioning System

h – Convective coefficient

I – Direct shortwave energy

IFC – Industry Foundation Classes

ISO – International Organization for Standardization
K \uparrow – Shortwave component radiating energy from the surface
K \downarrow – Shortwave component transporting energy to the surface
L \uparrow – Longwave component radiating energy from the surface
L \downarrow – Longwave component transporting energy to the surface
LOD – Level of Development
M – Mass per unit area
MRT – Mean Radian Temperature
OGC – Open Geospatial Consortium
PET – Physiological Equivalent Temperature
PMV – Predicted Mean Vote
Q – Shortwave Radiation
Q* – All-wave net radiation flux
Q_E – Latent turbulent heat flux
Q_F – Anthropogenic heat flux
Q_H – Sensible heat flux
Q_m – Thermal Storage
Q_i – Conductive Heat Transfer
Q_v – Convective Heat Transfer
R – Reflected shortwave energy
RH – Relative Humidity
S_{STR} – Radiation flux density
SVF – Sky View Factor
T_a – Air temperature
T_i – Internal Temperature
T_{MRT} – Mean Radiant Temperature
T_S – Surface temperature
U – Average transition, U-value
UBL – Urban Boundary Layer
UCL – Urban Canopy Layer
UHI – Urban Heat Island
USGBC – United States Green Building Council
 ϵ_i – Emissivity
 Θ – Solar incident angle
 σ – Stefan-Boltzmann constant

1

INTRODUCTION

This first chapter has the purpose to introduce the studied subject, starting with its framework (1.1), followed by the objectives (1.2) and, finally, the thesis structure (1.3).

1.1 Framework

The urban environment is vulnerable to climate change. High temperature amplitudes, heat waves, cold waves, sudden floods and raising sea levels can interfere with the city structure and interrupt or damage its functions. Public space, in particular, suffers the influence of weather conditions, according to the positioning of buildings and the presence of diverse infrastructures. Changes in finishing materials of buildings and public spaces can affect greatly the hydrothermal conditions both in indoor and outdoor spaces.

More dense built areas have higher temperature. Construction materials have higher capacity to store heat during the day and release it during night time, heating the urban environment to what sometimes can be perceived as an uncomfortable temperature. It is difficult to predict how these new buildings or new solutions to refurbish existing buildings and public spaces will affect the urban environment and, in many cases, this is achieved by trial and error practice. There are some cases where the reflective finishes of buildings create “death rays” of reflected light that can raise the near building temperature up to 15 °C, melt cars or even fry eggs [1].

Up to this moment, there is little to no concern, when designing a building or an urban public space, about how it will affect the thermal comfort of the open space and the surrounding urban areas. This can lead to great discomfort for the citizens and make public spaces an unwelcoming environment. The gap between urban planning and AEC industry, made by the freedom of choice on different finishing materials needs to be closed or, at least, tightened. So, there is the need for a tool that can assist in this challenge both designers and local authorities.

Until now, urban planning has relied mainly on *Geographical Information Systems* (GIS). They are used for gathering information, visualising, managing and analysing proposals and changes in the urban structure. Although they present some restrictions when handling more delicate problems like the ones mentioned above. The problem is that although GIS involves the consideration of raster, vectors, points and polygons with related information, it usually does not have data about the material of each building structure or urban public space and the availability of materials is limited.

Building Information Modelling (BIM), on the other hand, is specialized in dealing with the construction process and management of the lifecycle of individual buildings. The concept is to achieve interoperability between different software and tools that cover almost every aspect of the building process. It has diverse analytical properties and with the help of visual programming tools,

like Dynamo, it can be adapted to many purposes. Even though it is very effective in the AEC industry, it has model size limitation that can restrain its use in urban planning.

City Information Modelling (CIM) is new concept that gains popularity each year, whose objective is to integrate all aspect of the urban systems into one environment by representing the interactions between public and private spaces. CIM theoretical methodology grounds on the interoperability between GIS, BIM and the capacity to create unified standards to bridge between them.

In this dissertation, BIM capability to characterise open spaces were tested, in order to create a tool to study the effect of construction materials and coating surfaces on the quality of urban spaces. Creating a tool for simulating the response of the built environment, under different weather conditions, and different design alternatives, will enable decision-makers to support their final decision in order to create more sustainable and comfortable public spaces.

1.2 Objective

Given the previous framework, the aim of this dissertation is to create a tool that will close the already identified gap between urban planning and AEC industry.

Using BIM tools for urban planning can prove useful for analysing the physical environment, related changes, and the interaction with cities environment and the population. Simulating thermal exchange, heat storage and sky view factor can prove challenging to recreate thermal comfort conditions in 3D modelling. It depends on building geometry, the sky view factors, surface temperature and mean radiant temperature to analyse heat transfer between surfaces and to outdoor environment (urban climate). This also relates to weather conditions, solar radiation, construction materials and building positions. All of those factors follow physical laws, simplified in this dissertation using chosen parameters and constants, although one is aware of the risk of incorrect representation due to these simplifications. A balance must be found between the software capacity and limits of simplification. Heavier models require more time to execute and too much simplifications can lead to unreliability in the results. One of the objectives of this work is to find reasonable solution to this problem, without to compromise results.

This dissertation will connect urban planning with present and future built environment by creating a tool for the estimate of the main parameters used for thermal comfort determination. Having an instrument that can predict how new or refurbished construction will affect public spaces will give planners a powerful tool for simulating different scenarios for future projects, analysing the best ones, avoiding unnecessary costs and improving citizen's quality of life.

This dissertation follows the methodology explained bellow:

- Initially, relied on the study of how GIS and BIM can be used for urban planning and address what has been done and what is still missing;
- Clarify what is CIM, what has been done and what are the future potentials and challenges;
- Explore the possibility of using BIM environment for creating new tool for urban planning;
- Create a tool for estimating mean radiant temperature based on surface temperature;
- Validate the tool: creating 3D model of a chosen part of the city, take measurements and compare the estimates to the real values;
- Simulate different scenarios and see how diverse materials and colors can change thermal comfort of the public space
- Address the difficulties and challenges encountered during the elaboration of this work
- Suggest future work for optimization of the tool

The listed methodological steps seek to find a new way of looking at urban planning, using new tools to support technical and political decisions, regarding changes to the built environment, intended to be more sustainable, using the most suitable construction materials and reducing the need to fix unexpected mistakes, considering the final purpose of the interventions. This is not only a tool for aiding the decision-making process in urban planning but also has the objective to qualify urban public spaces, and with the chosen case study, to guarantee user comfort of that public space.

1.3 Overview

This dissertation is divided in five chapters whose description follows:

- Chapter 1:
This chapter introduces the topic of this dissertation and sets the main objective and the methodology.
- Chapter 2:
Here are clarified the basic concepts of Geographical Information Systems (GIS) and Building Information Modelling (BIM) and how they can contribute to the creation of unified and integrated platform for urban planning and construction sector. It is also discussed the subject of City Information Modelling (CIM) and what remains to be done.
- Chapter 3:
Introduces and clarify the concept of urban comfort by braking it down to basic parameter and physical laws that can be measured, quantified and qualified.
- Chapter 4:
This chapter presents the tool developed during this work, the case study chosen for validation, the comparison between estimated and real values and it also gives some examples of how the tool can be used.
- Chapter 5:
General conclusions about this dissertation, what was achieved, the main difficulties and future challenges and objectives.

Also includes the list of used References and some Annexes to complement the information given in the body of the document.

2

GIS, BIM AND CIM

2.1 Introduction

With the growing urbanization and decreasing of non-built-up areas in the city, urban planning is becoming more complex by the day. The existing city is one of the restrictions that urban planners must work more efficiently to manage the issues arising from the confrontation between the ‘new’ and the ‘old’.

Undeveloped land within or around the city is hard to find but may have a huge potential to influence the whole region, as the correct changes introduced to an existing built space can increase livelihood and improve working conditions in the area. In this context, land is the most valuable resource of a city and deserves a careful attention to every detail. Planners around the world had always searched for the most efficient practice for planning to optimize the gain a city can receive from its given local conditions. Some type of physical or numerical evidence that they work fittingly for the given scenario always supports those practices. Technologies are the tools that can give that type of physical proof and have the advantage to support the whole planning process as they increase the number of possible solutions. They also provide easy way of communication and collaboration between the participants. Technologies can serve as platform for spatial and demographic data analysis, they can provide base for studying all aspects of interaction between city and citizens but also have the possibility to study the influence of each individual structure in urban area.

Urban area consists of buildings, public spaces and supporting infrastructures together with human daily life happening in between.

For the purpose of this dissertation, we consider that there are two types of cities:

- cities that have been evolving through the centuries, with an ‘organic’ development and
- fully planned and built cities.

The first one is ‘natural’ and happens over time with the collective planning effort of many generations while the second is modelled and designed according the desire of certain town planners and authorities and it is regulated from the beginning. In both scenarios, the final purpose is the economic growth, prosperity and comfort of that urban area.

When creating an urban space, it always focuses on the harmony between comfort and function. The people using it must feel welcome and wish to stay and use the outdoor for different types of activities. The same happens when constructing a building. It is created with the thought of creating a safe indoor space with controlled environment and compartments corresponding to its function. When constructing a building there is always a concern about its structure, function and vision rather than how the building will change the environment around it. Single building can change the microclimate of an urban space making it hotter by releasing trapped heat or making it colder by giving unwanted shading. A building can be constructed and demolished in short period of time compared to creation of urban areas. When a process consists of known variables and parameters it means that it can be automated and optimized with the help of digital technologies such as Building Information Modelling (BIM) in the AEC industry while Geographical Information Systems (GIS),

on the other hand, helps with the organization of the know parameters in urban planning. This chapter will explain the uses and limitations of both GIS and BIM and introduces the recently developed concept of City Information Modelling (CIM) that has the potential to eliminate the gap between urban planning and individual structures, in terms of digital connection.

The general expectation for a 3D city model is that it must represent city's topography and related spatial objects, but with the rapid development of the technologies, there are more requirements that the existing models must meet. The models not only must account for the correct visual representation, but also must have relevant data related to the images. In practice, most of the 3D city models currently available are relatively poor in attributes [2]. These models can be divided in two categories:

- *Design models* generally represent single buildings, still not built as they are intended to satisfy the needs of AEC industry. The focus is to represent the maximum level of detail and development so that the digital model can be as close as possible to what will be constructed in the future.
- *Real-world models* typically includes the representation of existing objects, in the form of geospatial information system. They are ready to receive the design models in order to study the interaction in between [3].

Sun-hours per day received by a building, division of urban space, underground metro network management are problems that cannot be solved only with two-dimensional data, there is evidence for the need of 3D models to develop and advance. Researchers are interested in the development of 3D parametrical urban modelling, because it gives new opportunities for more objective view over the problems from different angles and perspective with integrated information from other sectors. Those models give not only visual representation of the space but also analytical capabilities that can take height, geometry and material of a building into the equation. The development of those models becomes an interesting matter in some fields like urban planning, land use management and traffic administration [4]. In most developed countries, the urban infrastructure is represented by geospatial data using GIS technology.

One of the issues is information sharing between different participant is the absence of any standards and norms are much needed to set guidelines for construction of digital city and clarify the interoperability between the sectors.

The interoperability between GIS and BIM have been object of many studies in the past years, intended to provide town planners with the benefits from both frameworks. 3D digital models have grown importance in urban planning not only for visualization but also for integrating different sources of data. 3D city models are presently scattered over different public and private sectors in different systems, different conceptual models, different data formats, different data schemas, different levels of detail and different quality. Results of integration efforts of BIM and geospatial models show that only 3D geometric information does not fulfil the integration purpose and may lead to geometrical inconsistencies [5].

2.2 Technologies and Urban Planning

2.2.1 GENERAL FRAMEWORK

Technologies are present in almost every aspect of everyday life, from application that shows the time of arrival of a bus and save time to complex simulations that helps mitigate and prevent disasters. In the development of the city, technologies have been used throughout the year to improve the process in different sectors from production of construction materials to planning and analysing efficiency for infrastructure scenarios. For the last few decades, planners, authorities and construction agents had been given the task of improving the quality of life and services in the cities and those

developments often must be supported by investments in technological development and innovations.

Urban planning is a complex process of controlled development of a city. Collecting data, analysis, predicting and estimating, setting objectives and public discussions are one of the many tasks urban planners have to cover. Technology is used to map the existing urban environment, merge it with the intended developments and predict how the outcome will affect urban systems. It helps transforming the vision of urban planners into implementation.

With fast development of urban areas and frequent events associated with climate changes, it is important to have better response plans for cities under risk. Technology can be an efficient tool that will allow resource rationalization. It is an answer to problems and challenges within the complexity of urban systems. Technologies can provide many alternative solutions for a given problem and help in decision-making by providing solid proof if a concept works before implementing it. It can increase productivity for the urban planner, boost team collaboration and have high precision when treating and analysing data. The technologies used to improve urban planning are [6]:

- *Geographical Information System (GIS)*: used for spatial location and associating geographical with statistical data in order to visualize tendencies and analysed them. Urban planning consists of many layers of detail on a single map and one of the advantages of GIS is multi-layered mapping. GIS can be used to investigate different things, including agricultural land, surface water, high flood frequency, forest fire hazard and protected areas. This multi-layered capability can make a significant difference when developing an area.
- *Virtual Reality Technologies*: Uses 3D models for simulating and representing the reality of urban areas allowing precise decision-making. These techniques increase the efficiency and flexibility for urban planner by reducing the time and effort required to finish the task. It helps represent and understand the processes, which take place in the city. Models can be used to easily represent the planner's vision for the city, assisting non-professional participants to understand complex planning issues.
- *Measurement systems*: Divers measurements tool applied directly to the urban environment for example laser measurement system that capture 3D geometric data with high resolution. There are tools virtual planning support, control and validation.
- *Remote Sensing*: allowing gathering of info without physical contact through aerial photographs and satellite images. Can detect the changes of land use, can monitor natural resources and monitor and control unwanted/uneven growth in the cities, meteorological data.

Managing resources and minimizing energy loss is one of the main goals in creating a sustainable urban environment. Technology can be used to record and observe where the most energy losses occur and can help in elaboration of efficiency plan. 3D models allow planners to get the bigger picture and can be used to improve accessibility of pedestrians and cyclists, reduce pollution and make it more likable for the people using it.

With the help of Global Positioning Systems (GPS), cities have become easy to navigate in. Steady telecom network and monitoring of building and public space can assure adequate assistance and reaction in emergencies. Good and comfortable living conditions improve the quality of life, reduce the stress level of the citizens, which can raise the productivity and help the growth of a city. Deep understanding of the integration of technology in the city is essential for finding smart ways of managing a city [7].

Introducing technology in urban design can lead to greater level of connectivity between residential and commercial locations. Sharing and collaborating is emerging as powerful concept and is gaining more attention through open data, open governments and in part through the increase in remote work. Working from home, reduce commute time and improve traffic conditions. It can help solve the

problem with the migration to the big cities by allowing people to work remotely from their homes and so diminishing the costs related to artificial growth of urban areas. Technologies and its applications can help connect urban planners and experts around the world, providing them with platforms for learning, sharing experience and boosting competitiveness. Connecting different parts of the world with similar problems can help partitions understand better the challenged and find more well-suited solutions.

2.2.2 GEOGRAPHICAL INFORMATION SYSTEM (GIS)

A geographical information system or GIS has acquired many definitions throughout the 40 years of existence from it easily conceptualization. One of the more accurate is given by ESRI (1990) [8] and it describes GIS as “an organized collection of computer hardware, software, geographical data and personnel designed to efficiently capture, store, update, manipulate, analyse and display all forms of geographical referenced information.” It represents the world as a map and describes it in terms of longitude and latitude and/or other projection systems consisting of hierarchical structure of graphical objects. GIS is used in large scale urban studies and projects for gathering, managing and analysing information to understand relationships, patterns and movements throughout the space and it contains four major components connected to spatial and non-spatial data [9]:

1. A data input system;
2. A data storage and retrieval subsystem;
3. A data manipulation and analysis subsystem;
4. A data reporting system.

GIS software represents the world via raster and vectors linking geographic information that indicate where the objects are situated with descriptive quantitative and qualitative information of what those objects are. As a tool, GIS allows planners to complete complex spatial analysis using geoprocessing functions as map overlay, connectivity measurement, and buffering [10]. Map overlay is one of the most valuable resources, as planners have a long tradition of using map overlay in land administration analysis [11]. Some of the GIS benefits include [12]:

- *improved mapping* – better access to maps, improved map currency, more effective thematic mapping, and reduced storage cost;
- *greater efficiency* in retrieval of information;
- *faster and more extensive* access to the types of geographical information important to planning and the ability to explore a wider range of “what if” scenarios;
- *improved analysis*.

Since 1980, urban planners adapted GIS for regional planning in the developed countries. Current GIS supports efficient data retrieval, query and mapping and can collaborate with spatial analysis programs and can also be used as open data platform for better collaboration and coexistence between the elements of urban planning to create inclusive communities diminishing manual labour of planners, giving bigger overview potentials and increasing time for thinking over the decision. It has huge potential to make planning more transparent by providing a platform for data management and sophisticated model simulation and enabling communication between large group of users [13].

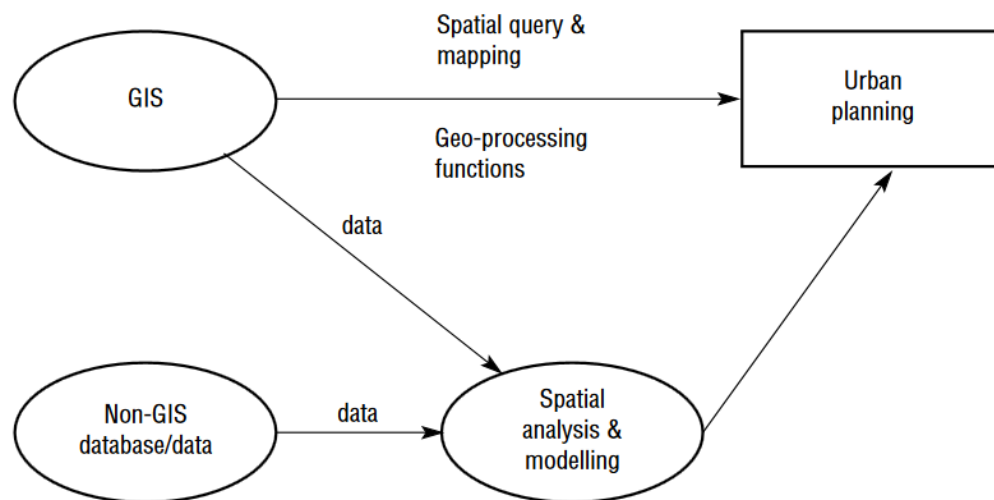


Figure 1. GIS and Urban Planning [14].

GIS and Urban Planning

GIS can be used in various aspects of a city function. Almost every department in the city governance can benefit from it. GIS can be used to manage all the information related to maintaining an inventory of all parcels, roads and other land features and can perform analysis for special projects and other public interests.

Municipality can benefit from providing public access to GIS, allowing information exchanges with the citizens. Public Safety is another sector where GIS can prove to be useful. It can help to create quick connection between responsible units and an address when emergency signal is given. GIS is also used to map location and types of incidents and is a key tool used in planning for future situations. It can also be used to compile the address file that is loaded into the computer-aided dispatches system that gives vital information to the responding emergency units. GIS is used for economic development, planning and zoning in analysing existing and long-range land use in future planning exercises. In addition, it is used to prepare maps for staff reports and other planning documents and to help with site selection on potential new businesses looking to locate in the city. Public transportation on the other hand uses GIS to trace and map comprehensive road projects, traffic modelling, site plan/plan review, and graphic illustration for meeting and court cases. Maps and other special project are created upon request to assist in solving citizen inquiries, court cases and general presentations. It can help managing the finances by using GIS as a tool to view parcel information such as size, shape, topography, zoning, proximity to geo-spatial data and can track price variation. It can graphically dispel feedback and provides a historic archive of how a parcel has changed over time in relation to their geospatial features. GIS can be used to track the Storm Water Drainage Systems Inventory, Storm Water Management Program, Emergency Management Flood Hazard Areas, Wetlands, Land use, Soils and other Environmental issues etc.

GIS limitations

Although all the advantages and uses mention above GIS is still application with specific purpose and restricted fields of action. It targets the treatment of geo-related information and even thou in recent year has enchanted 3D representation capabilities it still cannot account for all the needed studies and analyses in the urban environment. It has been present on the market for many years the technology is constantly improving, and yet the price for both software and hardware remains high. The free open source software, but it does not have the advanced analytical capability as the payed ones. It also has complex interconnections between the hardware and the software components of a

GIS and it also requires fully trained human personnel to operate the system which is expensive to train and acquire. In case of malfunction of a hardware it will take long periods of time to bring back the system into operation. Other problem is that integration with traditional maps is difficult because a GIS has a complex map structure. Due to this it is difficult to gain any meaningful information from traditional maps which mean that GIS only works and reads information that has been composed using the software from the beginning. The data structure is complex, and the information collected and stored in GIS often requires restructuring that require special skill. Often interoperability with other programs is impossible due to the structure of the data output. Also, there can be problems with analysing the data because of the lack of consistency or simply because not all information captured can be analysed completely. In performing data analysis using a GIS, there is a lot of generalization due to the massive data being analysed. The user stands to lose a lot of information due to the generalization of data. GIS stores extremely large amounts of data at any given time. This may generate problems when it comes to analysis due to the complexity of the data and the risk of generalization. It also creates problems when it comes to interpretation. Due to the large data sized GIS require large storage spaces which also increases the cost of storage and the manpower required to manipulate the data. Gathering the data can also be expensive in the long run since not all the data collected will prove to be useful but it will require sorting, storage and treatment. The process of collecting, storing and analysing of information using a GIS system is long and tedious and therefore time consuming. It may take a long time to get complete information regarding a set of data due to the vastness of the data available [15].

For more sustainable city environment and efficiency in energy and recourse use GIS must “learn” to cooperate with other programs. Interoperability and data exchange throughout various platforms have been challenging in recent year and it yet to be resolved. For optimizing cities performance planner must look not only in the big picture but also pay attention how the separate elements, building and structure that consume the energy preform. GIS is incapable of such analysis and therefore the concept of BIM will be introduced next.

2.2.3 BUILDING INFORMATION MODELLING (BIM)

The early beginning of BIM conceptualization can be traced back since the early days of computing in 1960s. In 1974 Professor Charles M. Eastman, relisted the first papers outlining the base line for the concept and marking new beginning in the solid modelling programming[16]. Many viewed the development of ArchiCAD software program in 1982 in Hungary as the begging of BIM even thou the term *Building Information Modelling* was introduces later in 1992 by G.A. van Nederveen and F. Tolman [17]. The development of the Revit software program in 2000 has made big impact on the market and marks the real shift of the AEC industry to effective BIM implementation [18]. Building Information Modelling can be described as a methodology of information shearing and communication between all the stakeholders involved during all the phases of life cycle of a construction that is supported by a digital 3D model accessible with appropriate software, which permits the manipulation of the virtual construction.

In comparison to CAD that consists mainly of vectors, associated line-typed and layer identifications, BIM tools are objected oriented and can support multiple views of the data models including 2D and 3D. This includes information about the element, material, price, resistance, and any assets that can be uses in different analysis in bettering the construction quality. It allows easy communication between the architects, engineers, contractors and owners and allows precise coordination between the different stages from project throughout construction till facility management and can help to avoid many unnecessary error and costs associated.

BIM is defined “as a modelling technology and associated set of processes to produce, communicate, and analyses building models” and building models are characterized by [19]:

- Building components that are represented with intelligent digital representations (objects) that ‘know’ what they are and can be associated with computable graphic and data attributes and parametric rules.
- Components that include data that describe how they behave, as needed for analyses and work processes, e.g., take off, specification, and energy analysis.
- Consistent and non-redundant data such that changes to component data are represented in all views of the component.
- Coordinated data such that all views of a model are represented in a coordinated way.

To describe the concept of BIM models, they have been classified according to two different approaches software vendors who deal with the building industry take [20].

- *Transitional Approach* where the building model is divided in to groups of objects, each representing a portion of the complete BIM. Then these groups are aggregated to form the complete view of a building, reports and schedules.
- *Central Project Database Approach* where a central database is used to store a building model and manages using a software or integrates system. The benefit of this approach is that the building of model parts can be organized and managed in one central database and any modification or design revision made in the model immediately appears in the model and coordination issues can be detected.

Additional to this classification the general characteristics of BIM can be specified as follows [21]:

1. *Object-oriented*: most of BIMs are defined in an object-oriented nature to facilitate the navigation and tracing processes through the model parts.
2. *Data-rich/Comprehensive*: BIMs are data rich and comprehensive as they cover all physical and functional characteristics of the building.
3. *Three-dimensional*: In contrast to CAD, BIMs always represent geometries of buildings and their spatial objects in three dimensions.
4. *Spatially-related*: Spatial relationships between building elements are maintained in the BIMs in a hierarchical manner.
5. *Rich in semantics*: BIMs store a high amount of semantic (functional) information about the building elements.
6. *Supports view generation*: The model views are subsets or snapshots of the model that can be generated from the base information model. BIMs therefore support view generation.

BIM Dimensions

As mention above, BIM is not only a 3D model used for visualization; it contains diverse information layers used in categories known as “BIM Dimensions”. As show in Figure 2, 3D BIM refers to the shape and it is basis for all other dimensions; 4D introduces the element of time; 5D is related to the costs. 6D and 7D BIM, respectively, referring to Sustainability and Facility Management are relatively new concepts and are still under discussion.



Figure 2. BIM Dimensions [22].

This are the main dimensions of a BIM methodology, they can be translated and transfer to serve the urban planning and even 8D can be introduces as a basis for using BIM tools for studying the comfort in the buildings and the open spaces, as it depends on the properties of the materials and variables that follow the physical laws and it can be represented by semantic data.

Parametric Objects

One of the basic elements in BIM is the used of parametric object with consist of geometric definition and associated data and rules. Parametric rules for objects automatically adapt to related geometries when inserted into a building model or when changes are made to associated objects. For example, a door will fit automatically into a wall, a light switch will automatically locate next to the proper side of the door, a wall will automatically resize itself to automatically butt to a ceiling or roof, etc. Parametric objects can be defined at diverse levels of aggregation, so we can describe a wall as well as its associated components. Objects can be defined and managed at any number of hierarchy levels. For example, if the weight of a wall subcomponent changes, the weight of the wall should also change. Objects rules can find when a specific change disrupts object integrity regarding size, manufacturability, etc. [19].

Level of Development - LOD

Level of Development (LOD) is BIM concept that refers to the amount of information a 3D model must contain to satisfy the requirement and reliability for different stages of the project development. It contains geometrical data linked with structural information and corresponding documentation. LOD also assures the quality of the information passed for the next stage of development. It is not to be confused with Level of Detail which is requisite for rendering a model.

There are five different levels LOD100, LOD200, LOD300, LOD400, LOD500 divided by difference in information requirement with one intermediate level LOD350 that comes from the specification in BIMForum and it is not universal. To meet the expectation of LOD100 minimum amount of information is needs while LOD 500 is considered digital model equal to the final product of construction. Basic LOD definitions are given by the American Institute of Architects (AIA) for the *AIA G202-2013 Building Information Modelling Protocol Form* [23] and is organized by CSI Unifomat 2010.

- LOD 100:” The Model Element may be graphically represented in the Model with a symbol or other generic representation but does not satisfy the requirements for LOD 200. Information related to the Model Element (i.e. cost per square foot, tonnage of HVAC, etc.) can be derived from other Model Elements.”;
- LOD 200:” The Model Element is graphically represented within the Model as a generic system, object, or assembly with approximate quantities, size, shape, location, and orientation. Non-graphic information may also be attached to the Model Element.”;
- LOD300:” The Model Element is graphically represented within the Model as a specific system, object or assembly in terms of quantity, size, shape, location, and orientation. Non-graphic information may also be attached to the Model Element.”;
- LOD 350:” The Model Element is graphically represented within the Model as a specific system, object, or assembly in terms of quantity, size, shape, location, orientation, and interfaces with other building systems. Non-graphic information may also be attached to the Model Element.”;
- LOD 400:” The Model Element is graphically represented within the Model as a specific system, object or assembly in terms of size, shape, location, quantity, and orientation with detailing, fabrication, assembly, and installation information. Non-graphic information may also be attached to the Model Element.”;
- LOD 500:” The Model Element is a field verified representation in terms of size, shape, location, quantity, and orientation. Non-graphic information may also be attached to the Model Elements.”;

The *Level of Development (LOD) Specification* is a guideline for BIM practitioners for assuring quality and high level of precision of Building Information Models (BIMs) at various stages in the design and construction process [22].



Figure 3.LOD levels and project stages. Source:[22]

In the context of this work, BIM methodology will be applied in the initial phase of urban planning so the requirement for the LOD must be low. Proposed software/methodology for this work the goal is set to LOD300, which indicates location, shape, orientation, information about different layers of each element and the material’s thermal and physical properties.

Industry Foundation Classes - IFC

One of the most established and recognized semantic models that implements BIM concepts is the Industry Foundation Classes (IFC). It follows ISO 16739:2013 and it represents an open international standard for BIM data that is exchanged and shared among software applications used by the various

participants in a building construction or facility management project [24]. It is an object-oriented file format with a data model developed by *buildingSMART* to simplify interoperability in the building industry and is a commonly used format for BIM. It is a standard used to unify all applications used in BIM, providing a common language and allowing information sharing between all the participants. Today, there are several CAD/AEC applications (such as ArchiCAD, AutoCAD and Bentley MicroStation) as well as many analysis applications (such as Solibri, SAP 2000, etc.) that can import and export their internal models according to the IFC standard [25].

Revit

Autodesk Revit is a BIM authoring tool for architects, structural engineers, MEP engineers, designers and contractors that allows users to design a building and structure and its components that accurately represents the real world through 3D graphic with all the related semantic information. It can store time related 4D information and to plan and track various stages in the building's lifecycle. Offers tool to improve the efficiency of the workflow of all the project participants by allowing them to visualize their work, run test, correct and avoid errors.

Revit is composed of parametric categorized components or the so-called 'families' which divide into three groups:

- System Families, such as walls, floors, roofs and ceilings which are built inside a project
- Loadable Families / Components, which are built with primitives (extrusions, sweeps, etc.) separately from the project and loaded into a project for use
- In-Place Families, which are built in-situ within a project with the same toolset as loadable components

Revit can produce schedules and extract quantities like area, price and number of needed unites in small fragment of time. It has a great interoperability with all BIM applications and it uses IFC standards as basis for collaboration and sharing. Is has variety of Add-Ins and tools available.

Although Revit and the BIM methodology were specifically developed to aid the AEC industry, some of the methodology can be applied in urban planning thru adaptation and scaling. Small districts can be correctly represented and studies in all of the 7 BIM dimensions plus hydrothermal studies of the environment can be elaborated and conducted with the help of Dynamo.

Dynamo

Dynamo is a visual programming tool that has the objective to be accessible and understandable for both non-programmers and programmers alike. It gives users the ability to visually script performance, define custom pieces of logic, and connect elements together to define the relationships and the sequences of actions that compose custom algorithms. It can be used for processing data to generate geometry to making vector-based analyses [26].

In this work the focus will be on the developed Dynamo software tool for seeking measurements of the urban comfort in BIM environment. The tool is easy to be used even by non-programmers and give a liberty of constructing and preforming space analysis tool that can be applied not only to inside of the building but also to open spaces.

“Dynamo is, quite literally, what you make it.” [26]. This citation describes Dynamo perfectly because it gives user the ability to freely change and adapt the modelling process to meet their needs

BIM for Urban Planning

BIM is used mainly in the AEC industry. It allows going from a virtual building or component, to the coordination between the specialties, before the actual construction is done, until the construction

itself. As so, BIM for Planning can be a powerful tool for urban design as it has the capacity to link data with physical form and connects planning regulations with the city and vice versa. BIM Visualizations is an effective communication tool and can aid public and private sectors [27].

BIM methodology is not practical for urban modelling because it misses essential tools for creating a large-scale urban area. However, it can be adapted to study small urban areas with *Dynamo*.

BIM process involves usage of different application that exchange information via IFC format and allow this way of having the possibility of extracting both schedules and quantities, extracting detail drawing of a building component, but also run analysis and compatibility checks. 3D models can contain a lot of data and can get quite heavy. This is one of the main concerns when BIM tools are applied in creating a city or neighbourhood models with high detail and information input.

2.2.4 CITY INFORMATION MODELLING (CIM)

CIM is an analogy to BIM for urban planning, it combines the capabilities of GIS with the detailed data form BIM allowing easy information management and variety of analyses in 3D geometrical space [28]. The term city information modelling evolves around the creation of an urban 3D model enhanced with semantic elements. At present, there is no single name for this type of modelling, and different terms and expressions has been encounter during the literature review, such as urban informational model, digital city, intelligent city, city information model, GIS city, smart 3D city, procedural city, etc. [29]. Digital methods and parametric procedural modelling have been used to develop software packages which can be utilized to design new urban structures and run various simulations. The technology available today is far more advanced than the methods currently used by professionals. Major software producers that usually produce architectural design software have launched an initiative over the last couple of years to create new platforms that would allow information to be taken from BIM and connected with other types of data.

Complex city environment with static structure and dynamic object, movement patterns transportation organization, logistics must be considered. Currently there is more information pollution so sorting of useful data is needed. The typical use of a 3D city model is broadly for visualization and design, while the functional and analytic capacity of the modes can be limited due to the software interoperability. The difficulty in the integration of IFC and CityGML models comes from translating the information from one to the other.

CIM structure

CIM if relatively new concept that derived from BIM with similar objective as to have the possibility to virtually construct the city to locate possible critical points and to eliminate them before the actual investment. A city structure can be divided into sub-modules each representing essential part of the city. The lack of unifies model for CIM can be compensated by using BIM-tech to build these parts into information models, and then use GIS-tech to locate every part of city [30]. Figure 4 illustrates the analogy between the needed component for construction of BIM model and CIM model.

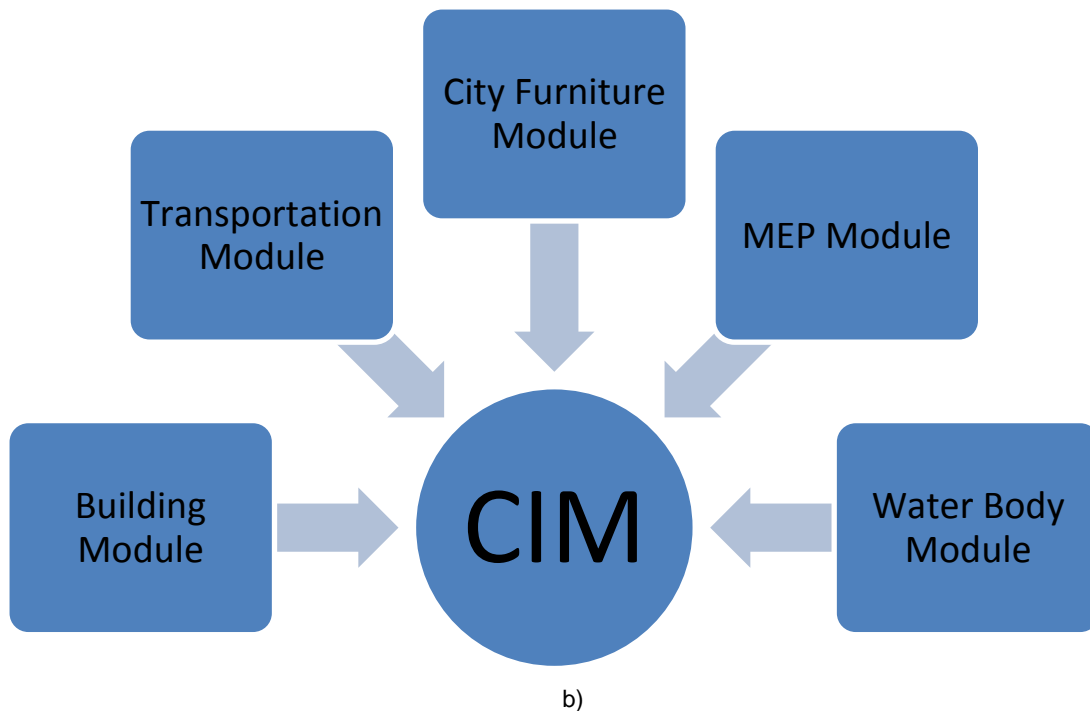
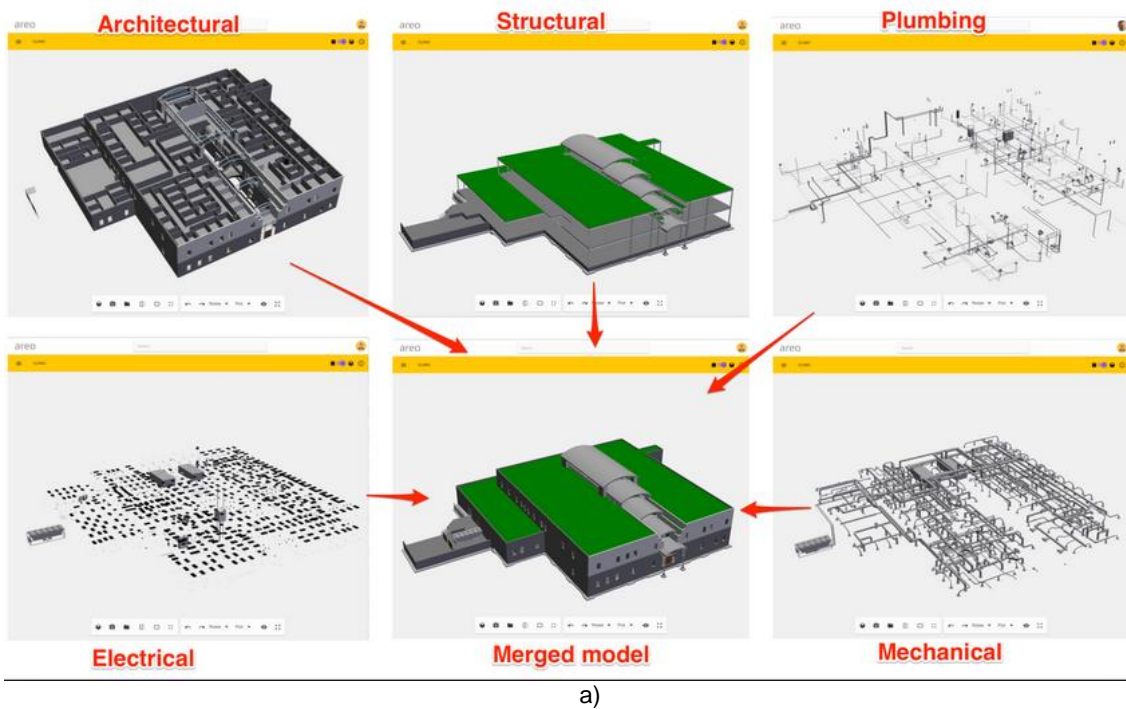


Figure 4. a) Sub-models of BIM [31]. b) Sub-modules of CIM, Adapted after [30].

Much like the BIM, CIM can also be divided into different modules. Each of them will represent different aspect of the city and together they will contribute to the overall representation of the urban scenario:

- **Building Module:** Buildings and adding structures are the main elements in a city. Each of them possesses unique characteristics like architecture, structure and function. Due to this diversity it is difficult to collect all the information needed for construction of this module. Some of the recent construction have their design in CAD or Revit that can be imported directly into the building module, while some older building dose not even have paper plans.

Technology like laser scanning can be used to fill in the blanks about exterior, materials, structure etc. [32]. Information in this module can be used for example comparing older to newer buildings by energy consumption, comparing the property value and studying how modification to the city texture can reflect on the urban environment.

- *Transportation Module*: It contains information about the road infrastructure about name of the street, length, width, parking slots, traffic expectation and all the related restrictions like speed limit, street direction etc. It can contain information about the layer structure of the street, expected maintained schedules and cost. Also, it can be used for real time monitoring, traffic management and detours routes for the system, avoiding traffic congestions and for quick response to emergencies.
- *City furniture module*: Contains information about public utilities and commodos. Much like facility management in the building city require continues uphold. Plus, public spaces can be stable source of collecting information with real time monitoring or other type of data gathering technologies that can be uses as reference point of how the space is performing.
- *MEP module*: Analogy to BIM MEP but city scale, HVAC system, underground piping system, electrical and lightning system and circuit system. Revit MEP provide segmented information that can be completed by using GIS data. It is not to be confused with the building MEP system as it is on a large scale and show the position of the network in the city infrastructure and it can help with maintains and performance optimization.
- *Water body module*: Include all rivers, pounds, lakes seas, infiltration systems. Water is becoming more of a scares recourse as it is important not only for human and industrial consumption but also for the ecosystem. This module can prevent water pollution and related disaster, minimized the losses in the system also can help with water management and treatment of city wastewater.

Those are the are the 5 “physical” modules needed for the construction of 3D city model, but the information contain in each of them can be used for analyses, queries and monitoring of the whole city.

CIM Methodology

Collect/input information, store and analyses it and show the results. This is a typical workflow of almost every program available on the market. CIM methodology is not so much different. First data must be collected about the present reality. Various specialties can participate in this process, so it is important to have solid collaboration platform that can serve for information exchange. A 3D model must be elaborated with associated building and infrastructure information divided in individual categories and ordered by given hierarchy. Preferably, each specialty will have their own 3D mode much like in BIM. For example, the underground network will have separate model then the building. 3D street can be generated automatically by using grammar-based modelling software from polyline GIS data. And the waterbodies and city furniture must have model on their own. All of the layer must be oriented in the same coordinate system and get on a top of each other perfectly. With this each specialist can work independently and during the workflow clashes and incompatibility can be detected in early stage of the model development. This model must not only respect representation requirements but also it must possess the semantic information needed for performing spatial analyses and queries. Automatization can be made to for a given set of rules to produce for example the 3 best solutions that planner can compare. New proposal can be given based on the analyses results and implementation process can be managed. Results of the new urban changes can be recorded as new data and the process repeats.

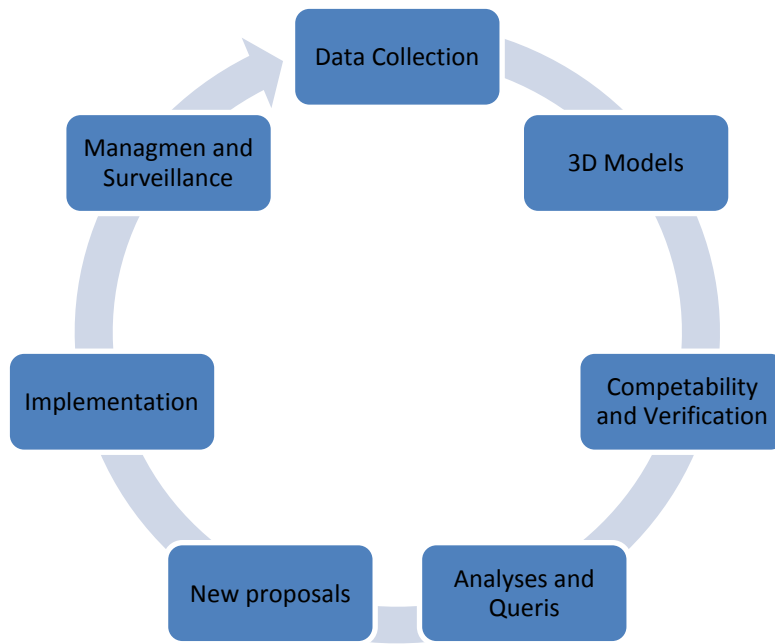


Figure 5. Methodology of CIM [33].

As the GIS and BIM model are quite different, both have special assets that make the essential in their fields. For creating CIM, both must be integrated. Integration of GIS and BIM has been subject of various studies for the last decade. Those studies focus on finding the cross-section of similar semantic information between the IFC standard and CityGML standard. It is a complicated process and may vary from case to case.

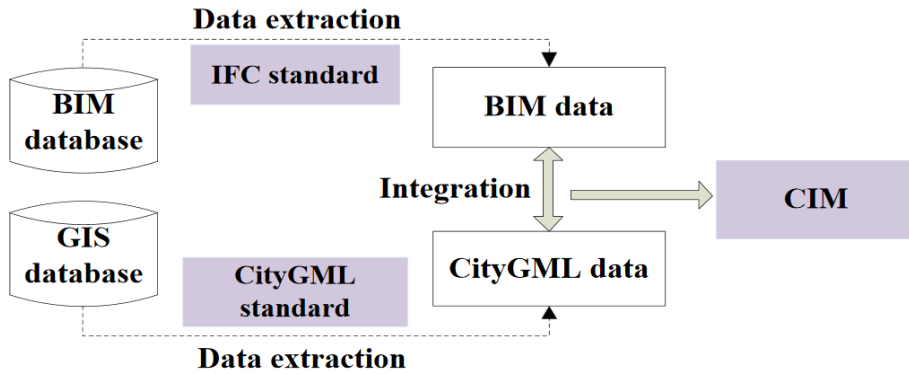


Figure 6. GIS and BIM integration for creating CIM [30]

Elaborating unified CIM standard that can be used by both GIS and BIM is much needed and it will help giving the bases for a solid workflow that all the cities around the world can adapt to their own realities.

CIM initiatives around the world

CIM is very ambitious and expensive initiative, although the theory is lacking there has been several attempts for creating application that can be integrated and few of them have succeeded.

Here are the most famous ones:

- **ESRI CityEngine**

CityEngine is a 3D modelling software developed by Esri R&D Centre Zurich and it is used for generation of 3D detailed and large-scaled urban environment by using procedural modelling approach. The main features of this program are its capacity to automatically generate buildings and streets by using predefined aesthetics and architectural rules. It uses a grammar to reduce building complexity, which allows this method to turn into a new computer-aided architectural design method for elements ranging from individual buildings to entire cities [34]. Traditional 3D modelling uses Computer-Aided Design (CAD) based tools, while CityEngine uses a rule-based system comparable with GIS [35]. It is integrated with ArcGIS and fully supports the Esri file geodatabase (including textured multi patches) and the shapefile format and allows users to import/export any geospatial vector data. It can compare planning proposals, analyse design and generate fully customized rule-based reports in order to automatically calculate quantities such as density or floor area. CityEngine scenes can be published directly on the web for sharing 3D models, analysis results, or design proposals with decision makers or the public [36].



Figure 7. CityEngine Data Flow [37].

Automation of the modelling process is the final objective, but it also depends on the preparation of the rule set which can get expensive and time consuming at the beginning. The model generation itself is done in a small fraction of the time compared to classic manual modelling but unique objects (such as landmark buildings) are best modelled by hand and usually do not need the procedural approach since often none of the modelling tasks on that object can be automated [38].

A series of different projects have been carried out using this software. These are some of the projects [37]:

1. *Redlands Redevelopment*. This example focuses on the site of an abandoned mall and proposes a scenario to redevelop the centre of Redlands. Using CyberCity3D buildings and existing GIS data, the current conditions of the downtown were quickly recreated inside CityEngine and several redevelopment scenarios were created by altering the building dimensions and zoned functions. The final design was chosen after comparing efficiency metrics to overall building cost and finally to the total floor area of entire site.
2. *Vitoria-Gasteiz Reconstruction*. It is a project that recreates Medieval Vitoria by using archaeological footprints of the town. Rules created with CityEngine describe the typical XV century Spanish elements such as walls, towers, houses, paths and orchards and serves as a hypothesis of how the ancient town of Vitoria-Gasteiz may have looked.
3. *Munich Reconstruction*. A project between GTA Geoinformatik GmbH and Procedural uses GTA's GIS data for creating volumes in relating them with their highly detailed facade data to create a rich real-world 3D reconstruction of the centre of Munich, Germany.
4. *3D Rotterdam in the Cloud*. This is a collaboration between ESRI, Procedural Inc, and mental images® with the goal to explore new techniques for smart 3D city solutions based on GIS data and grammar-based modelling technology.
5. *YouCity Real Estate*. Uses CityEngine to identify the volumetric of underused real estate in comparison to the actual state and the maximum possible exploitation predefined by current building regulations. As a result, maximum densification options as well as the current physical condition of the built environment were visualized and enhances the monitoring process of real estate investment potential for great institutional investors.
6. *Swiss Village for Masdar City*. CityEngine is used to procedurally create 3D models and master plan reports for the corresponding 210,000m² of build area. The goal is to create sustainable city with that is only dependent on renewable energy.
7. *Marseille Urban Planning*. This project shows an urban planning project of the big French construction company Eiffage, where a compelling master plan and 3D visualization has been created.

CityEngine is relatively new way of modelling and has huge potential for development, but there is still more to be wanted in some respects like integration and interoperability with other types of analytical software. It's useful for visualization and demonstration and some spatial analysis but it lacks in performing vectored based spatial analyses and calculation like Dynamo or Grasshopper.

- **Bentley**

Bentley's 3D City GIS integrate a series of products from various specialties to create smart 3D city model, manages the related components and follow its development throughout the lifecycle. It is closer to the concept to CIM than any other existing brands by following the CIM methodology and

Here are some of the key products for 3D City GIS for the different platforms [39]:

- **CAD (MicroStation, GenerativeComponents, ProjectWise Navigator)**. The MicroStation family of products provides traditional CAD capabilities and the

power and versatility to precisely view, model, document, and visualize information-rich 2D and 3D designs of all types and scales, working for professionals in every discipline on infrastructure projects of every type.

- **3D GIS (Bentley Map, Bentley Descartes)**. Create, maintain, analyse, and share your geospatial, engineering, and business information in a powerful, yet familiar MicroStation environment. Work confidently with engineering-quality GIS to produce quality maps and unify disparate 2D/3D data.
- **Web (Geo Web Publisher)** is a comprehensive application for the conception and management of web-based geospatial data and it can be used to create an easy-to-use web interface to disparate data sources for a wide range of Web GIS applications such as municipal information systems, image or drawing archives, map-based navigational sites, project sites, and public information portals [40].
- **Collaboration (ProjectWise family)** is a collaboration software that helps project teams to manage, share and distribute engineering project content and review in a single platform. While ProjectWise can manage any type of CAD, BIM, geospatial and project data, it integrates with Bentley applications, and other products including Autodesk software and Microsoft Office.
- **Architecture (Bentley Architecture, Bentley Hevacomp)**. Bentley Architecture is an advanced, yet intuitive and easy-to-use architectural **building information modelling (BIM)** application that allows architects and designers to create with unlimited freedom, to explore more design options, to make better informed design decisions, and to predict costs and performance.
- **Utility (Water, Wastewater, Stormwater products)** water management products that can help to understand and effectively design these types of systems, from small land development projects to large-scale municipal studies.
- **Civil (InRoads family, PowerCivil)**. Comprehensive tool for 3D modelling, design, and analysis applications for transportation, land development, water, and civil projects. It can be used to design, build, operate, maintain, and rehabilitate projects.

Bentley's CIM solutions have already been widely used in large-scale city modelling projects in Montreal, Helsinki, and in London's Crossrail project. A more recent example is their use to produce 3D map data and the city model for the city of Singapore [33].



Figure 8. 3D model of Singapore created using Bentley's CIM products [41].

- **Autodesk**

Digital City is an Autodesk initiative to create a single tool that would allow a cooperative environment for the visualization, analysis and simulation of future interventions in a city and the development of cities in the future. Digital City combines several applications and platforms [34]:

- 3D/4D City Modelling using Autodesk products, 3ds Max, AutoCAD, Revit, AutoCAD, Civil 3D, Navisworks and AutoCAD Map 3D.
- 3D modelling using LIDAR, Terrestrial Laser Scanning and other automated data capture methods.
- 3D/4D visualization and the ability to accurately model and evaluate existing and proposed developments in their proper geospatial setting.
- Digital City business practices and opportunities, including urban development, transportation, infrastructure, real-estate, tourism and historic preservation projects.
- Industry standards and consortia, including the Open Geospatial consortium (OGC), City GML, IFCs, BuildingSMART Alliance, and the US Green Building Council (USGBC).

The initiative was launched in 2008 and several pilot cities were selected for case studies but unfortunately, the Digital City project has remained theoretical to this day. Namely, Autodesk, like Bentley, has an wide range of different applications, whose integration and mutual exchange of formats and information has huge potentials for producing intelligent structures and data gridding [34].

Even thou Autodesk still has various platforms that can be integrated and used to create accurate city model. CIM is not limited concept but rather it integrates all sort of spatial studies and analyses using 3D model with related semantic data. Revit on its own can perform small scale urban analyses by using Dynamo, but models can get quite have in size and information so there are certain limitations.

Main Problems and Challenges

Interoperability is essential key element to for creating sustainable 3D city environment and creating and unified stander is essential. The idea of CIM is not to create a single software or tool that contains all the city aspect, but to include and integrate in its workflow GIS and BIM alike.

CIM is a project that must be developed mainly by city government initiative because it gives to much information about the structure and function of an urban area. There is a high sensibility regarding the treatment of private data and protection of this information is essential which can become quite expensive. It requires also multidisciplinary qualified personal. It is not a rapid process that happens overnight it is a prolonged process. 3D “intelligent” city model can be compared to a complex multidimensional puzzle, but if participants in the planning process put each year a piece of the puzzle together with the same goal in mind, after few generations it will be complete.

Not considering how construction will affect the environment around can have great negative consequence for the urban space. The infrastructure has certain limits and although the planning is done by looking into the forecast for the future there is no reliable way of determining how changes of today will affect tomorrow. Urban areas tend to grow, materials and colours become more and more diverse, city climate is changing with every new structure. When planning and building there is little to no consideration of how this will influence the environment. With 3D model planner can view the shadow analyses and how much sunlight the building received, but most of the information is used to look from the outside to the inside of a building considering the indoor comfort. Considering that closed environment is relatively easy to control by cooling and heating system the outside doesn't have the same advantage. Each change can be crucial and raise or lower the temperature making it uncomfortable for pedestrians.

CIM is a continues process that much like the city itself is constantly evolving and renewing. It does not have to be big and complex model of huge urban area it can be simple as studding a single district or public space. All digital information and all technologies working in favour of the urban development can be consider CIM assets. Regulated gathering of BIM models can be the be the begging of the process of making virtual cities reality and this work will go step further into using this information for controlling complex phenomenon like heat islands by using BIM environment for preforming thermal comfort analysis.

Beginning somewhere is vital and with today's technology it can be possible and not so expensive to start conceiving a new way of thinking about how information can be used to make each step taken in urban planning better than the previous.

3

URBAN COMFORT

3.1 Climate Change and the City

In the rapid changes of today's growing urban areas one of the main challenges, that remains its adaptation and response to climate alterations. The aggregation of growing population, disappearing natural green spaces and air pollution can alter the city's climate and have deep impact on the urban comfort. The quality of housing and infrastructure in the city can directly influence the scale of the risk from extreme weather conditions. Urban planning and land use management can positively ensure risk reduction within urban expansion and benefit key emergency services [42].

Climate change is dominated by human influences which is the main source of global warming [43]. The most significant anthropogenic influences on climate are the emission of greenhouse gases associated with energy use and changes in land use, such as urbanization and agriculture because both tend to increase the daily mean surface temperature [44]. Climate change deriving from expanded fossil fuel use and deforestation has received substantial attention in recent decades [45]. A temperature increase can cause discomfort, economic loss, migration and increased mortality rates on a global level [46]. According to the UN-Habitat, 2011, Chapter 4 [47], urban areas may encounter two categories of risks due to climate changes: direct and indirect.

Direct consequences of climate changes are those that can damage the city form. They can vary from rising sea levels, flooding, landslide, heavy precipitations to extreme heat events and droughts. The indirect impacts are those that can damage not only the physical part of the city but also the functional in long term. Some of them are shown in Table 1.

Table 1. Projected impacts upon urban areas of changes in extreme weather and climate events [46].

| Climate phenomena | Major projected impacts |
|---|---|
| Fewer cold days and nights | Reduced energy demand for heating |
| Warmer and more frequent hot days and nights over most land areas | Increased demand for cooling |
| Warmer temperatures | Reduced disruption to transport due to snow, and ice effects on winter tourism Changes in permafrost, damage to buildings and infrastructures |
| Warm spells/heat waves: frequency increases over most land areas | Reduction in quality of life for people in warm areas without air conditioning; impacts upon elderly, very young and poor, including significant loss of human life Increases in energy usage for air conditioning |
| Heavy precipitation events: frequency increases over most areas | Disruption of settlements, commerce, transport and societies due to flooding Significant loss of human life, injuries; loss of, and damage to, property and infrastructure Potential for use of rainwater in hydropower generation increased in many areas |
| Areas affected by drought increase | Water shortages for households, industries and services Reduced hydropower generation potentials Potential for population migration |
| Intense tropical cyclone activity increases | Disruption of settlements by flood and high winds Disruption of public water supply Withdrawal of risk coverage in vulnerable areas by private insurers (at least in developed countries) Significant loss of human life, injuries; loss of, and damage to, property Potential for population migration |
| Increased incidence of extreme high sea level (excludes tsunamis) | Costs of coastal protection and costs of land-use relocation increase Decreased freshwater availability due to saltwater intrusion Significant loss of human life, injuries; loss of, and damage to, property and infrastructure Potential for movement of population |

Indirect impacts can be divided in three major groups depending on how they influence the urban environment [47].

Impact on Physical Infrastructure:

- Substantial damage to residential and commercial structures due to the increased occurrence of climate-change related hazards and disasters like flooding due to increased precipitation.
- Disruption in transportation systems through weather condition that has immediate consequences for travel and damage causing lasting service interruptions. Sea-level rise can inundate highways and cause erosion of road bases and bridge support while heavy precipitation can cause flooding and landslide. The increasingly higher temperature during long periods of drought and high daily temperature can compromise the integrity of roadways and necessitate more frequent repairs.
- Energy demand increases due to rising temperature and the need for cooling interior spaces. In turn, greater use of air conditioning can worsen the urban heat-island effect and further increase the cooling demand in urban areas. Also, extreme drought conditions can halt the work of water-based power generators.
- Water supplies can be reduced or increased through a change in precipitation patterns, reduction in river flows and falling groundwater tubes and with the growing population and the growing demand for supply water resource limitation can become more severe. Furthermore, excess heat from buildings and roads due to the urban heat-island effect can be transferred to stormwater, thereby increasing the temperature of water that is released into streams and rivers.

Economic impacts:

- Climate change can affect a wide range of economic activities, including trade, manufacturing, transport, energy supply and demand, mining, construction and related production activities, communications and real estate;
- The direct effects of climate change and extreme climate events on industry include damage to buildings, infrastructure and other assets;
- The tourism industry is highly dependent upon reliable transportation infrastructure, including airports, ports and roadways. Climate change has the potential to not only shift regional temperature distributions but also increase the incidence of severe weather events, which would increase transportation delays and cancellations;
- Climate change could result in increasing demand for insurance while reducing insurability. Insurance industry catastrophe models forecast that annual insured claims and losses are likely to significantly increase over the next century because of the increasing intensity and frequency of extreme storms;

Public health and social impacts:

- Climate change can lead to extended periods of heat (i.e. heat waves) and drought. More heat waves have the potential to increase the incidence of heat stress and heat-related mortality.
- Physical climate changes, including temperature, precipitation, humidity and sea-level rise, can alter the range, life cycle and rate of transmission of certain infectious diseases.
- Climate change is considered a distributional phenomenon because it differentially impacts upon individuals and groups based on wealth and access to resources.
- Can threaten the children and the elderly due to the limited adaptation capacity to extreme weather conditions.

In this context, it is of high importance to identify the cities that are most vulnerable to those climatic changes and the correct mitigation practices that may be needed. Cities are also places where resources are being concentrated and are centres for new ideas and technological innovation, therefore they may have the ability to respond to climate changes while providing tools and examples for other. Urban governance and planning can improve resilience to climate change impacts through a targeted financing of adaptation, broad institutional strengthening and minimizing the drivers of vulnerability[48].

This work will focus on how the negative effect of climate changes can be mitigated with the aid of 3D urban simulation and analysis for urban planning.

3.2 Urban Microclimate

Urban microclimate can be defined as the effect from local climate conditions encountering build environment and the resulting alteration in temperature, airflow and humidity in relation to surrounding areas. It has a vital part in building energy consumption and thermal comfort in outdoor spaces. Microclimate can be influenced by human activity via several factors such as urban morphology and density, properties of urban space and vegetation cover. It has been proven that the geometry and orientation of street canyon can affect the outdoor and indoor environment, solar access inside and outside the building, urban airflow and the potential of cooling the whole urban system [49], therefore, the street design influence the thermal comfort at pedestrian level as well as the global energy consumption of urban buildings [50].

City climate suffers unwanted thermal conditions due to changes in urban surfaces that alter the radiative exchange, humidity and thermodynamic properties of the environment. That causes a specific urban microclimate that can vary from city to city and is defined by higher temperature in urban areas compared to surrounding rural areas, which can lead to disturbing effects [51]. It is important because it has a direct relationship with energy consumption and thermal comfort. Urban

planning especially open spaces like squares or street canyons has a huge impact on local microclimate that can affect comfort and space quality inside a city [52]. It gives the opportunity of urban planners and design specialist to improve the quality of life and reduce the energy demand inside the city perimeters by manipulating the elements that have influence over the microclimate and to avoid damaging consequence from irresponsible planning like Urban Heat Island that will be explained in the next paragraph.

3.2.1 URBAN HEAT ISLAND

Urban Heat Island (UHI) is a consequence in temperature rise in an urban environment due to human activity and change in the land surface. The name comes from the resembles of the heat pattern to that of an island, where peaks represent the concentrated heat in the central zone of the city and cliffs are the temperature difference between the urban and rural area. Building materials have lower specific heat the natural materials like grass or earth and heat up more during the day, warming the air around. Concrete surfaces emit heat during the night which does not allow the cooler air to go down and substitute the hot air via convection. The trapped heat raises the night air temperature which can cause discomfort and an increase in cooling energy. Buildings also can act as blockades to winds which would distribute heat and cool the city. The urban geometry is treated as one of the most influential factors in the formation of heat island. It is more pronounced when the streets are narrow, and buildings are higher [53]. Building materials also have a strong influence on UHI, darker materials tend to store more heat, while reflective materials can heat up near structures by reflecting solar radiation. Other factors that influence the UHI are the time of the day and the station of the year; the geographical location that dictated the climate zona, topography and rural surroundings; the size of the city that is liked to function and form and the synoptic weather like the formation of clouds and wind [54].

Those factors can also be divided into two categories: controllable and uncontrollable, as shown in Figure 9. First can be influenced by UHI mitigation measurement in order to compensate the latter.

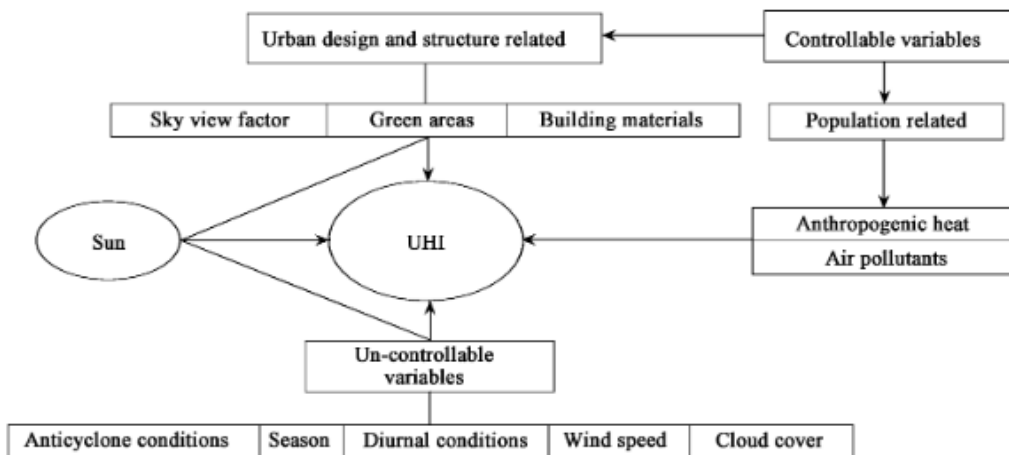


Figure 9. Generation of Urban Heat Island [55].

3.2.2 UHI SCALES

There are two scales when it is referred to UHI: mesoscale and microscale. This distinction, originally applied to UHIs by Oke (1976)[56], has been a guiding principle in urban climate research of all around the world.

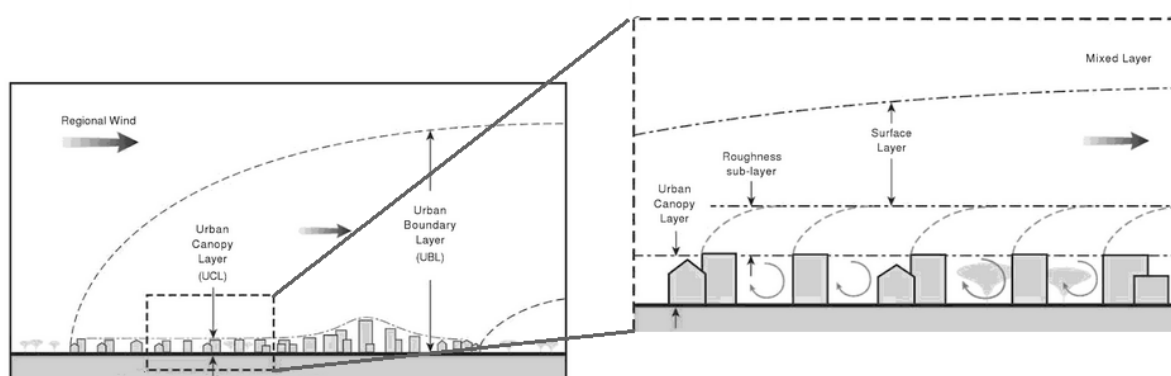


Figure 10. Schematic section of the urban atmosphere, showing the development of the urban boundary-layer (UBL) relative to the urban canopy-layer (UCL), which reaches the average building height (top), and the distinction between the homogeneous surface layer above the city and the heterogeneous urban canopy (bottom). The mixed layer and the roughness sub-layer are transition zones above and below the surface layer, respectively [57].

Figure 10 represents the two main types of urban heat island that can be distinctly distinguished: Urban Boundary Layer (UBL), Urban Canopy Layer (UCL)

Boundary Layer Heat Island is referred on the mesoscale. It is situated directly above the city and it represents the global heat output and temperature pollution. It also includes the additional heat from rooftops and urban canyons. It is influenced by chimneys and vents that send the heat above the city level. The rough urban surface slows the wind in the lower part of the boundary layer and the downwind region this layer may be separate from the surface as a new rural boundary layer develops underneath forming the so-called urban plume.

Canopy Layer Heat Island is contained between roofs of the buildings and the ground level and by nature is defined by the urban geometry and materials, and the influence of the comfort temperature it the main objective of this study. The urban environment has many conditions that can aggravate the rise of the temperature that must be taken into consideration. The main one is the result of the stored heat by thermal properties of urban material and increased surface area. Other includes:

- obstructed a sky view result in more trapped radiation
- warmer air temperature as a result from wind slowed
- increased wind turbulence increased
- impermeable surfaces reduced surface moisture and evaporation that are essential for lowering air temperature
- additional anthropogenic heat, humidity and pollution
- insulated surface lead to high daytime surface temperatures

3.2.3 URBAN HEAT ISLAND MEASUREMENT

Measuring the intensity of the UHI is important indicator of evaluation of the severity of the urbanization of an area [55]. The city has two main sources of heat: outside/resaved and inside/produced heat. The outside or receives heat is in form of solar radiation. The city consumes raw materials and produces secondary material and waste because of the filtration process. During this energy is consumed and produced. Whenever this energy is transfer to one form to another heat always involved in the transformation process. This process can be defined as inside heat production. The Surface Energy Balance or City Energy Balance can help understand how the heat moves within the city's parameters. Space technology, numerical modelling and small-scale physical models can complement the study of this phenomenon.

City Energy Balance

The city energy balance as the name implies is the energy outputs versus input that goes into the urban area. The energy balance of a city is one of the biggest concerns when it comes to sustainability and optimization of resources.

Full representation of an urban energy balance is given by Oke (1988) [58] and is shown in Equation 1 and is measured in W/m^2 .

Equation 1. Urban energy balance.

$$Q^* + Q_F = Q_H + Q_E + \Delta Q_S + \Delta Q_A \quad (1)$$

The equation balances the all-wave net radiation flux (Q^*) and anthropogenic heat flux (Q_F) with the sensible and latent turbulent heat flux (Q_H and Q_E), net heat storage (ΔQ_S) and net heat advection flux (ΔQ_A). Q^* , Q_H and Q_E can be measured directly using radiometers and eddy covariance techniques and is considered representative of the neighbourhood if instruments are at sufficient height above ground at UCL, where effects of individual roughness elements are mixed together [59]. ΔQ_A is often considered insignificant and left out if area adjoining observation site have similar urban characteristics [60].

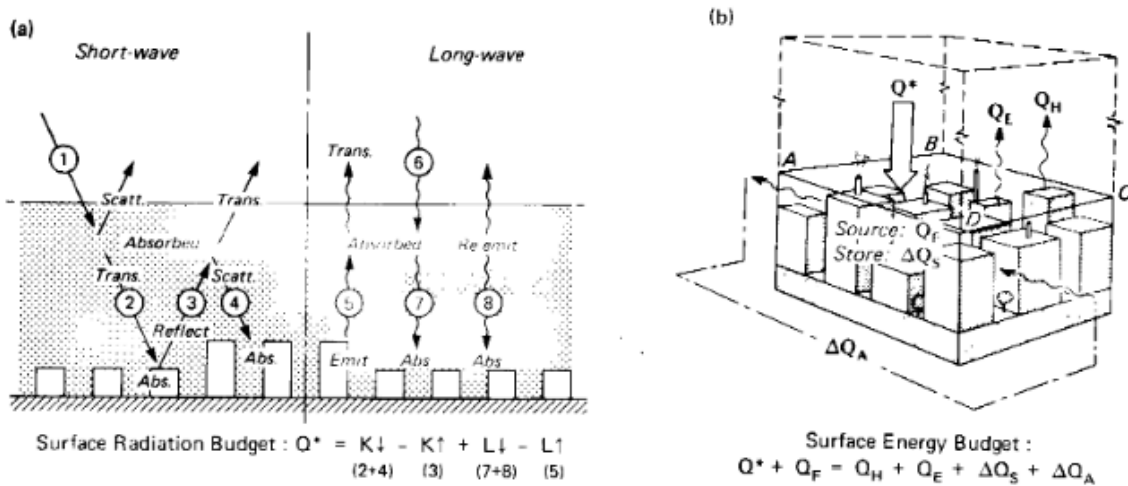


Figure 11. Representation of urban surface energy budget by Oke 1988 [58].

Net all-wave radiation Q^* , shown in Equation 2, is divided into shortwave and longwave components with the arrow showing the direction of the radiation flux densities. Components transporting energy to the surface (\downarrow) are positive and those radiating energy from the surface (\uparrow) are negative.

Equation 2. Components of net all-wave radiation.

$$Q^* = K \downarrow + K \uparrow + L \downarrow + L \uparrow \quad (2)$$

Storage heat flux density (ΔQ_s): the net flow of heat per unit area into and out of materials. It has an important role in the urban energy balance and dictates the heat storage and absorption in materials during the day and the heat release during night. ΔQ_s is difficult to determine because of the large number of surface materials, orientation and the interaction between, therefore ΔQ_s is determined as the result of the energy balance equation, assuming complete closure of the energy balance.

Additional methods

Space technology as the name implies uses advanced high-resolution radiometer satellite data to determine soil properties and surface albedo [61]. It can determine surface temperature by remote sensors, study evaporation rates [62] and determine sensible heat flux [63].

Numerical Modelling is another widely used tool for studying UHI. It can use numerical and weather data to simulate important influential factors like wind speed, anthropogenic heat release, and thermal properties such as albedo, sensible and latent heat. It has a wide range of application for example is used to evaluate that conduction of heat in buildings is the most significant contributor in CEB [64]. Other uses include: predicting air temperature, heat flux and humidity [65]; anthropogenic heat release trends [66] and quantification of artificial heat release by the air conditioners [67].

3.2.4 FACTORS THAT INFLUENCE THE URBAN MICROCLIMATE

In this section will be defined the most important factors that can impact urban microclimate and have a strong influence over the urban heat island formation. There is an extensive amount of study that show the relation between UHI intensity and physical parameters that can be controlled by urban planners like urban morphology, urban surfaces, building materials and green areas [68-72].

Urban Geometry

The city's microclimate is significantly affected by the geometric form of the urban canopy layer and the variation between open and closed spaces. Urban geometry is often characterized by the urban street canyon where the street is flanked by buildings on both sides. Urban street canyons can affect temperature, wind speed and wind direction and subsequently the air quality within the canyon. Urban street canyon can be classified by the H/W ration and sky view factor. Orientation is also one of the key elements in the urban geometry and influences the wind speed, shading and sunlight received by each building which can condition the energy storage flux of a building. The most representative geometrical indicator about a street canyon is the ratio of the canyon height (H) to canyon width (W). The higher the H/W ratio, the smaller the area of visible sky which reduces the dissipation of long-wave radiation and, therefore, lowering the air-cooling in urban areas leading to a positive thermal change [73].

Solar Radiation

Solar radiation is radiant energy emitted by the sun and received by the earth surface in form of electromagnetic radiation. It is measured in the power per unit area (W/m^2). The sun emits shortwave radiation because it is extremely hot and has a lot of energy to give off. Once in the Earth's atmosphere, clouds and the surface absorb the solar energy and dived the shortwave radiation into direct, diffused and reflected radiation (Figure 12).

Direct radiation is also called "beam radiation" or "direct beam radiation". It is used to describe solar radiation traveling on a straight line from the sun down to the surface of the earth. Diffused radiation, on the other hand, describes the sunlight that has been scattered clouds or gases in the atmosphere but that has still made it down to the surface of the earth. Reflected radiation is radiation reflected from the ground.

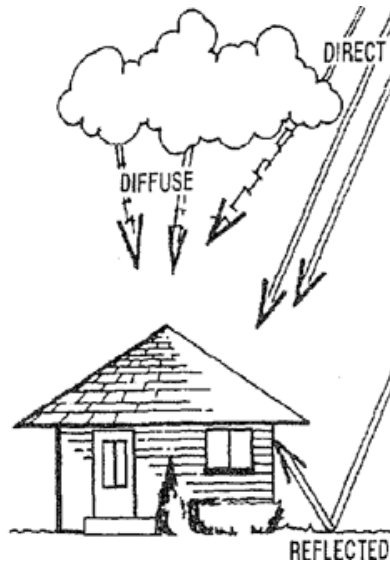


Figure 12. Three types of solar radiation: direct, diffuse and reflected [74].

After the ground heat, up it re-emits energy as longwave radiation in the form of infrared rays. Both the reflection of short-wave radiation and the emission of long-wave radiation have the potential to interact with and be absorbed by another surface, increasing its sensible heat. The increase in both the number of emitting surfaces and the amount of radiation emitted by each within a confined space can alter the net radiation of the whole urban environment tending to make the radiation field higher than that of a rural environment [75]. Measurements for solar radiation are higher on a clear, sunny day and usually low on cloudy days. During night-time or when there are heavy clouds solar radiation is measured at zero.

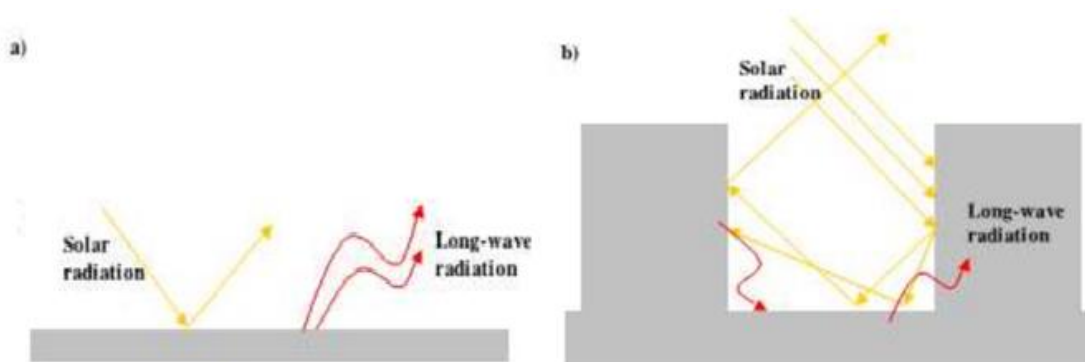


Figure 13. Radiation reflected and emitted from: a) a surface in an open environment, b) surface within urban canyon [75].

Airflow

Another one of the main climate factors that can influence the city's microclimate is the wind velocity. The 'surface roughness' of the city modifies the airflows passing through and when an air mass encounters a building, it is forced around, causing a series of whirlpool flows, due to the unsteady separation of the flow from the buildings. This can reduce wind velocity causing low air renewal when the wind velocity is between 0-5 m and its related to higher temperatures. Wind velocity above 5 m/s like a strong breeze is related to complete ventilation of a space but it starts getting uncomfortable at a speed of about 10 m/s, and possibly dangerous at a speed of around 20 m/s. Figure 14 shows the difference in air movement between straight and parallel (a) and narrow and winding (b) streets [76]. Ventilation paths are important to improve and maintain the thermal comfort level of an urban neighbourhood.

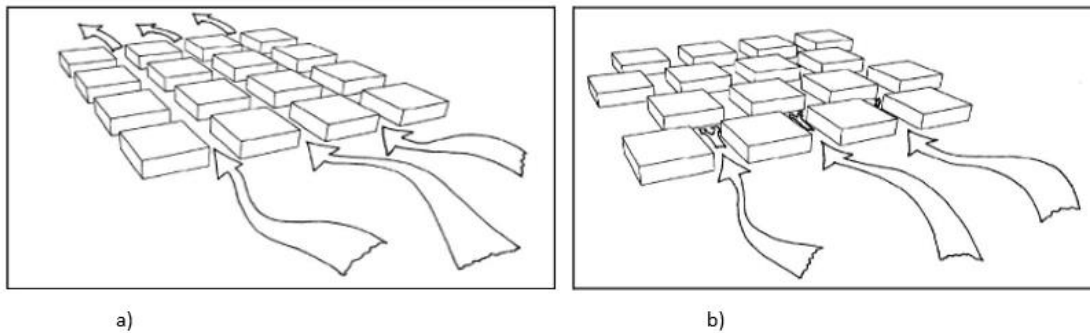


Figure 14. Airflow within a city: a) Straight and parallel streets improve airflow. b) Narrow and winding streets make airflow slow [76].

Air Pollution

The consumption of energy in a city and the metabolic exchange can result in air pollution. Elements emitted through evapotranspiration or by human activity can form a condensed layer of gases above the urban area that is referred as air pollution. It can absorb some of the upward direct thermal radiation from the surface and re-emitted back down words to warm the ambient air. Airborne pollutants not only cause higher heat island temperature but also alter the vertical temperature structure in a way that delays dispersion [77].

Building Materials

Emissivity

Emissivity is the capacity of materials to emit thermal radiation and is defined as the ratio of energy radiated from a material surface to that radiated from a perfect emitter (black body) at the same temperature and wavelength and under the same conditions. For any wavelength and temperature, the quantity of thermal radiation released depends on the emissivity of the object's surface. It is a dimensionless and varies between 0 (for a perfect reflector) and 1 (for a perfect emitter). It depends not only on the material but also on the nature of the surface. For example, a clean and polished metal surface will have a low emissivity, whereas a roughened and rusty metal surface will have a high emissivity. Knowledge of surface emissivity is important both for accurate non-contact temperature measurement and for heat transfer calculations.

Albedo/Reflectance

Albedo is the capability of a surface to reflect portion of the received sunlight radiation depending on the colour of the material. It has no dimensions and it is measured on a scale from 0 (corresponding to a black body that absorbs all incident radiation) to 1 (corresponding to a body that reflects all

incident radiation). Surface albedo is defined as the proportion of irradiance reflected to the irradiance received by a surface. This definition applies both for uniform surface and heterogeneous, complex ones. On average urban albedos are in the range between 0.10 and 0.20 but in some cities these values can be exceeded. Figure 15 illustrates the relation between surface temperature and albedo by hypothetical approximations of a white coloured city comparing it to an average city [78].

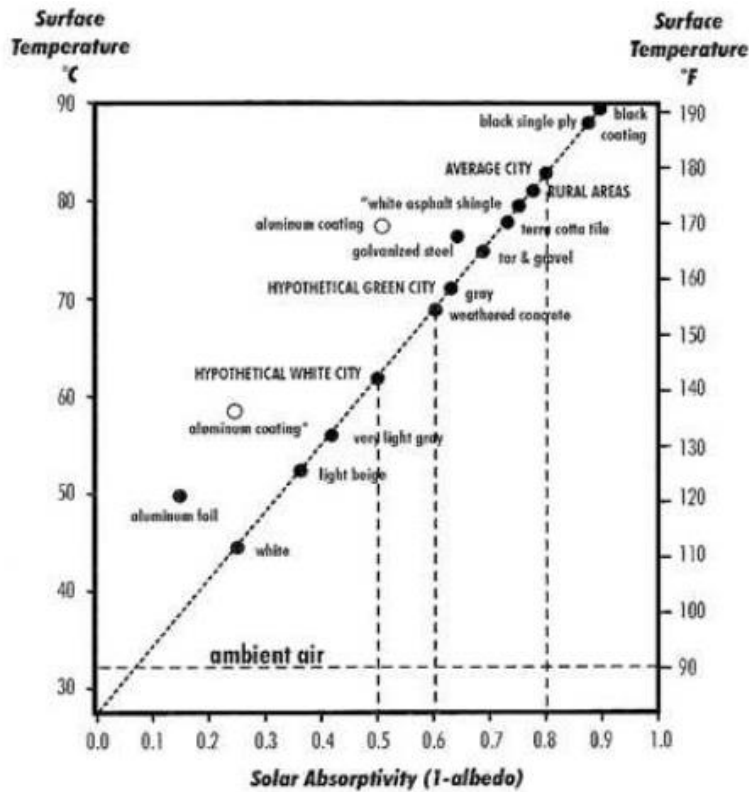


Figure 15. Albedo and surface temperature for different surface materials and colours [14].

Anthropogenic Heat

Anthropogenic heat refers to the heat released by human activity and is often denoted as QF. Metabolic heat (body heat) is negligible, but the heat released from vehicles, central heating (alternatively, in some warmer areas, from air conditioning systems) and industrial activities is substantial. All of these inject heat into the canopy layer and the upper boundary layer. Some large, densely packed cities in colder areas can release more heat from human activity than the urban area receives in its net input from the sun. Can be estimated from energy balance measurements [58] and inventory of energy consumption [79]. It was reported that anthropogenic heat release has greater potential for modifying the daytime thermal environment and wider buildings are better than small tall pencil buildings [80].

3.3 Outdoor Thermal Comfort

Since early 1960 wide range of studies for thermal comfort in different climatic zone resulting in different approaches and definitions, but all is revolving around the energy balance between the human body and an environment [81]. The definition given by the international Standard ISO 7730 is one of the key references for thermal comfort studies. It states that thermal comfort is “condition of mind which expresses satisfaction with the thermal environment” [82].

As mentioned before, big cities are more susceptible to extreme weather conditions due to climate changes. More comfortable an outdoor space is more used by pedestrians which can reduce use of car and can lead to more sustainable urban environment and can be a good indicator for economic and social advantage. Making the open urban space more attractive to pedestrian is an important goal in urban planning and design [83].

There are extensive and wide-ranging studies for indoor climates, but matters are more complicated in naturally ventilated and outdoor spaces. Comfort within these environments involves different conditions and issues not encountered in studies performed on indoor comfort [84]. Thermal sensation is an objective response to a specific location as a function of environmental parameters and is the subjective response that includes psychological factors. It is harder to predict as it varies from person to person [75].

Outdoor spaces are essential for a sustainable urban environment. Outdoor planning is complex and includes interaction between climatic behaviour and build environment. Several studies in the last decade focused on outdoor thermal comfort as a complex and subjective parameter to quantify [84-89]. To predict a comfort for urban environment there are two main components that must be considered: simulation of urban surface temperature and consequent the mean radiant temperature calculation. Knowing the factors that influence thermal comfort can be translated to knowledge of how to model, create and manage it and can be beneficial to researchers and planning practitioners [90].

3.3.1 FACTORS THAT INFLUENCE THERMAL COMFORT

When defining thermal comfort two main group of factors must be taken into consideration, one that has all the objective parameters that can be measured and quantified like environmental and personal and another that has the preceptive or subjective parameters which are individual from person to person. Figure 16 shows the most important factors needed for the precise estimation of the thermal comfort. They can be divided into three main groups: environmental, personal and perception factors.

Environmental Factors

- Air Temperature*
- Wind Velocity*
- Solar Radiation*
- Relative Humidity*
- Mean Radiant Temperature*

Personal Factors

- Metabolism*
- Clothing*
- Activity*

Perception Factors

- Adaptation*
- Tolerance*
- Preference*
- Expectations*

Figure 16. Factors that affect thermal sensation. Adapted from [75].

3.3.1.1 Environmental Factors

The five main environmental factors include the air temperature, mean radiant temperature, air velocity, and relative humidity. have influence over the thermal comfort indoors and outdoors. The effect of these parameter on an urban space's microclimate is usually estimated at the average height of a standing adults centre of gravity which is typically around the height of 1.1 meters above the ground [91]. Help on acquiring the climatic parameters is available from ISO 7726 [92].

Air Temperature

Air temperature (T_a) is defined as the dry-bulb temperature of the air surrounding the occupant for determining heat transfer by convection between the skin and the environment [93]. Temperature is usually measured in degrees Celsius ($^{\circ}\text{C}$), kelvins (K), or degrees Fahrenheit ($^{\circ}\text{F}$). Most people will feel comfortable at room temperature around 22 ± 2 $^{\circ}\text{C}$ but it can vary greatly in outdoor open spaces with the change in humidity and wind velocity. Thermal comfort depends directly on the air temperature. It is the main factor that can define directly thermal sensation although the other environmental factors only can have amplified the sensation effect of air temperature.

Wind Speed

Wind speed (U) is the rate of air movement at a point, without regard to direction and it is the average speed of the air to which the body is exposed, with respect to location and time [93]. It is taken into consideration when estimating heat transfer between the body and the environment and it is usually measured in (m/s). When the wind speed is high, particularly in cases when the mean radiant temperature is high, and T_a is low a greater heat loss can be observed [82]. For the same values, the wind speed can be considered desirable or undesirable: for example in cold climates "wind will almost always decrease outdoor comfort conditions, whereas the opposite is the case of hot climates" [94]. Changing wind speed from 0m/s to 5m/s greatly reduces thermal comfort. The outdoor thermal environment can affect the indoor thermal environment and that the change in wind speed has a significant impact on the thermal comfort levels [95]. Improvements in the outdoor thermal environment could lead to enhancing the indoor thermal environment, relieving the stress of indoor thermal control [96]. Wind speed exerts a strong influence on the thermal comfort indices. Even a small increase in wind speed leads to a significant decrease in the thermal sensation. Additionally, as mentions above the effects on the surrounding built environment are more pronounced with increasing wind speed.

Direct Solar Radiation

Definition of this parameter is given in the section above. Direct solar radiation is the radiant flux from direct solar radiation received by the surface has possibly the most important effect on its microclimate [97] and can result in the highest discomfort values [85].

Values of 100 W/m² correspond to low insolation (e.g. overcast or late sunny afternoon), 400 W/m² to average insolation (e.g. partly cloudy or winter clear day), and 800 W/m² to high insolation (e.g. summer clear sky conditions). As mention before global solar radiation is divided into direct and diffused which depends on the cloudiness condition of the sky, so logical clearer the sky - higher values of K_{\downarrow} .

Relative Humidity

Relative Humidity (RH) can be defined as the amount of water vapour present in air expressed as a percentage of the amount needed for saturation at the same temperature and depends on temperature and the pressure of the environment. Usually is expressed as a percentage (%) – the higher the value indicates that the air–water mixture is more humid. At 100% relative humidity, the air is saturated and is at its dewpoint.

The human body is sensitive to high humidity because it uses evaporative cooling, enabled by perspiration, as the key mechanism to release unwanted heat. Evaporation of perspiration from the skin occurs slowly under humid conditions than under arid. When the air temperature remains constant, the body placed under greater discomfort at high humidity than at lower humidity.

Depending on the temperature humans can be comfortable in with range of humidity - from 30% to 70, but ideally between 50% and 60% [94]. Very low humidity can be damaging for the human health creating discomfort, respiratory problems, and even aggravate allergies in some cases.

Mean Radiant Temperature

The mean radiant temperature T_{MRT} is defined as the “uniform temperature of an imaginary enclosure in which radiant heat transfer from the human body equals the radiant heat transfer in the actual non-uniform enclosure”[98]. Is rather difficult to determine outdoors with accuracy and is required for the estimation of the thermal comfort. The exact workflow of determining T_{MRT} will be discussed further in paragraph on its own.

3.3.1.2 Personal Factors

Those are factors that are different from person to person either by choice like clothing and activity rate or involuntarily – metabolic rate, age and health conditions. They can affect the thermal sensation and can be quantified.

Metabolic Heat Production

Metabolic Heat Production or metabolic rate (M) is the amount of energy produced by the human body (converting food into heat by inhalation of oxygen) per unit time and expressed in watt per square meter of body surface or often in Met units (1 Met = 58 W/m²) [99]. ISO 8996 standard, “Determination of metabolic heat production,” provides guidance for metabolic rate values for standard physical activities [100]. Metabolic rate can differ from person to person for the same type of activity which can influence the body’s ‘perception’ of the surrounding thermal environment. Higher core body temperatures increase metabolism while cooler core body temperatures lower the metabolic rates. More demanding physical activities like running can cause a rise in body temperature and an increased metabolism during physical activity. In fact, muscle has a higher metabolic rate than body fat, so the more muscle mass you gain by exercising, the higher your metabolism will be, even during periods of rest [101].

Clothing

The clothing can be described as lyres of thermal insulation that can help to adjust the body to the present thermal conditions. It prevents unwanted heat losses or heat gains depending on clothing thickness, colouring and permeability to air [97]. Difference in worn clothing can be due to individual preferences like style, gender etc. and thermal reasons, linked to the weather conditions. Clothing transmits convective, as well as radiative and evaporative heat exchange [102]. ISO 9920 standard provides means for estimating the thermal characteristics (resistance to dry heat loss and evaporative

heat loss) based on tables with insulation values for a clothing ensemble based on values for known garments, ensembles and textiles [103].

3.3.1.3 Perceptions Factors

The perception or subjective factors include all the things that cannot be measured and that are based mainly on personal preference. Some people prefer hotter climates other feel better in colder depending on perception factors such as capacity of adaptation, tolerance to heat, preference and expectation. Tolerance of hot or cold climate conditions is define by personal limit beyond which the human body experience thermal stress.

Three different categories for adaptation can be identified: physical, physiological and psychological.

- Physical adaptation can be expressed in terms of the changes a person makes, to adjust oneself to the environment for example to decide on level of clothing, or change in the environment to improve their comfort conditions like opening a window, closing the curtain etc.
- Physiological adaptation suggests changes in the physiological responses resulting from repeated exposure to the same climate conditions, leading to a gradually decreased in stress levels from such exposure [104].
- Psychological adaptation can be explained more as a personal choice, memory and expectations for satisfaction with given thermal environment. Expectation can be expressed if person is content with the weather for given station of the year such as “is it too cold this summer” or “ is it too hot in the winter”, this however can change day to day, so it influences thermal sensation in short-term [105].

3.3.2 OUTDOOR THERMAL COMFORT CALCULATION/INDICES

Biometeorological indices- describing human thermal comfort level by relating it to local microclimate condition and thermal sensation. These method are call ed steady-state assessment methods that assume that people exposed to local microclimate can reach over time thermal equilibrium allowing the use of the energy balance equation governing thermoregulation almost all inside of this category have been summed in [106].

3.3.2.1 PMV

Predicted Mean Vote (PMV) is parameter designed by [107] is one of the most used to predict thermal response of large group of people. PMV has been included in the International Organization for Standardization (ISO) standard. It takes into account personal and environmental and the resulting values are organized according to 7-step ASHRAE thermal sensation scale that ranges from -3 to 3 as shown of Figure 17.

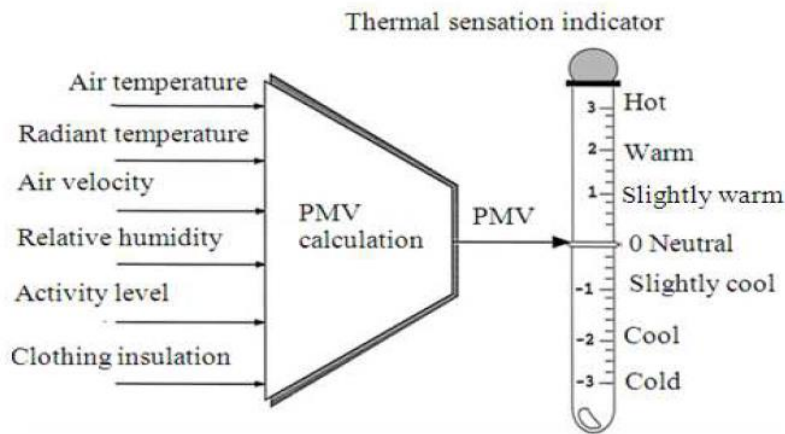


Figure 17. PMV and Thermal Sensation [108].

It was initially developed as an indoor thermal comfort index but has been adopted in outdoor thermal comfort studies in which a large population of people is being surveyed [109-111]. PMV is calculated using the equation described in ISO 7730 [82].

3.3.2.2 Physiological Equivalent Temperature (PET)

Like PMV gives an estimation of a thermal component of a given environment. PET index uses a heat balance model of the human body based on the Munich Energy-balance Model for Individuals (MEMI), which models the thermal conditions of the human body in a physiologically relevant way [112]. PET is defined by using the concept of equivalent temperature: the air temperature at which, in a typical indoor setting (without wind and solar radiation), the heat budget of the human body is balanced with the same core and skin temperature as under the complex outdoor conditions to be assessed [113]. There are various studies of PET application for both the indoor and outdoor environment study. Table 2. shows some of the variations of the PET values depending on the season.

Table 2. Variation of PET in different scenarios [113].

| Scenario | T _a (°C) | T _{mrt} (°C) | V (m/s) | VP (hPa) | PET (°C) |
|---------------|---------------------|-----------------------|---------|----------|----------|
| Typical room | 21 | 21 | 0.1 | 12 | 21 |
| Winter, sunny | -5 | 40 | 0.5 | 2 | 10 |
| Winter, shade | -5 | -5 | 5.0 | 2 | -13 |
| Summer, sunny | 30 | 60 | 1.0 | 21 | 43 |
| Summer, shade | 30 | 30 | 1.0 | 21 | 29 |

The MEMI model is based on the energy balance equation for the human body show in Equation 3:

$$\text{Equation 3. Energy balance for the human body.}$$

$$M + W + R + C + E_D + E_{Re} + E_{sw} + S = 0 \quad (3)$$

Where, M is the metabolic rate, W the physical work output, R the net radiation of the body, C the convective heat flow, E_D the latent heat flow to evaporate water diffusing through the skin (imperceptible perspiration), E_{Re} the sum of heat flows for heating and humidifying the inspired air, E_{Sw} the heat flow due to evaporation of sweat, and S the storage heat flow for heating or cooling the body mass. Each individual component in the equation has positive signs if they result in energy gain for the body and negative signs when there is energy loss (M is always positive; W , E_D and E_{Sw} are always negative). The unit of all heat flows is in Watt [113]. Each of the individual heat flows in Equation 3 depend on the following meteorological parameters [113, 114] as follows:

- Air temperature: C , E_{Re}
- Air humidity: E_D , E_{Re} , E_{Sw}
- Wind velocity: C , E_{Sw}
- Mean radiant temperature: R

Thermo-physiological parameters are required in addition:

- Heat resistance of clothing (clo units)
- Activity of humans (in Watt)

As demonstrated above mean radiant temperature plays a great role in thermal comfort modelling. In the next paragraph, a methodology for estimating T_{MRT} in urban environment will be summarized.

3.4 Mean Radiant Temperature

3.4.1 DEFINITION:

Mean Radiant Temperature (T_{MRT}) is one of the most significant meteorological factors controlling human energy balance and thermal comfort. It is a result of all short and longwave radiation fluxes (both direct and reflected), to which the human body is exposed [115], as demonstrated in Figure 18.

According to ASHRAE (2010), T_{MRT} is “the uniform temperature of an imaginary enclosure in which the radiant heat transfer from the human body equals the radiant heat transfer in the actual non-uniform enclosure” [93].

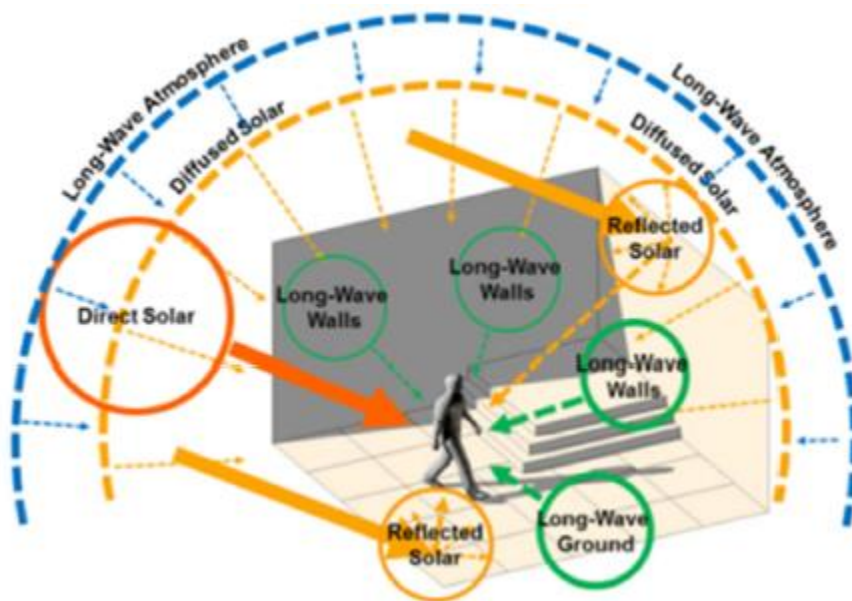


Figure 18. Components of T_{MRT} in urban environment [116].

The influence of T_{MRT} over the thermal comfort has been a subject of various studies both for indoor and outdoor environment. T_{MRT} can differ depending on time of the day and the station of the year and between outdoors and indoor conditions. In hot summer day without shade and clouds, T_{MRT} can be more than 30°C higher than air temperature. During night time radiation exchange is exclusively due to longwave radiation. In urban environments, the radiation energy received by a standing man is resulting primarily from the longwave component and less than 30% comes from solar radiation during daytime [117].

3.4.2 CALCULATION OF T_{MRT}

In this work, the methodology follows one of the most complete researches regarding the subject [118]. It summarizes all the needed information that will be used in this work to estimate T_{MRT} .

In order to calculate the mean radiant temperature, there are three main components that must be considered: surface temperature, view factors and thermal properties of the materials composing the built environment. The body posture and orientation relative to the geometry of the open space is also important because the T_{MRT} for a standing person is different as for a seated one. The clothing level of the human body is also important because it can reduce the incoming radiation as shown in Table 3.

Table 3. Absorption coefficient for short and longwave radiation [118].

| Absorption coefficient | skin | clothing | Standard value |
|--|-----------|----------|----------------|
| for long wave radiation (a _l) | 0.99 | 0.95 | 0.97 |
| for short wave radiation (a _k) | 0.55-0.85 | 0.4-0.9 | 0.7 |

Fanger [107] provides the most complete methodology for numerical determination to the mean radiant temperature by dividing the environment into n isothermal surfaces with proper surface temperature (T_s), emissivity ϵ_i , and F_i as view factors from the surface to its surroundings ($i=1, \dots, n$). According to the Stefan-Boltzmann's law Equation 4, each of these n isothermal surfaces (ground, surroundings, and also the sky) emits E_i [W/m²] longwave radiation:

Equation 4. Stefan-Boltzmann's law for long wave radiation.

$$E_i = \epsilon_i * \sigma * T_i^4 \quad (4)$$

Where σ is the Stefan-Boltzmann constant ($\sigma=5.67*10^{-8}$ W/m²K⁴).

The T_{MRT} equation can be expressed through radiation flux density (S_{STR}) which consist of two main components as shown in Equation 5: shortwave (direct (I), diffused(D) and reflected(R)) and longwave (E) (emitted from the environment). Figure 19 demonstrated all the important components that play part in the equation. In yellow is represented the direct sun radiation affected by the absorption coefficient for shortwave radiation a_k and f_p is the surface projection factor which describes the orientation of the human body. The orange component represents the diffused and reflected components multiplied by a_k and the view factors (F_i) and in red is the longwave component multiplied by F_i and coefficient for longwave radiation a_l .

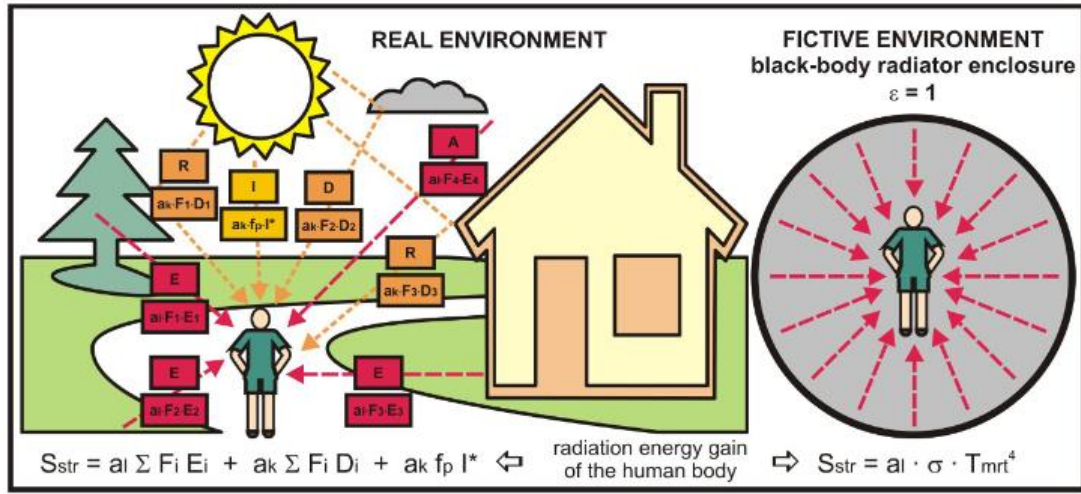


Figure 19. Illustration supporting the understanding of the definition and calculation of the T_{MRT} [118].

Equation 5. Radiation flux density.

$$S_{STR} = (a_k * (I^* * f_p + \sum_{i=1}^n F_i * D_i))_{shortwave} + (a_l * \sum_{i=1}^n F_i * E_i)_{longwave} \quad (5)$$

Mean radiant energy gain of a human body located in a real environment is equal to that in the fictive environment (Figure 19) which is a black-body radiation ($\epsilon=1$) in an isothermal enclosure with T_{MRT} [K] temperature. It emits $\sigma * T_{MRT}^4$ longwave radiant energy from which human body received part according to its absorption coefficient ($a_l = \epsilon_p$).

Equation 6. Relation between radiation flux density and mean radiant temperature.

$$S_{STR} = a_l * \sigma * T_{MRT}^4 = \epsilon_p * \sigma * T_{MRT}^4 \quad (6)$$

Solving the equation for T_{MRT} :

Equation 7. Mean radiant temperature.

$$T_{MRT} = \sqrt[4]{\frac{S_{STR}}{\epsilon_p * \sigma}} \quad (7)$$

For the complete clarification of the mean radiant temperature calculation, the surface temperature and the view factor will be needed. The methods used in this work will be described in the paragraphs below.

3.4.2.1 Surface Temperature

The methodology used in this work is taken from [116]. Figure 20 illustrates all the component needed to make the estimation. As shown T_s is the result of heat balance equation for radiation, convection conduction and thermal massing effects.

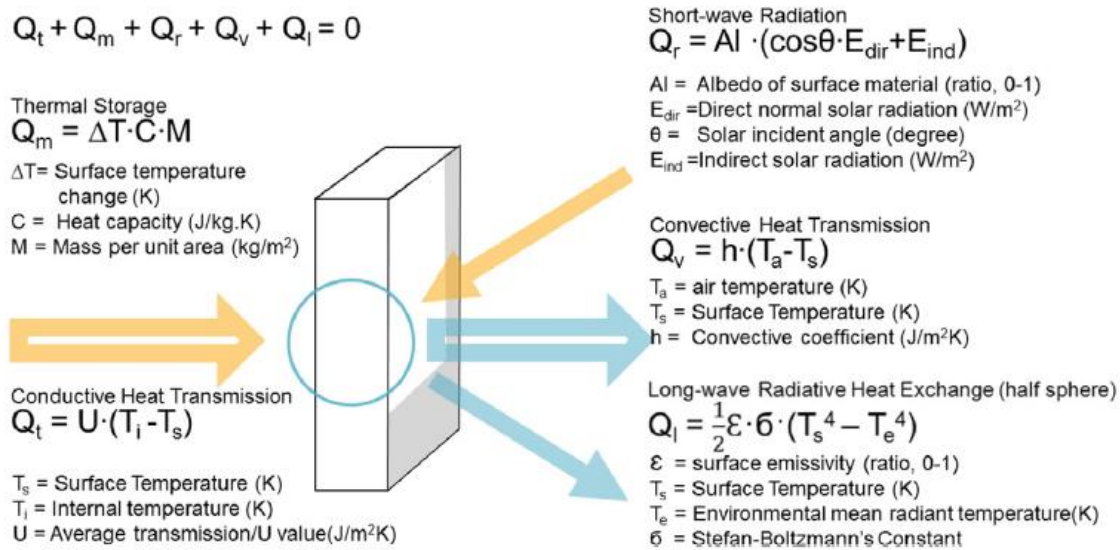


Figure 20. Heat transfer equation for urban surfaces [116].

When surface or plane receives solar radiation, it heats up to a specific temperature depending on the material qualities. Heat transfer equation is used to estimate the urban surface temperature. T_s is a function of solar radiation, surface albedo, emissivity, specific heat capacity, material density, average U-values for external walls and the ground, building internal temperature and soil temperature. Isothermal conditions are applied for each surface which mean T_s remains constant during the time frame for each surface where is measured.

For the initial interval of the study (at sunrise) the initial value of T_s is set equal to 3.4K below the ambient temperature [116].

3.4.2.2 View Factors

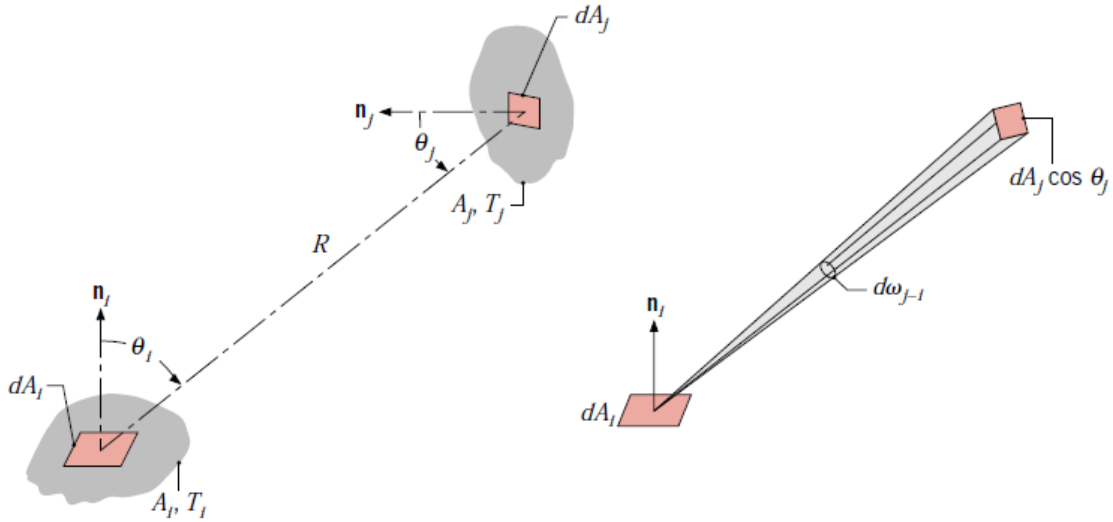
Surface to Surface

As referred before emissivity is a property of a surface A_i of a material to give up stored heat in form of radiant energy in all hemispherical surroundings according to Stefan-Boltzmann law Equation 8:

Equation 8. Stefan- Boltzmann's law for multiple surfaces.

$$E_i = \epsilon * \sigma * T_i^4 * A_i \quad (8)$$

Only a fraction of this energy will reach a second arbitrary oriented surface A_j . This fraction (F_{i-j}) is referred as the view factor which depends only on the geometrical orientation of two participating surfaces [119].



It can be expressed as Equation 9.

Equation 9. View Factor between different surfaces.

$$F_{ij} = \frac{1}{A_i} \int_{A_i}^0 \int_{A_j}^0 \frac{\cos\theta_i * \cos\theta_j}{\pi R^2} dA_j dA_i \quad (9)$$

where

dA_i and dA_j are differential elements within the two arbitrary surfaces with direct view one to another.

R is the length of the line connecting the centre of the surface that forms polar angles θ_i and θ_j respectively with the surface normal n_i and n_j .

All the described values vary with the position of the elemental areas on A_i and A_j .

In an enclosed environment the sum of all view factors from a point to a surface is equal to 1 given the fact that this represents the fraction of energy received by all surroundings.

Equation 10. Summary of all view factors to a plane.

$$\sum_{j=1}^N F_{ij} = 1 \quad (10)$$

In a real outdoor environment, this sum is lesser than 1 since there is no closed box and some of the energy is radiated back to the atmosphere.

To estimate the surface temperature and mean radiant temperature the view factors are needed to be taken into account.

Ray tracing is one of the most used methods to measure the value of the view factor. It has been used to solve diverse problems from generating images with a high degree of photorealism to complex radiative heat transfer modelling. Figure 21 illustrates simplification that can be used to estimate the view factor in outdoor opens space considering only the six main directions.

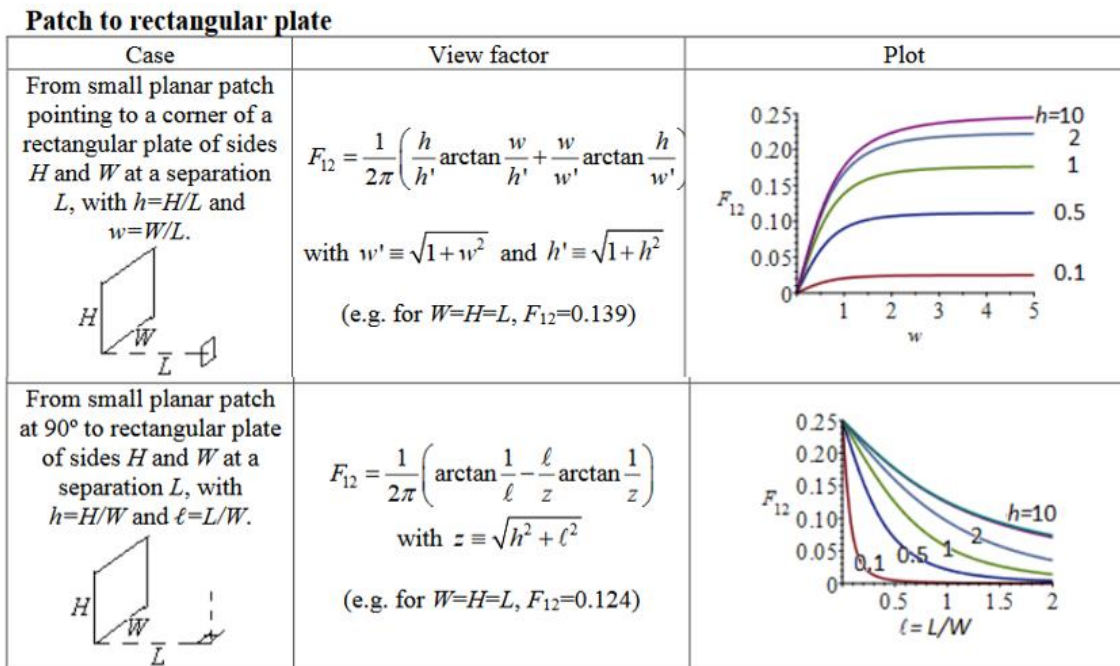


Figure 21. View Factors from patch to rectangular plate [120].

When the view factors are intended for T_{MRT} regarding the human body position they are estimated as 1.5m above ground which is standard height for thermal comfort estimation.

Sky View Factor

The sky view factor (SVF) is a value that represents the ratio between the area of open space and that from the entire hemispheric radiating environment (Figure 22) and is calculated as the fraction of sky visible from the ground up. SVF is a dimensionless value that ranges from 0 to 1. An SVF of 1 means that the sky is completely visible, for example, in a flat terrain. When a location has buildings and trees, it will cause the SVF to decrease proportionally. The reduction of the visibility of the sky leads to a decrease of long-wave radiation loss and increase in heat sensation.

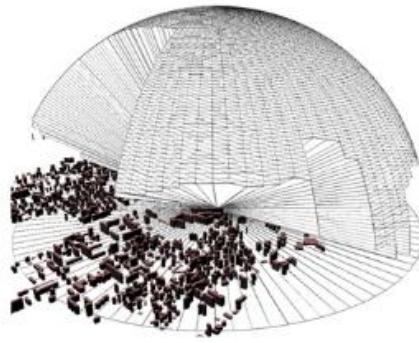


Figure 22. Sky View Factor is the ratio between the area of open-space and the total area of the hemisphere.
Source:[121]

In this work, the calculation of the SVF is following the methodology described in [122].

The technique used is similar to the method of integral calculus; it is its adaptation for a hemisphere. The border of the visible sky is defined by polygon $g(x)$ is, under the polygon the sky is not visible because of the building obstruction. After dividing the hemisphere equally into n equal slices by rotation angle(α) ‘rectangles are created with heights equal to the $g(x)$ values in the middle points of the intervals. The SVF value determined by $g(x)$ polygon is estimated with the sum of the SVF values of these rectangles on the hemisphere as shown in Figure 25 [122].

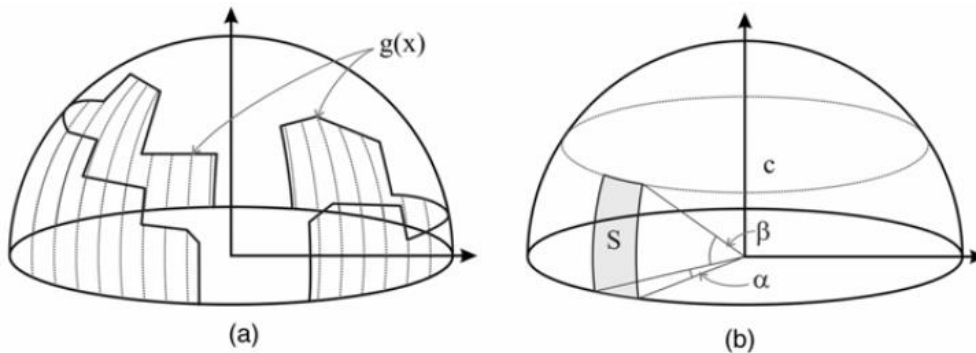


Figure 23. (a) Polygon $g(x)$ as a border of the visible sky and dividing the hemisphere under $g(x)$ equally into slices by angle α (heights are equal to the $g(x)$ values in the middle points of the intervals) and (b) a slice of a ‘width’ of α (S) of a basin with an elevation angle β [122].

$$SVF = 1 - \sum_{i=1}^n \cos^2 \beta_i = \sum_{i=1}^n \sin^2 \beta_i \quad (11)$$

The accuracy of the method depends on the magnitude of the selected α . Smaller α angle (finer division) means better estimation of SVF but longer computation time.

3.4.3 METHODS FOR CALCULATING T_{MRT}

There are two most popular method for estimating the contribution to the build surroundings to the T_{MRT} values.

Firs is by using field measurement or globe thermometer: by knowing globe temperature, air temperature and air velocity T_{MRT} can be calculated using empirically derived equation [123]. The second method for estimation is by using software to make complex calculations involving radiant fluxes and the angle factors of surrounding surface. Over the years several models have been developed to estimate T_{MRT} values, the most popular one will be discussed in the paragraph below.

3.4.3.1 By integral radiation measurements

The simplest method of obtaining T_{MRT} with integral radiation instruments is based on the utilization of a globe thermometer. The standard globe thermometer is a flat black-painted hollow copper sphere (diameter is 150 mm, thickness is 0.4 mm) with a thermometer bulb at the centre (Figure 24).



Figure 24. Standard Globe Thermometer

It was developed for indoor application where the mean radian heat flux is relatively constant compared to open spaces but later has been adapted to outdoor measurements.

3.4.3.2 By modelling the radiation emolument

To avoid in-site measurements few methods have been developed in recent years to estimate T_{MRT} in theurban environment. The most popular are RayMan, ENVI-met and SOLWEIG and CityComfort+. They calculate T_{MRT} by reasonable approximation but also have their limitations. The Figure 25 illustrates some of the existing programs and tool and shows the need for a new tool to calculate the mean radian temperature without the limitation given by the other programs.

| Rayman 1.2 | ENVI-met 3.1 | SOLWEIG 2.2 | CityComfort+ | Propose tool |
|--|--|--|---|--|
| easy to use calculates Tmrt at one point at a time significant errors when solar angle is low can not account for reflected short-waved radiation | can compute Tmrt on a continuous surface can not process vector-based geometries (building vegetation etc. must be manually transformed into pixels) computationally demanding | fast and user friendly allows DEM data exchange (pixel geometry format compatible with GIS) no 3D geometry detail overly simplified-method is limited to dense urban space (SVF < 0.65) | simulation of spatial variation of Tmrt in dense urban environment urban surface categories as sunlit or shaded wall and ground with no spatial resolution lack in variations that urban surfaces exhibit in reality through change in shortwave and longwave radiation values in an open space | work in 3D BIM environment can calculate Tmrt from multiple points at a time calculates surface temperature calculate SVF works with calculated angles register sunlit and shadow surface and the time interval change counts the heat transfer from one time interval to another. |

Figure 25. Proposed tool vs different existing methods for estimating/simulating T_{MRT} [116, 124].

3.5 Sustainability, Adaptation and Mitigation

In current construction practice, the local microclimate does not have a very significant role. Building position for the site is more associated with the visual relationship with other buildings, views than microclimatic conditions. Open spaces are planned more by preference, type of use and activities and less consideration for microclimate [125]. Designing and planning with green areas is most broadly used mitigation measure that could achieve huge energy saving through temperature reduction [126]. Adaptation measures like “blue and green infrastructure” translating to more evaporation areas (i.e., water and vegetation) which, by evapotranspiration, improve thermal comfort by reducing air temperature and increasing humidity. can further decrease turbulent and convective heat transport and thus contribute to achieving a diminution of thermal discomfort. Providing more shaded ground and building surface can reduce the surface temperature. Shade can be provided by vegetation or building elements [127].

The effectiveness of individual adaptation measures depends on the kind (vegetation/ water / building parameters) and type (e.g., vegetation: grass/ park/ forest) of the adaptation measure, as well as on meteorological conditions. Vegetation areas achieve higher PET reductions than water surfaces due to a combination of evapotranspiration and shading and can reach their maximum PET reduction potential only with an adequate water supply. During the daytime can be observed a significant difference in thermal comfort levels of well-watered and non-irrigated vegetation [128].

Mitigation measures can be divided into three categories. First one is related to reducing anthropogenic heat release by designing more buildings with natural ventilation and switch off air conditioners. The second category is related to better roof design for example green roofs, roof spray cooling, reflective roofs etc and the third one includes all other design factors like humidification, increased albedo, photovoltaic canopies etc. [129]. It was demonstrated in a study that with proper building ventilation the energy demand could be reduced by 10% [130].

Knowing what to expect when building an environment it gives also the possibility to exercise control over the space to accommodate it to the required needs. By using prediction numerical model that can estimate the expected heat comfort with reasonable precision. The collision of those numerical models with the development of the 3D geometry analysis has given the planner a tool for estimating the damage before constructing and the possibility to see the weak and the strong point of the design considering all factors that a real environment has to offer.

4

CASE STUDY

4.1 Introduction

In this chapter will be presented the tool developed in for thermal comfort study. It will be explained why the tool is needed although there are some similar products on the market and how it is organized, and the methodology used for its operation. Each of the functions of the individual components will be explained in the paragraph below and detailed in its corresponding annex. For the validation of the tool, an urban area in Porto is selected and it will be categorized by surfaces and modelled in Revit.

For the location of the case study, the area around and above Metro Station Trindade was chosen. The motive for the selection was because it has two levels with different characteristics: lower level or Trindade Square that is made of granite (floor) and concrete (walls) and upper level near the elevator that is made mainly of green space and granite path. The figure below illustrated the developed simplified 3D model of the Metro Station and the square compared to the real-life scenario.

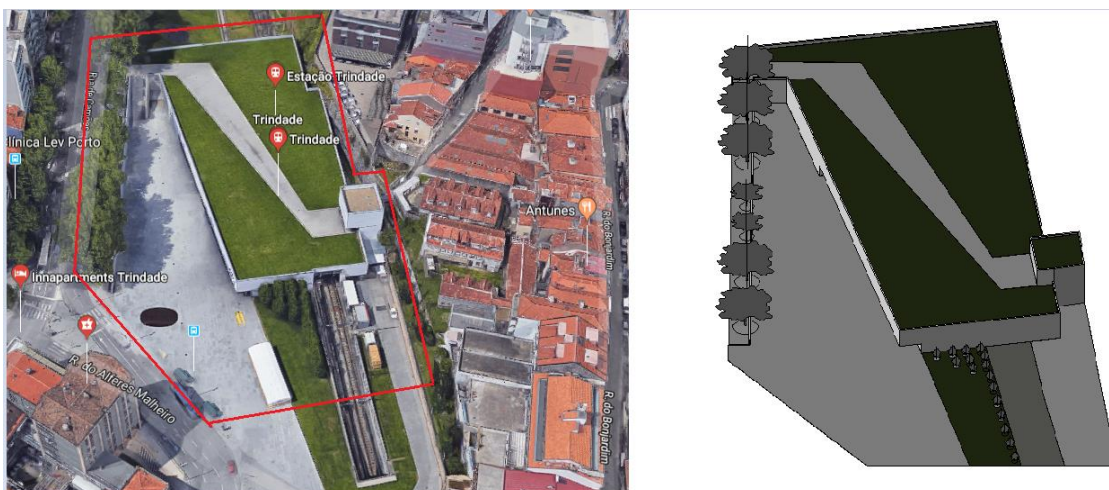


Figure 26. Metro Station Trindade: Real life scenario (Google Maps) vs. simplified 3D model

The Laboratory of Construction by providing the needed equipment for the validation of one of the components of this work and measurements were taken and compared with the result of the elaborated tool. Conclusions and results of the comparison between the estimation and the reality will be represented together with some hypothetical scenarios of how the urban environment will reach to the change in the material and colour.

4.2 Need for the tool

There is little to no integration between urban planning and build environment. Buildings are planned depending on their function and it is not of concern how they interact with the microclimate of the open public space. There are too many variables that need to be considered when designing the comfort of a public space but solving this problem can be the key to more sustainable environment. Each newly constructed building stores and reflects heat contributing to the temperature race in the urban environment and there is no tool or program that can see what effect this will have on the comfort level of the public space. GIS tools can only study a section of the urban life, but it cannot represent it as it is and their tools like EnviMet or Solweig used for estimating/calculating thermal comfort of an open space also lack in 3D representation, convenience and accuracy. There is a need for a tool that can be part of a CIM methodology by using BIM environment as a basis for the analysis. The software tool developed in this work had the objectives to:

- Create a connection between urban planning and build environment
- Study new dimensions for using BIM software – Comfort Study
- Register how different material influence the thermal environment
- See the surface temperature variation in the different alternative of an urban project
- Estimate basic parameters for Thermal Comfort study

This chapter will be divided into 3 main parts: first is the creation of the model by using Autodesk's Revit, second a Dynamo code will be introduced to provide the analytical part of the work and last different scenarios will be studied and compared.

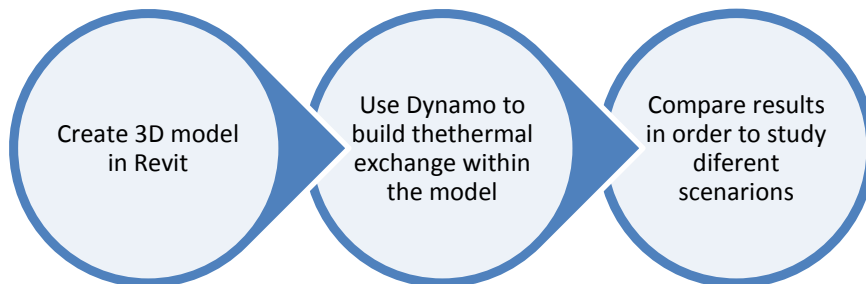


Figure 27. Workflow of the software tool.

Advantages of the tool:

- Use of BIM – accurate representation of surface/materials
- More variation in urban surfaces
- Solar Analyst accurate representation of the solar radiation from closes weather station
- Simplified ray-tracing using Dynamo
- Works in detailed 3D environment, it is possible to work in 4D (time interval included)
- Inbuild values inside Revit with the possibility to input more information
- The model can be made available through OpenBIM platform and shared with different users

4.3 Dynamo Methodology

The Dynamo model is divided into 4 main categories and other supplementary calculations. First data about Solar Irradiance is acquired by using Insight 360 Solara Analysis. Then supplementary data like air temperature and wind speed is added. For the calculation of surface temperature and mean radiant temperature view factors are needed and the is the second important component. The Sky View Factor and the View Factor between point/person position and Environment depend only on the geometry and it needs to be calculated only once – it is a constant for all time periods.

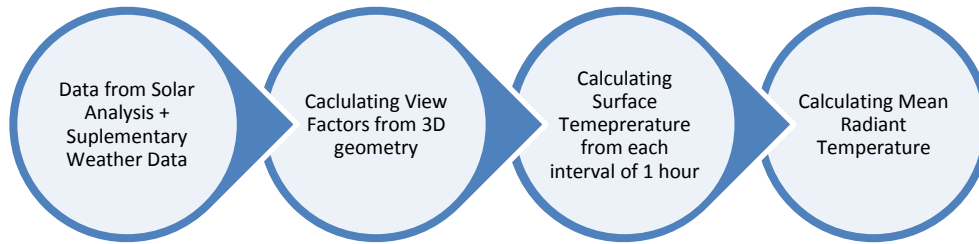


Figure 28. Dynamo methodology.

After this, the surface temperature is calculated for the given interval of time and from is mean radiant temperature incoming to standing person is calculated.

4.3.1 INSIGHT SOLAR ANALYSIS

Autodesk Insight is a powerful cloud-based analysis tool for maximizing BIM workflow by helping to improve energy and environmental performance throughout the building lifecycle. It allows integration of energy, lightning and solar analysis for optimizing building performance design. In this work, Insight Solar Analysis tool is used for obtaining the indecent solar radiation needed for calculation of surface temperature and mean radiant temperature and it is based on two primary components:

- **Direct radiation** (I_b) from the sun which is always measured perpendicular to the sun's rays
- **Diffuse radiation** that is both scattered by the clouds and atmosphere (I_d) and the ground in front of the surface (I_r). This is always measured on a horizontal surface.

From the total energy of the sun, up to one third can be lost (reflected into space), about 20% reaches the surface as diffuse radiation, and the rest reaches the surface as direct radiation [131].

Equation 11. Incident solar radiation in Revit.

$$Incident\ solar\ radiation = I_b * F_{shading} * cos\theta + I_d * F_{sky} + I_r \quad (12)$$

Where:

- I_b - direct beam radiation, measured perpendicular to the sun
- I_d - diffuse sky radiation, measured on horizontal plane
- I_r - radiation reflected from the ground

- $F_{shading}$ -factor (1 if a point is not shaded, 0 if a point is shaded, a percentage if measured on a surface)
- F_{sky} -visible sky factor (a percentage based on the shading mask)
- θ - angle of incidence between the sun and the face being analysed

For the tool to perform correctly first a Location must be provided (*Manage>Location*). It gives the option to choose the exact *Project Address* on the map and the nearest Weather Station. In this work the in the Validation paragraph the 2 closest weather stations will be compared by air temperature and the one closest to the measured temperature will be chosen.

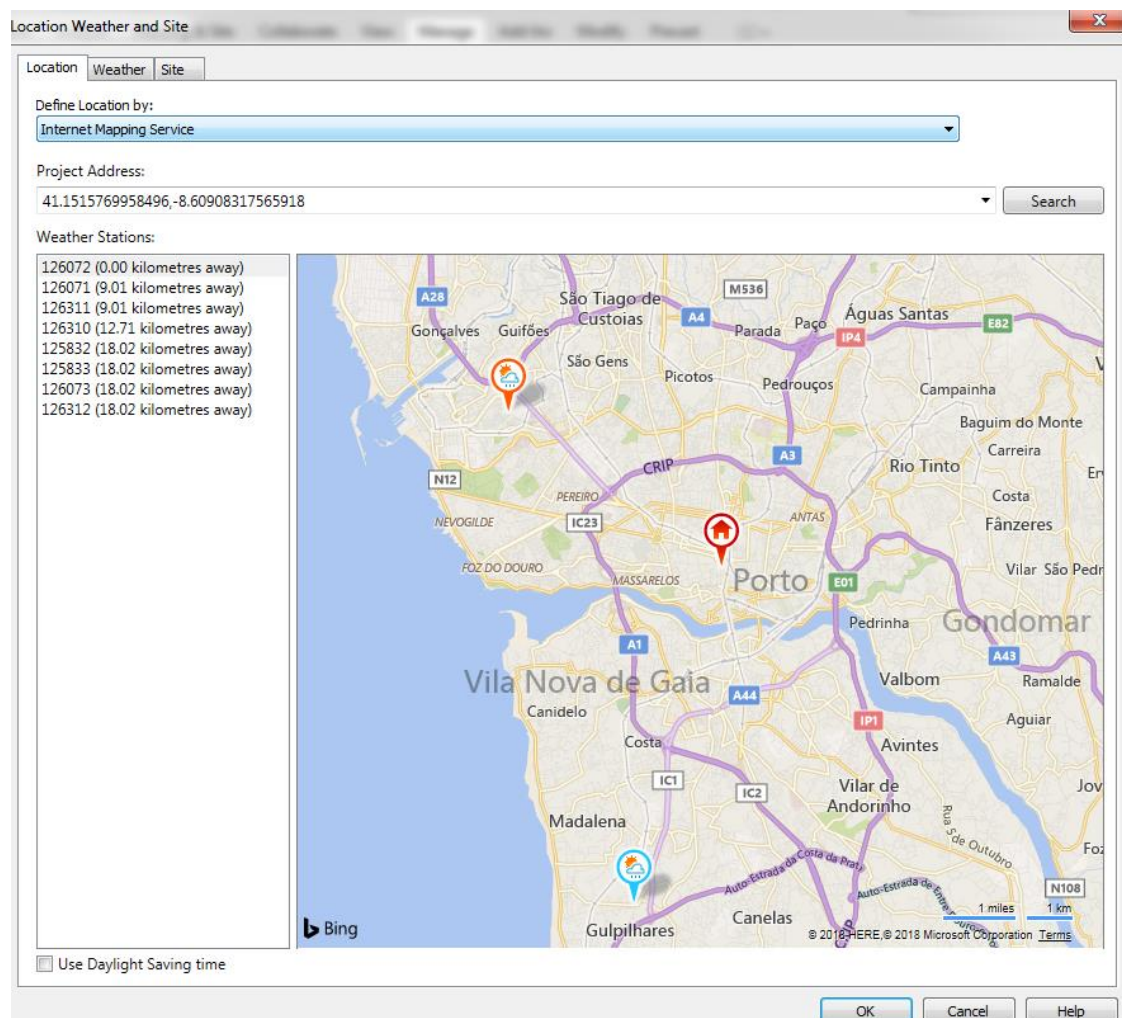


Figure 29. Location of the case study.

Then the sun setting must be adjusted for the desired interval of time by creating a desired time frame in *Manage>Additional Settings>Sun Settings*. For this work, Single Day study will be selected giving the possibility for the planner to select the most critical day of the year where the temperature is the highest. Figure 30. illustrates the time intervals that will be used in this case study.

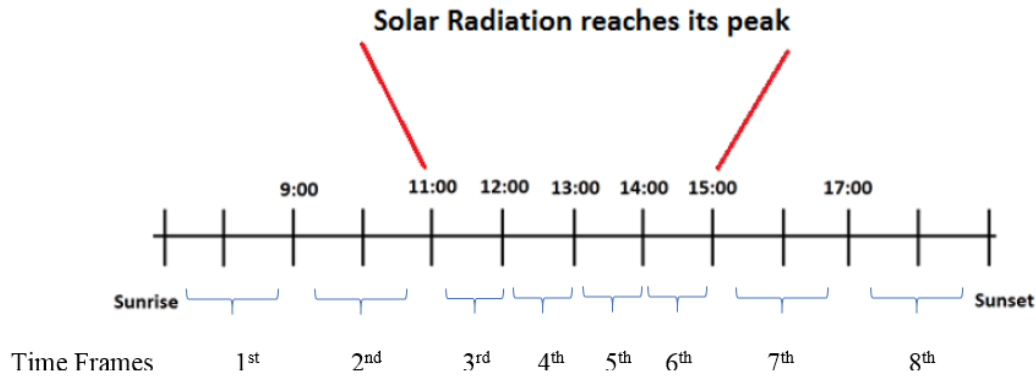


Figure 30. Case Study Time Frames for Solar Analysis.

In *Sun Settings* the desired *Date* and *Time* or *Time Frame* should be selected with *Time Intervals* of 15 minutes.

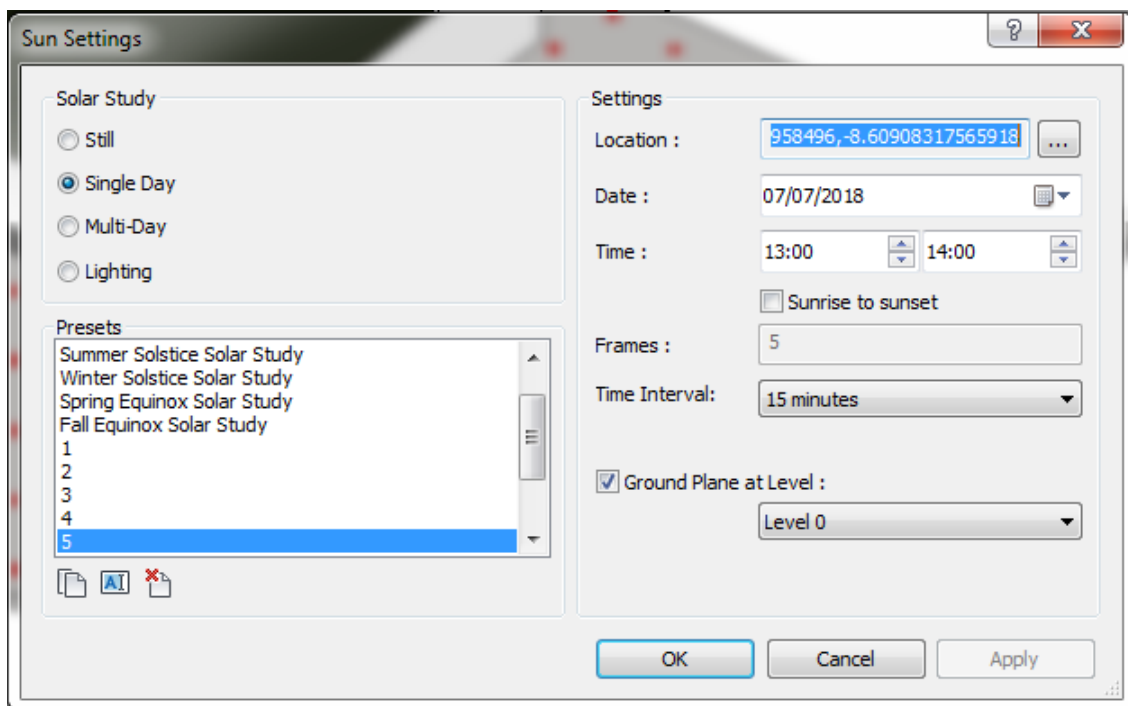


Figure 31. Revit Sun Settings Panel.

Next step is to adjust the Solar Analysis setting. In the Analysis tab, under the Insight section, there is an icon named *Solar* that activate the Solar Analysis tool shown in the Figure below. 1st step is to set the *Study Type* to *Custom*. 2nd is to select the desired surfaces, the selection can be made for multiple surfaces at once. 3rd is to set the *Study Settings* by selecting *Analysis Perios* “<use sun settings>” with the same sun settings selected described in Figure above and also *Analysis Grid* must be specified. The 4th step is to set the Result Settings: for the *Result Type*, there is choice between Cumulative, Peak and Avarage Insolation. This work has the objective to see the most critical heat

load for the time interval, so *Peak Insolation* that register the highest value for this time interval is chosen. The *Style* field is to choose the graphical representation for this analysis and it can be point or surface based. 5th step is to “*Update*” the model or to run the program. 6th is a window that represents summary for the result and 7th is an option to “*Export*” the results in .csv format.

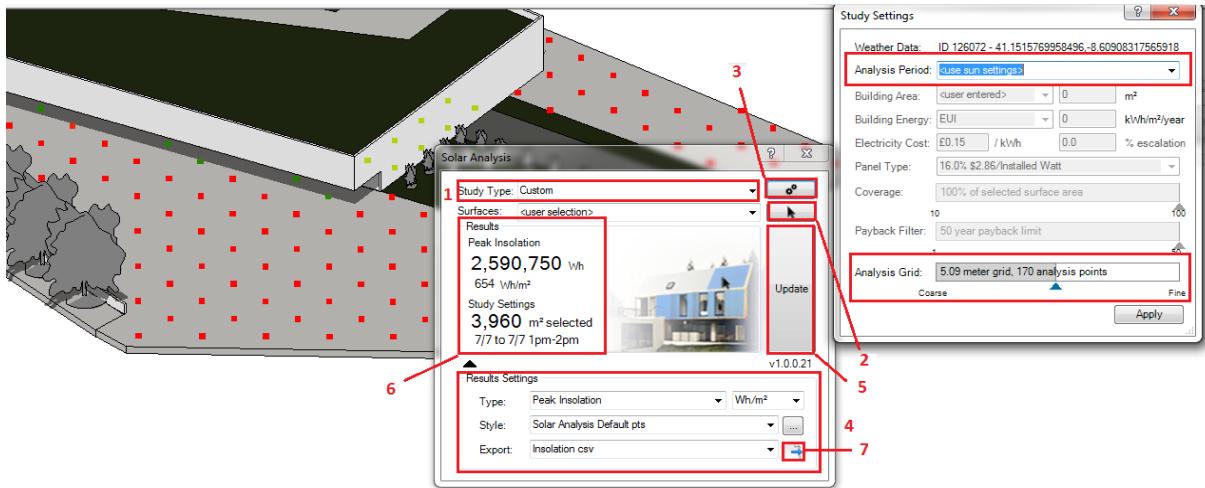


Figure 32. Configuring Solar Analysis Menu.

The exported file has is structured as show in the Figure below. It has information about the time and date of the performed analysis, name of the model, study date and time units etc. It contains data for the element category, ID, surface area and total surface insolation value. Also, associate each point of the grid with a given coordinate to insolation value. The .cvs format must be changed to .xlsx (Excel Workbook format) and the name of the sheet must correspond to the number of the time frame.

| | A | B | C | D | E | F | G | H | I | J | K | L | M |
|----|---|------------|------------------|------------|-----------|--------------------------------|--------------------------|--------------------------------|------------------|---------------------|-------------|--------------|-------------------|
| 1 | e | Date | Time | Model | Type | Study Average Insolation Value | Total Study Surface Area | Total Study Insolation Value | Study Date Range | Study Time Range | Longitude | Latitude | Unit |
| 2 | | Revit 2016 | 09/07/2018 | 19:12 | Trinidade | Cumulativ | 0.456549556 | 6063.233533 | 2768.166579 | 07/07/2018,07/07/20 | 13:00,14:00 | -8.609083176 | 41.151577 kWh/mA² |
| 3 | | | | | | | | | | | | | |
| 4 | | Analysis S | Parent object ty | Category | Parent ob | Average S | Surface Area | Total Surface Insolation Value | | | | | |
| 5 | | 1.06E+09 | Wall | Walls | 304233 | 0.325356 | 2932.834454 | 954.2158766 | | | | | |
| 6 | | 1.06E+09 | Wall | Walls | 305854 | 0.311384 | 5253.630213 | 1635.897847 | | | | | |
| 7 | | 1.06E+09 | Wall | Walls | 306274 | 0.098513 | 3850.433254 | 379.3171749 | | | | | |
| 8 | | 1.12E+09 | Wall | Walls | 306674 | 0.31556 | 627.6721652 | 198.0680737 | | | | | |
| 9 | | 1.06E+09 | Wall | Walls | 311290 | 0.085884 | 1905.864168 | 163.6840249 | | | | | |
| 10 | | 1.06E+09 | Wall | Walls | 312235 | 0.085168 | 151.9260134 | 12.93923692 | | | | | |
| 11 | | 1.06E+09 | Floor | Floors | 312523 | 0.396338 | 39525.48219 | 23570.56113 | | | | | |
| 12 | | 1.06E+09 | Floor | Floors | 312842 | 0.76801 | 5142.581198 | 3949.554255 | | | | | |
| 13 | | 1.06E+09 | Wall | Walls | 314336 | 0.306975 | 923.1948761 | 283.3981753 | | | | | |
| 14 | | 1.06E+09 | Wall | Walls | 316117 | 0.107781 | 877.6939326 | 94.59897596 | | | | | |
| 15 | | 1.06E+09 | Wall | Walls | 316117 | -3.40E-09 | 32.88771071 | -1.12E-07 | | | | | |
| 16 | | 1.06E+09 | Floor | Floors | 324493 | 0.769204 | 4039.930511 | 3107.530462 | | | | | |
| 17 | | | | | | | | | | | | | |
| 18 | | Analysis p | Insolation value | Parent sur | point x | point y | point z | normal x | normal y | normal z | | | |
| 19 | | 1 | 0.325356201 | 1.06E+09 | 116134.1 | 234565 | 13.12335958 | 0.1500441 | -0.9886793 | 0 | | | |
| 20 | | 2 | 0.325356201 | 1.06E+09 | 116173 | 234570.9 | 13.12335958 | 0.1500441 | -0.9886793 | 0 | | | |
| 21 | | 3 | 0.325356201 | 1.06E+09 | 116212 | 234576.9 | 13.12335958 | 0.1500441 | -0.9886793 | 0 | | | |
| 22 | | 4 | 0.292603821 | 1.06E+09 | 116038.6 | 234801.1 | 13.12335958 | -0.9530278 | -0.3028827 | 7.70E-34 | | | |
| 23 | | 5 | 0.304395569 | 1.06E+09 | 116052.4 | 234757.8 | 13.12335958 | -0.9530278 | -0.3028827 | 7.70E-34 | | | |
| 24 | | 6 | 0.313031738 | 1.06E+09 | 116066.2 | 234714.5 | 13.12335958 | -0.9530278 | -0.3028827 | 7.70E-34 | | | |
| 25 | | 7 | 0.316291412 | 1.06E+09 | 116079.9 | 234671.2 | 13.12335958 | -0.9530278 | -0.3028827 | 7.70E-34 | | | |
| 26 | | 8 | 0.318952179 | 1.06E+09 | 116093.7 | 234628 | 13.12335958 | -0.9530278 | -0.3028827 | 7.70E-34 | | | |
| 27 | | 9 | 0.323030945 | 1.06E+09 | 116107.4 | 234584.7 | 13.12335958 | -0.9530278 | -0.3028827 | 7.70E-34 | | | |
| 28 | | 10 | 0.101967911 | 1.06E+09 | 116006.5 | 234677.3 | 13.14502589 | 0.9999295 | -0.01187719 | 0 | | | |
| 29 | | 11 | 0.100902359 | 1.06E+09 | 116006.9 | 234718.9 | 13.14502589 | 0.9999295 | -0.01187719 | 0 | | | |

Figure 33. Exported Excel Data

This is the final step before preparing the Initial Data for Dynamo to use. It is to remark that this is a manual process that can be automatized. Also, there is a Dynamo node shown in the Figure below that can be used directly to avoid all this process, but it dose not represent shadows influence correctly

and only give information about insulation value with associated points and it does not contain information of the elements category or ID which is essential to this work and for this reason it hasn't been used in the program.

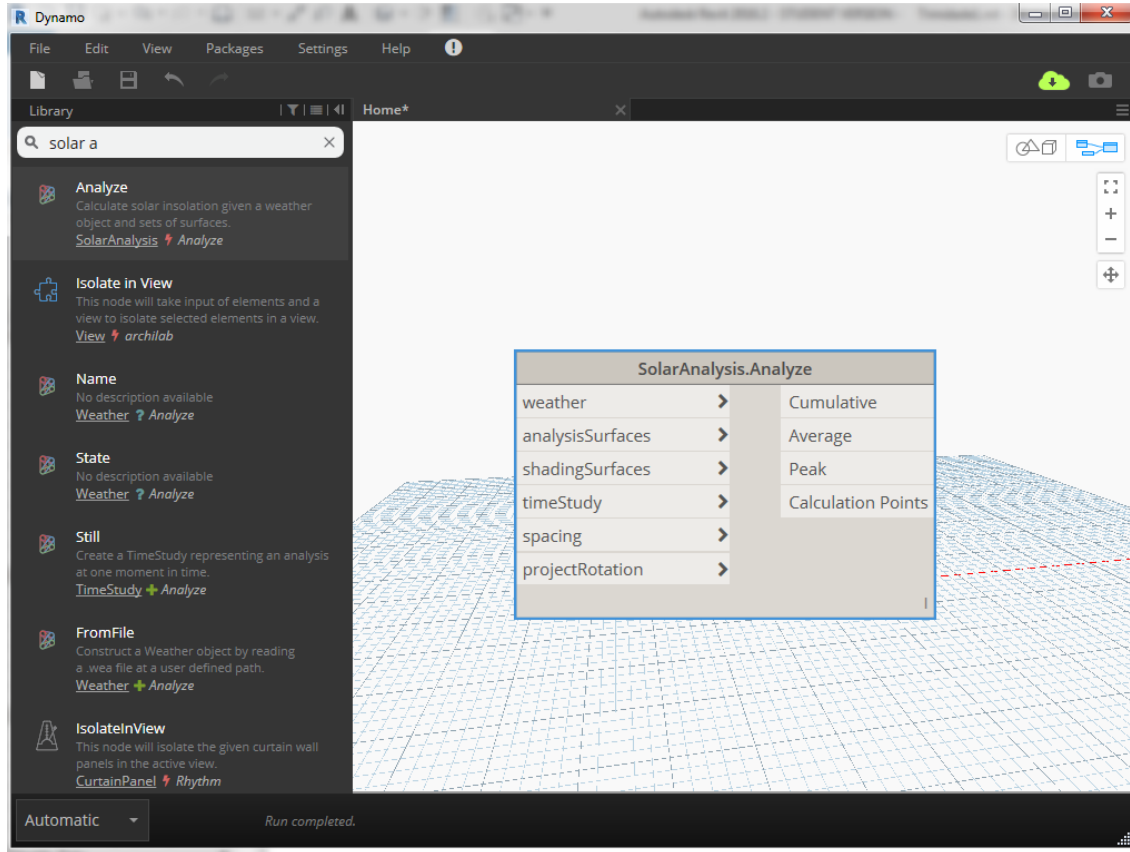


Figure 34. Dynamo node alternative for Solar Analysis.

4.3.2 INITIAL DATA

The outcome from the previous paragraph will be 8 separate sheets in excel one for each time frame. They will contain information about the peak insolation value registered during the time interval and they will be imported into Dynamo. The Initial Data has 3 main processes that will be briefly represented in this section in and it will be further discussed in the Annex A. First is the extraction of the insolation, corresponding coordinate point and the element they belong to (Figure 35), the second is the extraction of the thermal parameters from the corresponding elements (Figure 36) and the third is the separation of the Floors from the Walls (Figure 37).

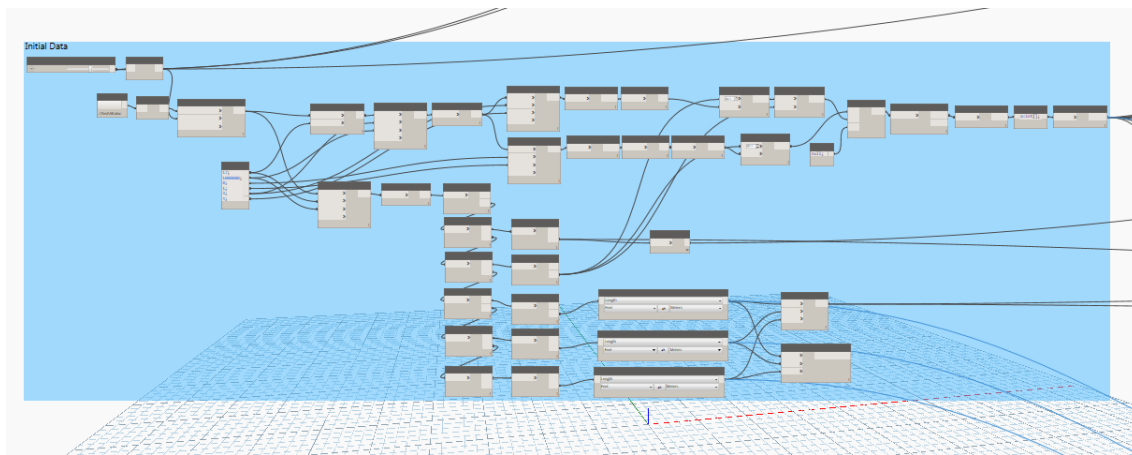


Figure 35. Initial Data

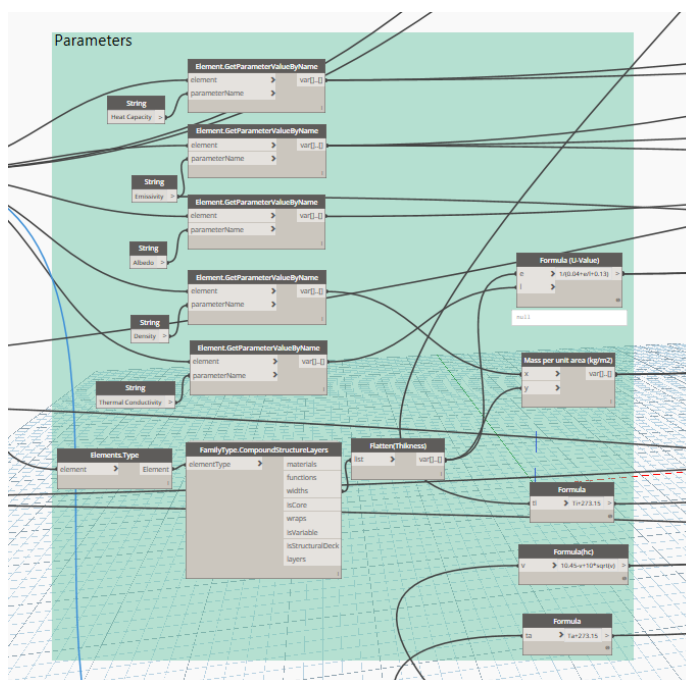


Figure 36. Parameters extracted from Initial Data

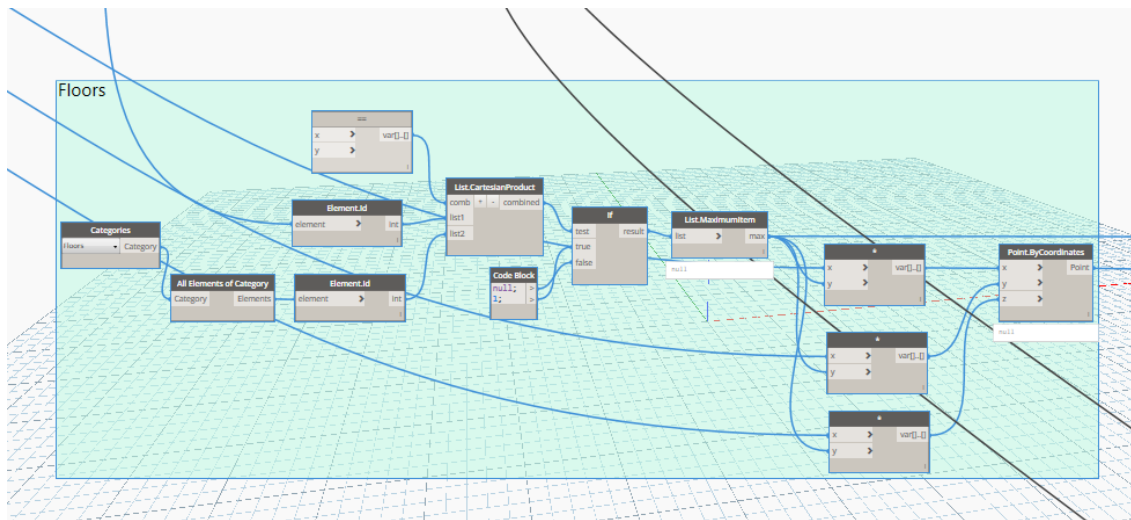


Figure 37. Separation of the Floors

The separation of the Floors from Walls is important because they have different thermal behaviour: Floors are horizontal components and the Walls are vertical which will influence the thermal transmittance of the element.

The result of this process will be used for the calculation of the View Factors, Surface Temperature and Mean Radiant Temperature and the process will be explained in detail in Annex A.

4.3.3 VIEW FACTORS

There are two main type of view factors used in this work: Sky View Factor (SVF) and view factor from standing person to surface (VF_{p-s}).

SVF

As explained in Chapter 3 SVF depends on the grid point of a dome. Finer grind means more accurate SFV values, but it also means that the model will get “heavier” and calculating time will increase. So, SFV will be calculated separately from the other model and the result will be exported in excel file which will be loaded in the main process.

Apart from the Initial Data this process has 6 main components: the first one generates 1 dome per point of the initial data, each dome has number of grid points depending of the given precision; 2nd finds the angle between the centre point of each dome and the dome’s grid points; 3rd is the chess if any of the vectors from the centre to the grid points intersect with any object; 4th step it to find the highest point of intercession; 5th is to calculate the SVF value and 6th is to export the result in excel file.

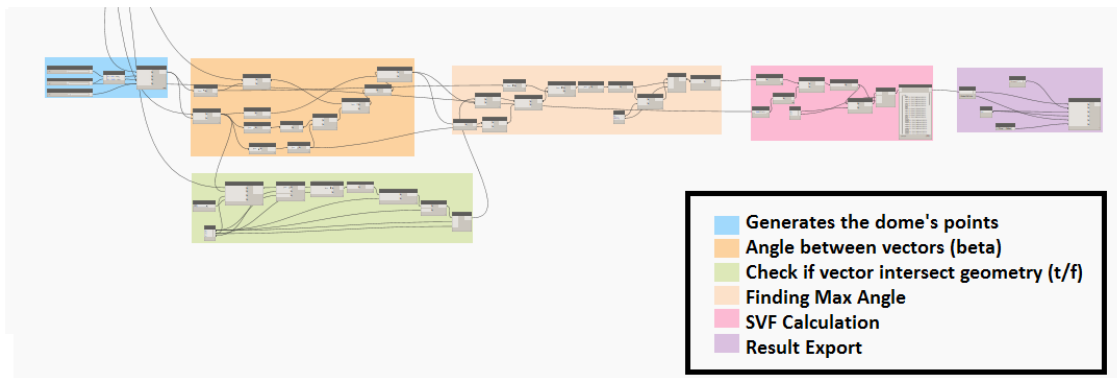


Figure 38. SFV calculation process

4.3.3.1 VF_{p-s}

Even though this component always gives a constant value, it is part of the main process because it also gives the surfaces' thermal parameters associated with the point, which is important for determining the emissivity of the elements they belong to. The method consists of “firing” large numbers of rays from any given point of an object at random angles into the 3D build environment. The first object that each ray intersects with is being recorded with the geometrical parameters between the two being recorded and processed into an equation to find what fraction of the energy that left the first surface has reached the other.



Figure 39. Ray Tracing methodology used to determine the View Factor.

It has three main parts: first is defining the start point of the analysis, which are only the points belonging to the Floors category or where the person can walk. The second part has four elements representing the main directions (front, back, left, and right); the fifth direction registers the radiated energy from the floor, which is constant at a height of 1.5m and the influential area is 1m². As it is open space, there is no incoming longwave radiation from above.

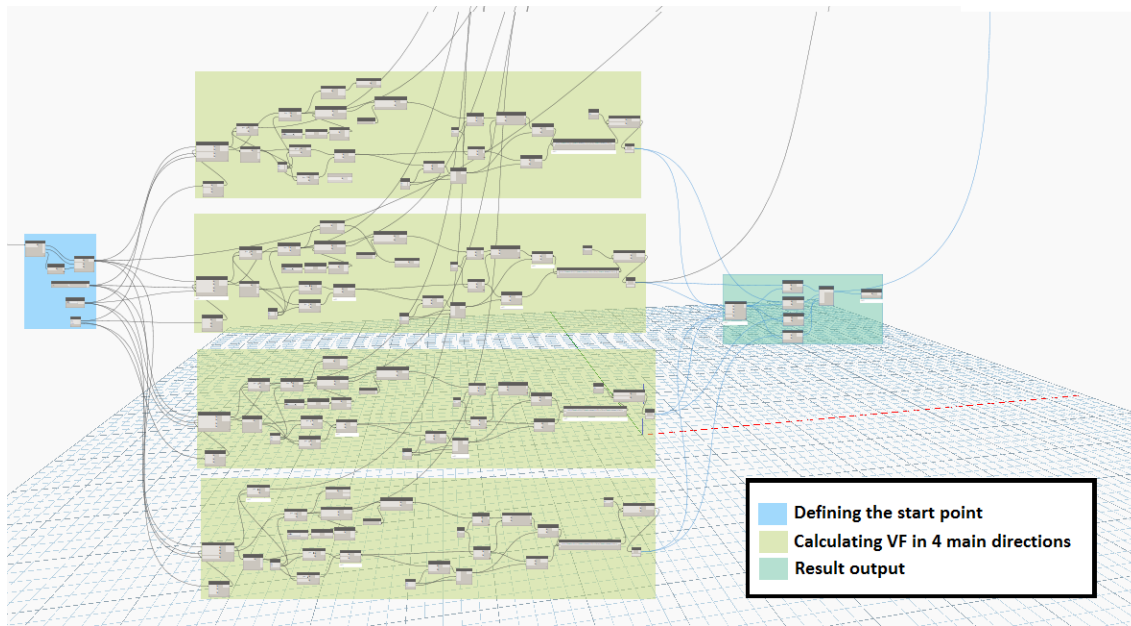


Figure 40. View Factor from person to surface at high 1.5m.

This process is a simplification because the human body receives radiant temperature from all directional and some errors may be expected in the result.

4.3.4 SURFACE TEMPERATURE

This is one of the two main processes of the program. It calculates the surface temperature base on thermal energy balance by using environmental data and solar radiation. It has 6 main components:

- environmental parameters like air temperature, wind speed etc.;
- internal temperature which has different values for Walls and Floors, one is the room temperature between 20-25 C and soil temperature is lower depending on the depth in this work is assumed to me around 20 C;
- initial temperature which is assumed to be 3.4 C lower than the air temperature in the first time frame but in every consecutive time interval it changes to surface temperature of the previous time frame;
- import of the previously calculated Sky View Factor;
- calculation of the surface temperature, and;
- result that is also imported in the 3rd step as new initial temperature.

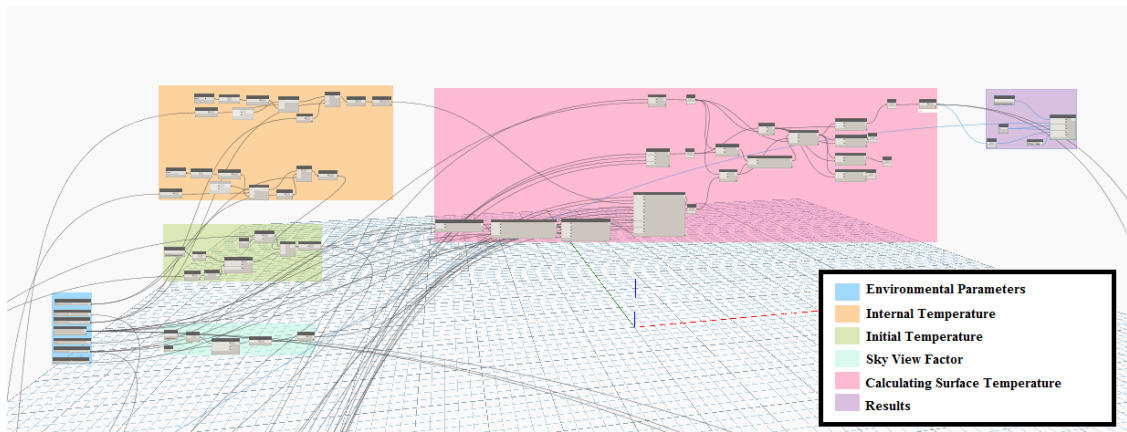


Figure 41. Process of calculating surface temperature.

4.3.5 MEAN RADIANT TEMPERATURE

This is the final outcome of the program and the result can be used for determining human comfort conditions. It uses only the point from the floor elements where a person can stand and also uses data from all previous steps and it contains four main components: 1st one is determining the closes point containing surface temperature information to the point containing view factor data. As the point of the surface temperature is not the same as the one from the ray tracing it is necessary to find the closest surface temperature. 2nd is to provide thermal parameters only for the floor elements; 3rd is the elements corresponding to points associated with the view factor as thermal information from them is essential for the calculation of the mean radiant temperature in the 4th panel.

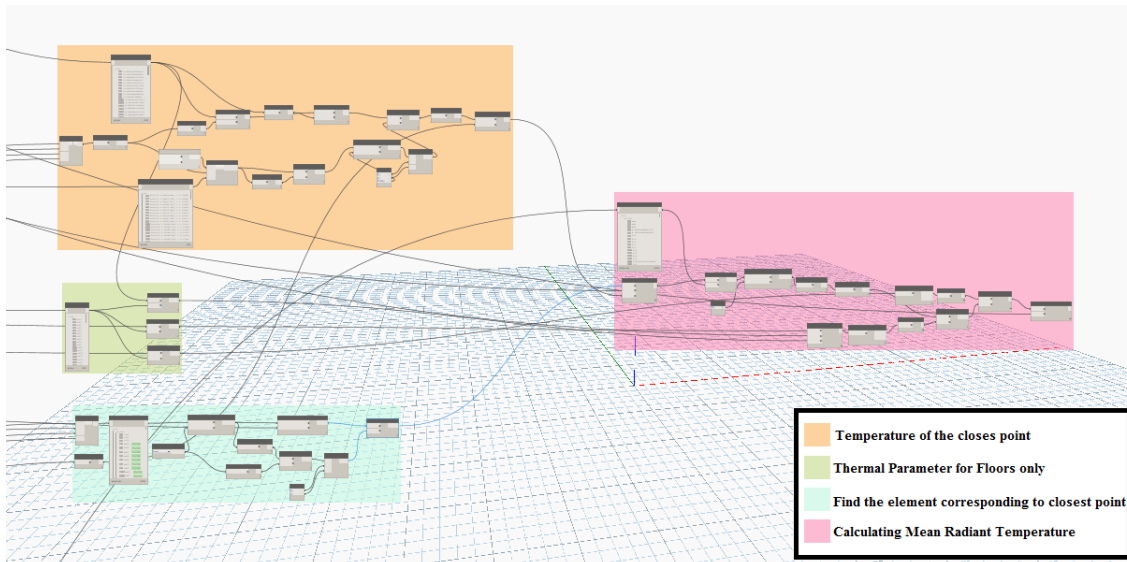


Figure 42. Process of calculating Mean Radiant Temperature.

4.4 Model Validation

For the validation of the model Trindade Metro Station and Square were chosen to verify if the developed tool can accurately represent the difference in the surface temperature and account for the thermal comforts of the pedestrians. This zone has two levels with different characteristics: lower level, or Trindade Square, with finishing layers of granite (floor) and concrete (walls) and an upper

level, near the elevator, that mainly is an open green space (green roof) with a granite cobblestone pedestrian path. So, the objective is to observe if the program correctly represents the temperature difference between the levels, and how the change in the materials and in the physical environment will reflect on the temperature.

A simplified 3D model was developed by using Autodesk Revit. The model contains two main categories: Floors and Walls with the corresponding types:

- | | |
|--------|-----------------------|
| Floors | ● Grass |
| | ● Granite |
| | ● Granite Cobblestone |
| Walls | ● Concrete |

As BIM is designated for the AEC industry, there are no categories that can cover urban elements like Street, Pavement, etc. so, the Floors category will be used instead.

The figure below illustrates the developed 3D model of the Metro Station and the square, compared to the real-life scenario.

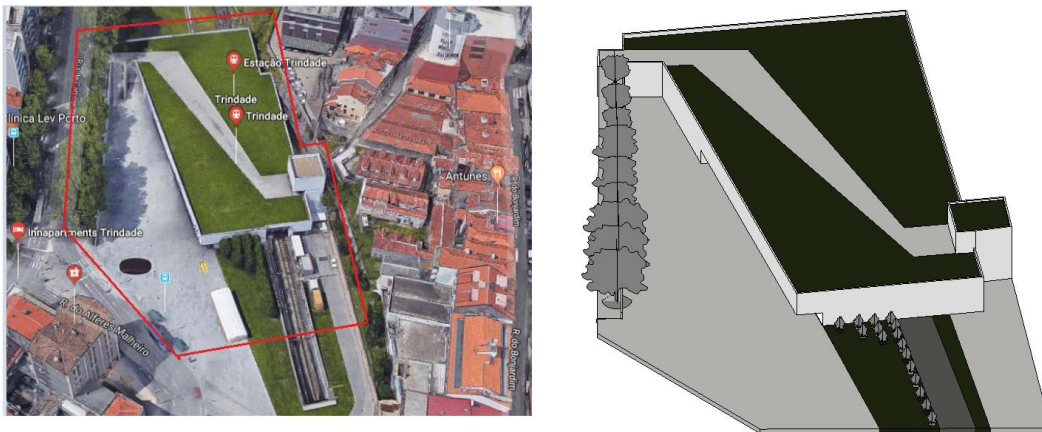


Figure 43. Metro Station Trindade: Real life scenario (Google Maps) vs. simplified 3D model

It is a simplified representation because the purpose is to aid in the design stage of an urban project to high LOD is not necessary. The graphic information is relatively low, and it represents simplified forms of walls and pavements and three that cast shadow on the square. Semantic information on the other hand contains details about the size, height, positioning, materials and thermal qualities of each elements. With this it can be concluded that the objective for LOD300 for the model has been covered.

4.4.1 BUILDING MATERIALS

As mentioned before the model has two categories with the corresponding types of materials. Revit posse's rich library for materials that have predefined data associated with them (Figure 44). The thermal properties value can be changed but additional parameters cannot me added.

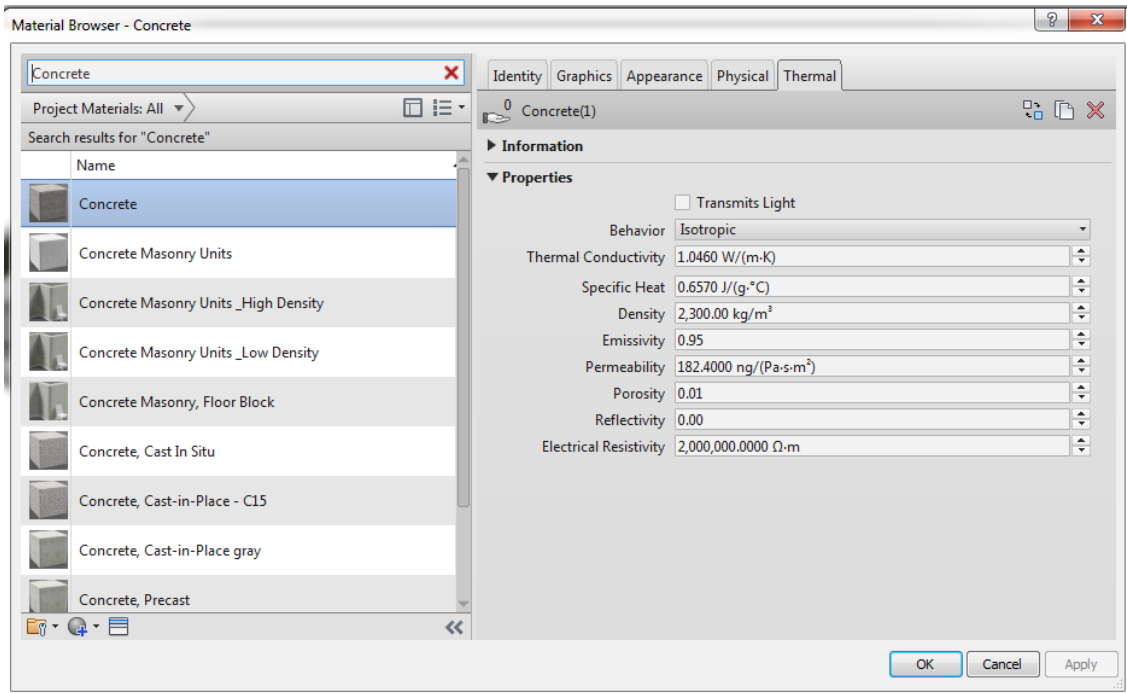


Figure 44. Thermal properties of the materials in Revit.

Due to this Project Parameters are used to equip the element type with the required data. Project parameters are “vessels” for information defined and then add to multiple categories of elements in a project. They can be two types: Instance Parameter that allows the user to modify the parameter value separately for every instance and Type Parameter enables a modification in the parameter value, which applies to all elements of the family type. In this work Instance Parameters are used because it gives more freedom to “play” with the different combinations. Project parameters are specific to the project and cannot be shared with other projects [132].

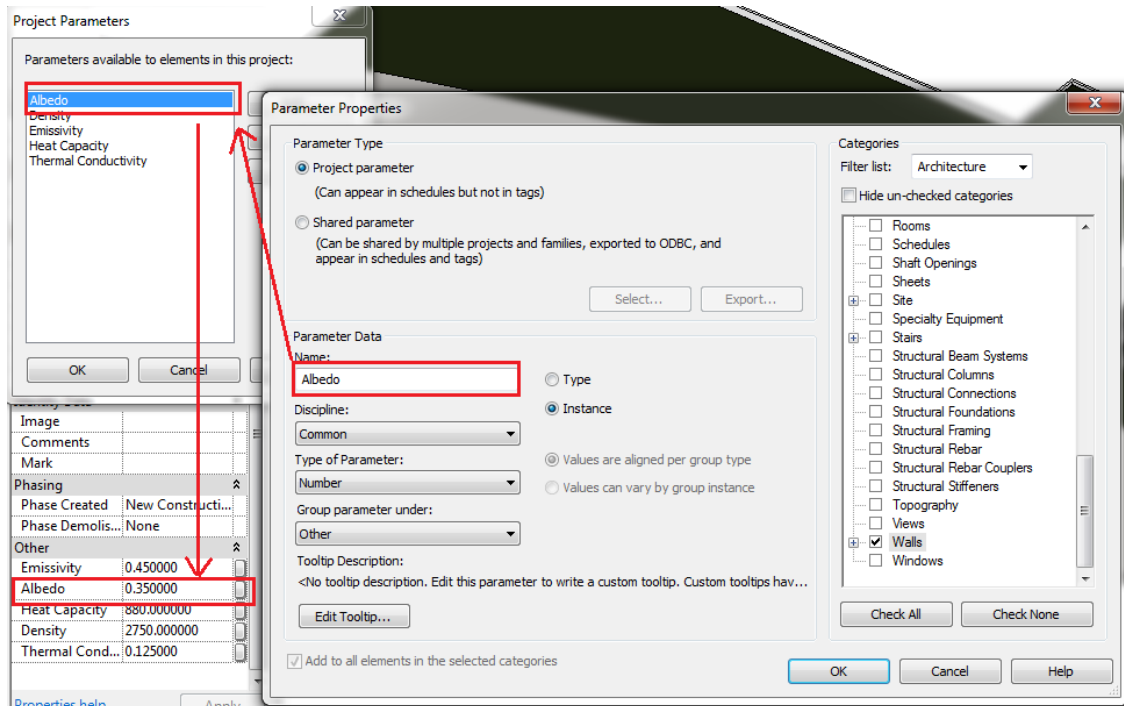


Figure 45. Revit Project Parameters Menu

The materials and their parameters needed for this work are described in Table 4.

Table 4. Thermal properties of the materials [133-136].

| | Soil (w/Grass) | Granite | Granite Cobblestone | Concrete |
|--------------------------------|-------------------|---------|------------------------|----------|
| Albedo (0-1) | 0.25 | 0.35 | 0.35 | 0.55 |
| Density (kg/m ³) | 1200 | 2750 | 2750 | 2200 |
| Emissivity (0-1) | 0.96 | 0.45 | 0.45 | 0.85 |
| Heat Capacity (J/kgK) | 800 | 790 | 790 | 880 |
| Thermal Conductivity (W/mK) | 0.25 | 1.8 | 1.8 | 2 |

These parameters will be used for the analytical part of the program and are essential for the correct calculations. Due to the equipment availability in the desired period from measurement, it was possible only to validate surface temperature.

4.4.2 EQUIPMENT

Equipment used for the study was Protimeter MMS2 is the industry's most advanced all-in-one moisture meter. Its ergonomic, 4-in-1 design allows one-handed operation to measure moisture on

and below the surface as well as ambient air humidity. An infrared thermometer which calculates the difference between dew point and surface temperature is just one of the many advances designed to assess moisture in new/refurbishing projects and help diagnose moisture-related problems in existing buildings [137]. It is design to measure the temperature at close range, so all points that are above two meters of the ground may contain some error.



Figure 46. Protimeter MMS2

4.4.3 METEOROLOGICAL CONDITIONS

The field measurements were taken on the 15th of July 2018 a warm and calm summer day, with a daily mean air temperature of 26.54°C (maximum 31.4°C between 14:00 and 15:00) and mean relative humidity of 62.78% (maximum 73% in the morning).

Table 5. Hourly measured air temperature and relative humidity.

| | 9:00-11:00 | 11:00-12:00 | 12:00-13:00 | 13:00-14:00 | 14:00-15:00 | 15:00-17:00 |
|--------|------------|-------------|-------------|-------------|-------------|-------------|
| Ta(°C) | 24.2 | 25.6 | 30 | 31.4 | 30.5 | 30.7 |
| rH(%) | 71.4 | 65.6 | 61.2 | 58.5 | 57.8 | 57.3 |

The sun rose at 05:16 and set at 20:04. In the morning there were some cloud formation in the morning that disappear around 11:00. Measurement were taken between the period of 9:00 in the morning to 17:00 in the evening. The Meteorological Station Chosen for the study was Weather

Station 126071 with mean dry bulb temperature of 27°C in July because is closer to the measured daily mean measured temperature of 26.54°C then Weather Station 126072 which has mean dry bulb temperature of 30°C.

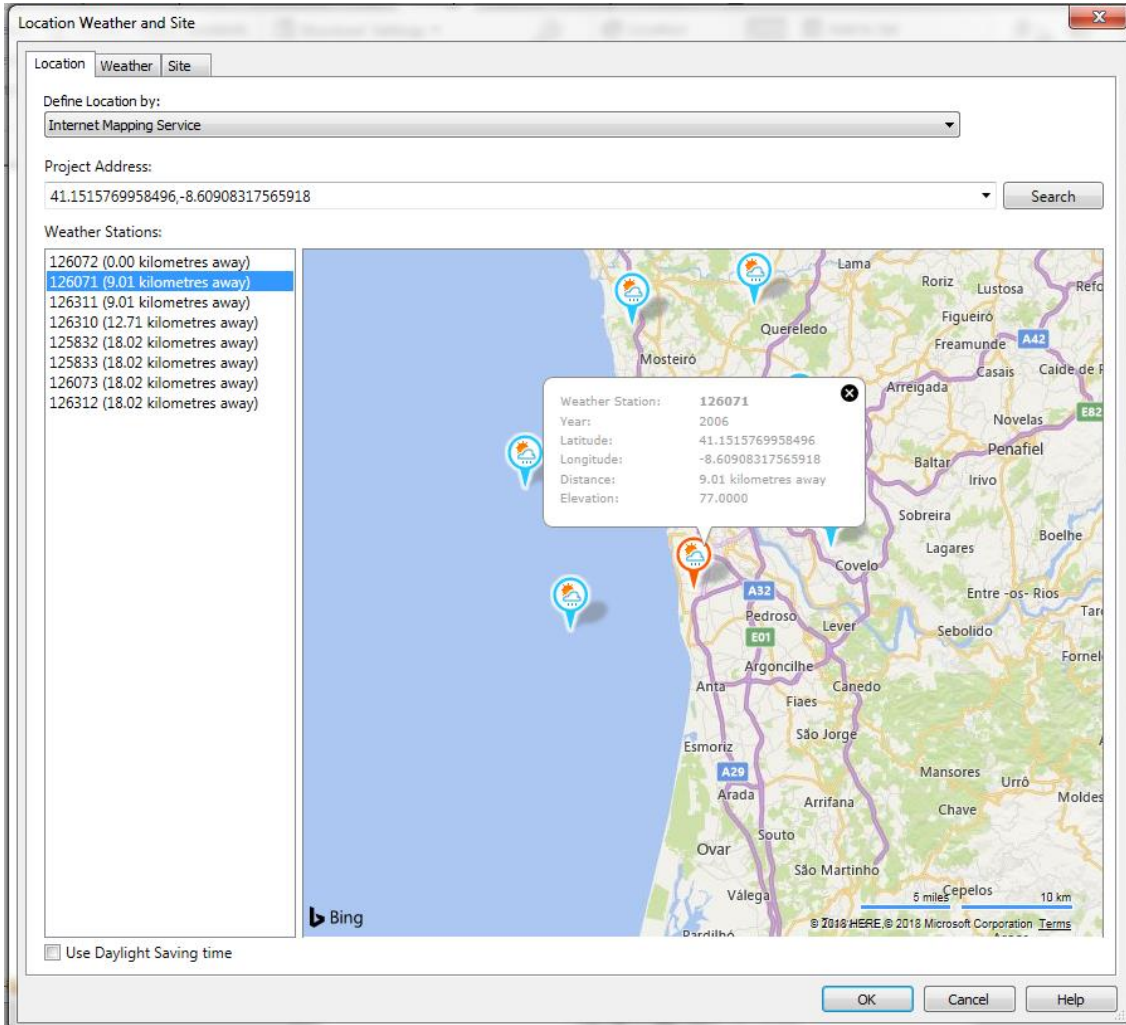


Figure 47. Weather Station 126071.

4.4.4 MEASURED POINTS

Points needed for this validation are selected on each surface. Floors are measured in grid approximately to 10m while Walls are measured in approximately 4m grid. Some of the points were too high or where obstructed by trees or structure to be measured. It was possible to register the temperature change of 144 out of 181 predefined points. Due to the extensively of the study plays it wasn't possible to guarantee measurements at the exact same point for each hour, so the results may have some error related to this.

It was registered that right after the surface started receiving sunlight and begun to heat up from temperature of 19 to 28 for green space and 20 to 46 for concrete and granite pavements. Due to the huge amount of point, it was impossible in the given time frame to compare each point of the surface to the corresponding of the model so, comparison between the estimated values and the average of the measured value for each surface will be made. The result of the measurements is shown in Annex A.

4.4.5 ESTIMATED RESULTS

The tool diverse from the measured results in intervals from -10 to +10 C with an absolute average difference of ± 2 to ± 3 depending on the time interval.

The figures below illustrate the difference between 853 points of the mean measured surface temperature and the calculated in each time frame from 9:00 to 17:00. In the first half of the graphic which represents the upper level till point 480 presents relatively low difference between estimated and measured and the second half represents the lower level where the space is closed and shaded compared to upper part and some variation in the results may be observed.

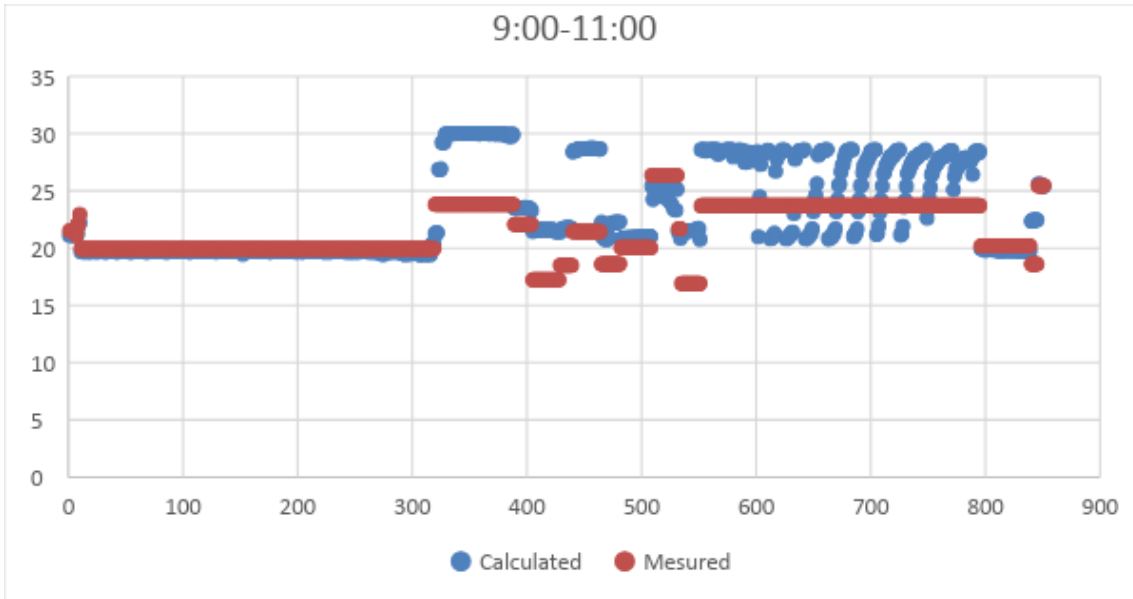


Figure 48. Difference between calculated by the tool and measured in reality from 9:00 to 11:00.

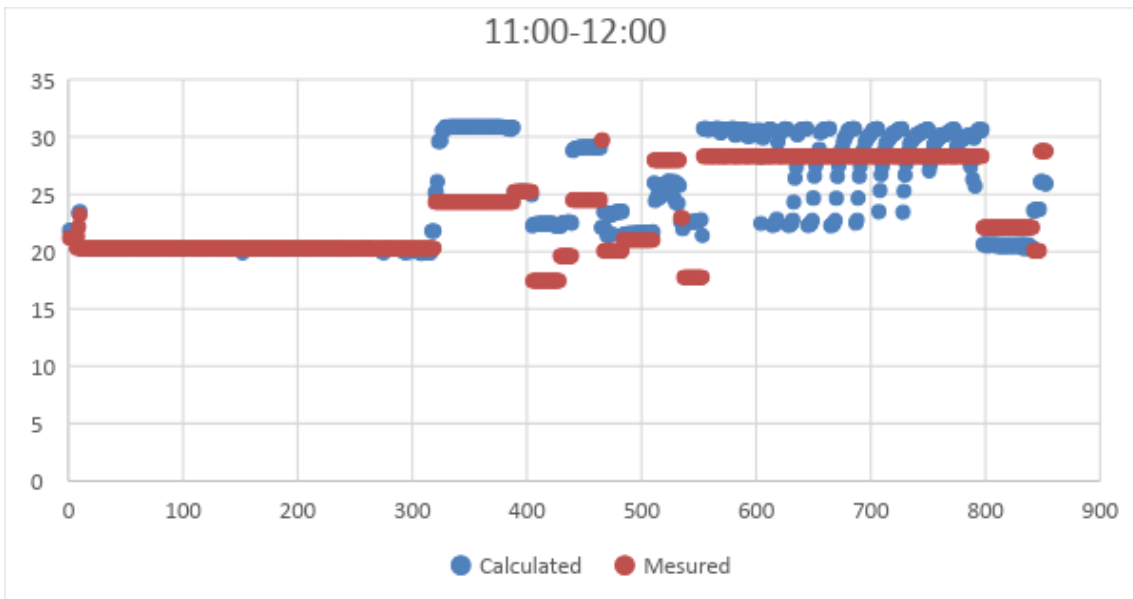


Figure 49. Difference between calculated by the tool and measured from 11:00 to 12:00.

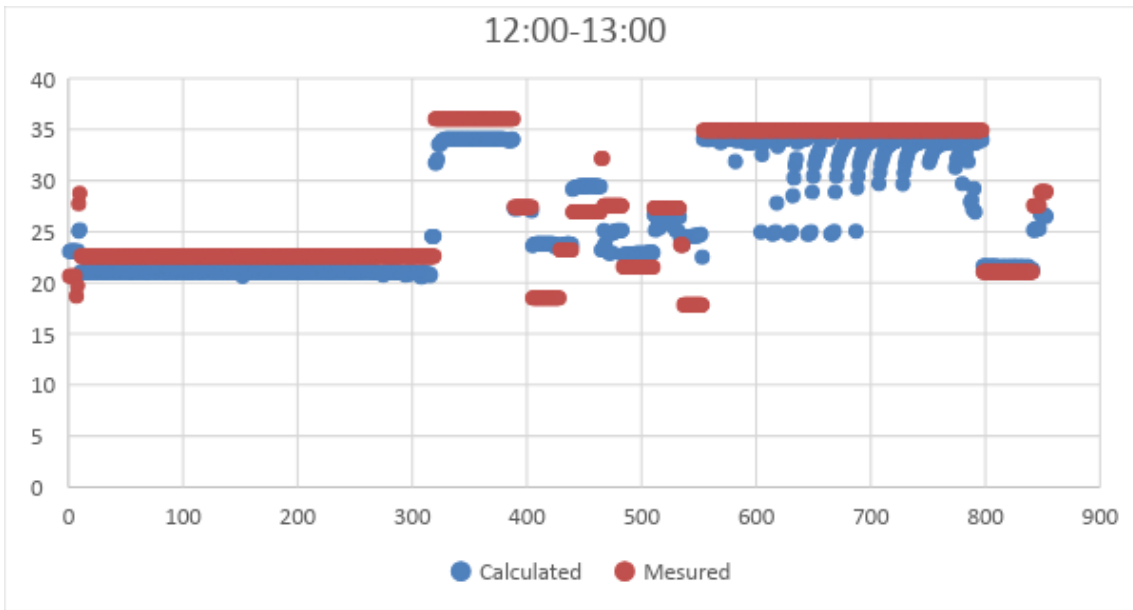


Figure 50. Difference between calculated by the tool and measured from 12:00 to 13:00.

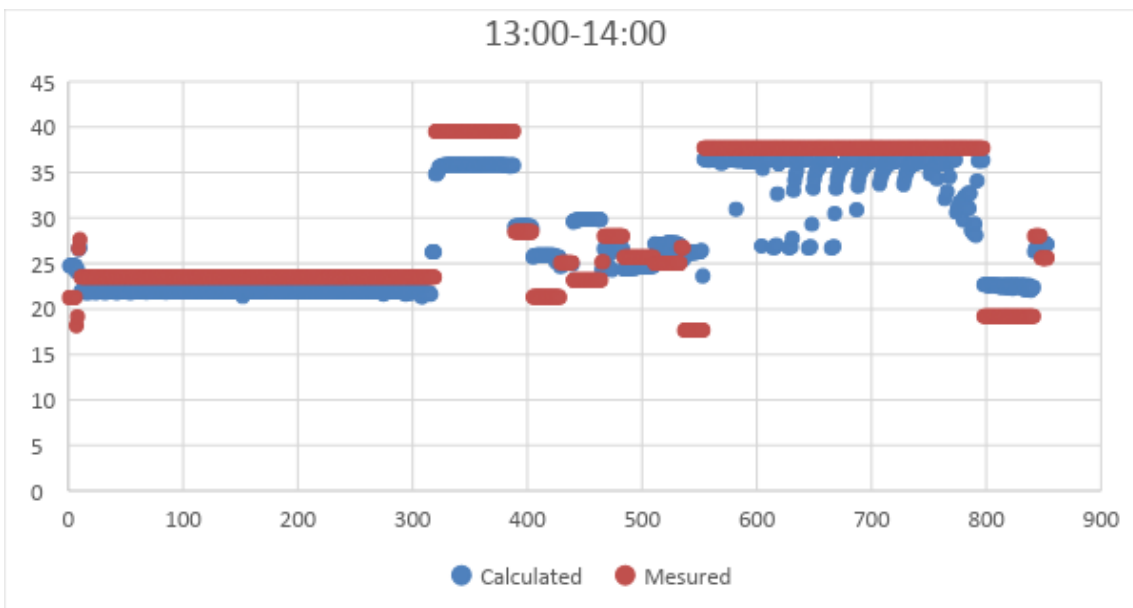


Figure 51. Difference between calculated by the tool and measured from 13:00 to 14:00.

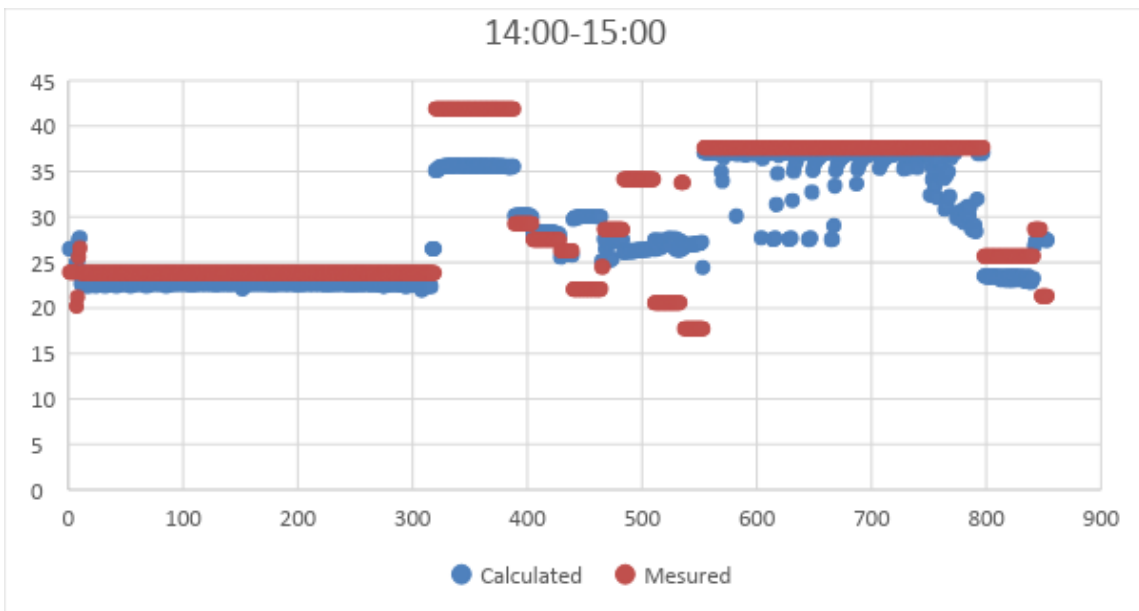


Figure 52. Difference between calculated by the tool and measured from 14:00 to 15:00.

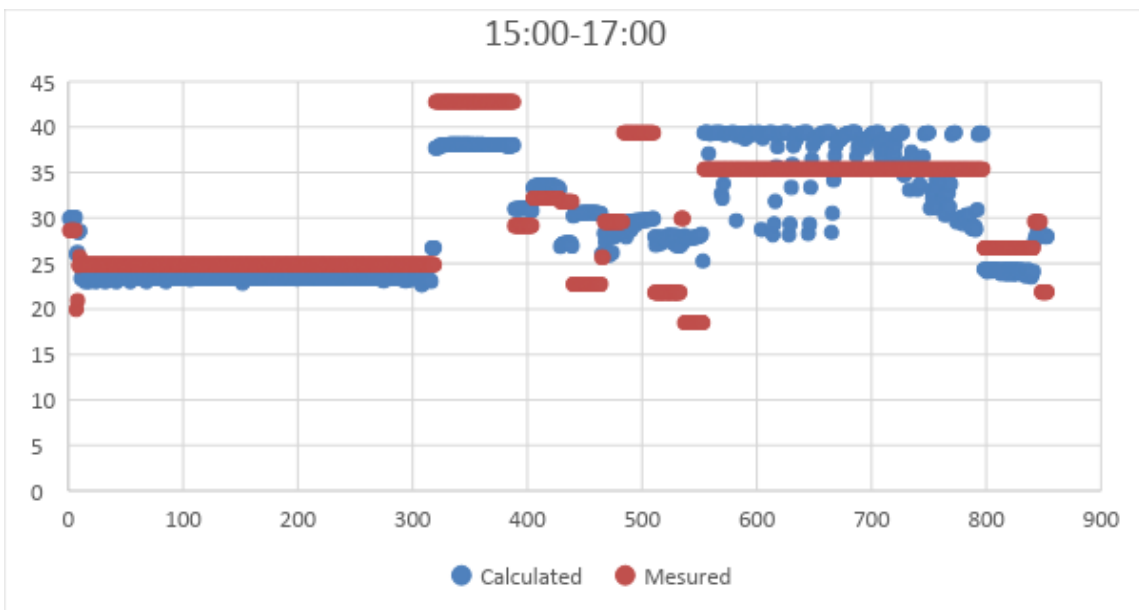


Figure 53. Difference between calculated by the tool and measured from 15:00 to 17:00.

The difference is coming mainly from flattening the measured results which at the lower level results in lowering the sunlit temperature and raising the shaded temperature. On the lower level, the biggest difference is observed near the vertical walls and in the shade, while on the upper level the difference is mainly on the granite pavement in the early hours and the sunlit walls in the afternoon, which may point to a necessity to adjust the heat storage part of the equation.

4.4.6 MEAN RADIANT TEMPERATURE

As mentioned before MRT has two important components, one from shortwave radiation influenced mainly by solar radiation and one from longwave radiation influenced by surrounding surface temperature and the view factor between standing person and shortwave the environment and the sky

view factor. The closer a person is to a wall higher the radiated temperature will receive but also the closer it gets to an open space more radiation it will receive from the sun. Also, the longwave component depends on the temperature received from the walls and floors and the

The following figures illustrated the influence of the different components on the mean radiant temperature. The results were not validated. So, there is no assurance if the results correspond to real values. This will be left for eventual future confirmation.

Unfortunately, this part of the tool gest very “heavy” for Dynamo to run and it can operate only with few analytical points which can lead to information loss and imprecision in the end results.

On Figure 54 the influence of the Longwave component is demonstrated by removing the Shortwave component of the S_{STR} in Equation (5). The tool returns almost constant result of around 24°C for all surface with slightly variation. It is demonstrated that surface temperature plays an important role in the mean radiant temperature but due to the low point capacity and the fact that the upcoming longwave radiation from the floor is only 6% of the total. There is no obvious evidence of change in the temperature from green space to pavement. In some of the corner of the model or where the distance between the surrounding walls is smaller maximum temperature is observed.

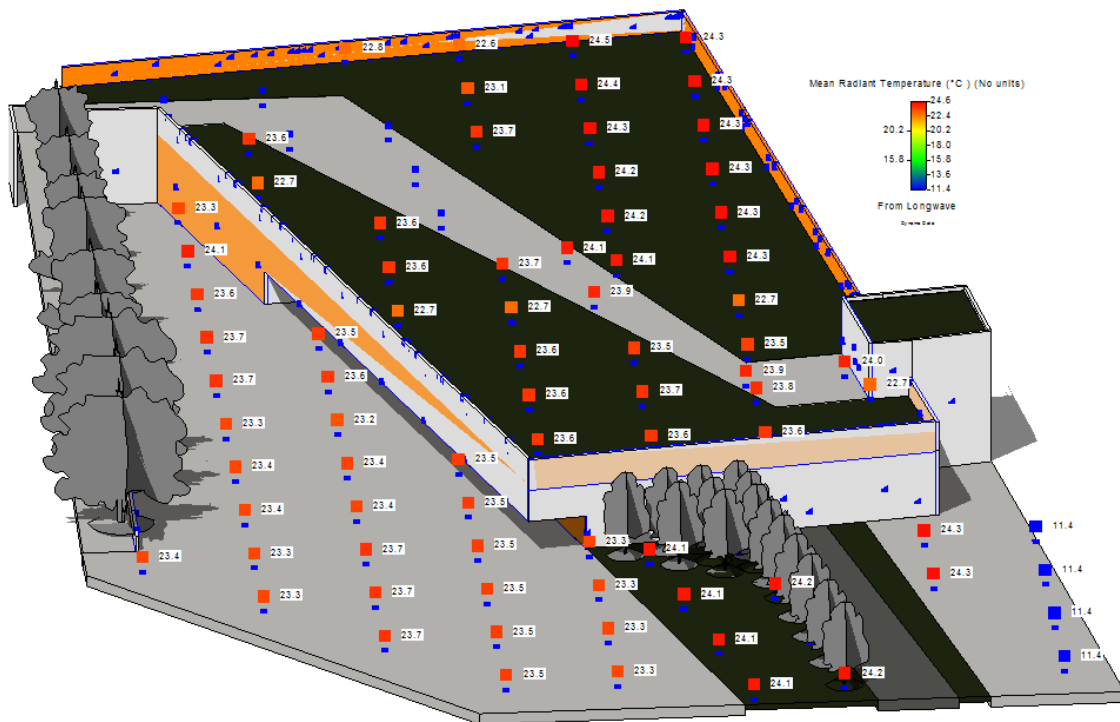


Figure 54. Influence of Longwave component over Mean Radian Temperature.

Figure 55 illustrated the shortwave component of the mean radiant temperature incoming from the sun. It depends only on the shadow/sunlit surface and the latitude and longitude of the sun. With temperature of around 42 °C this is the major contributor for the rise in the mean radiant temperature.

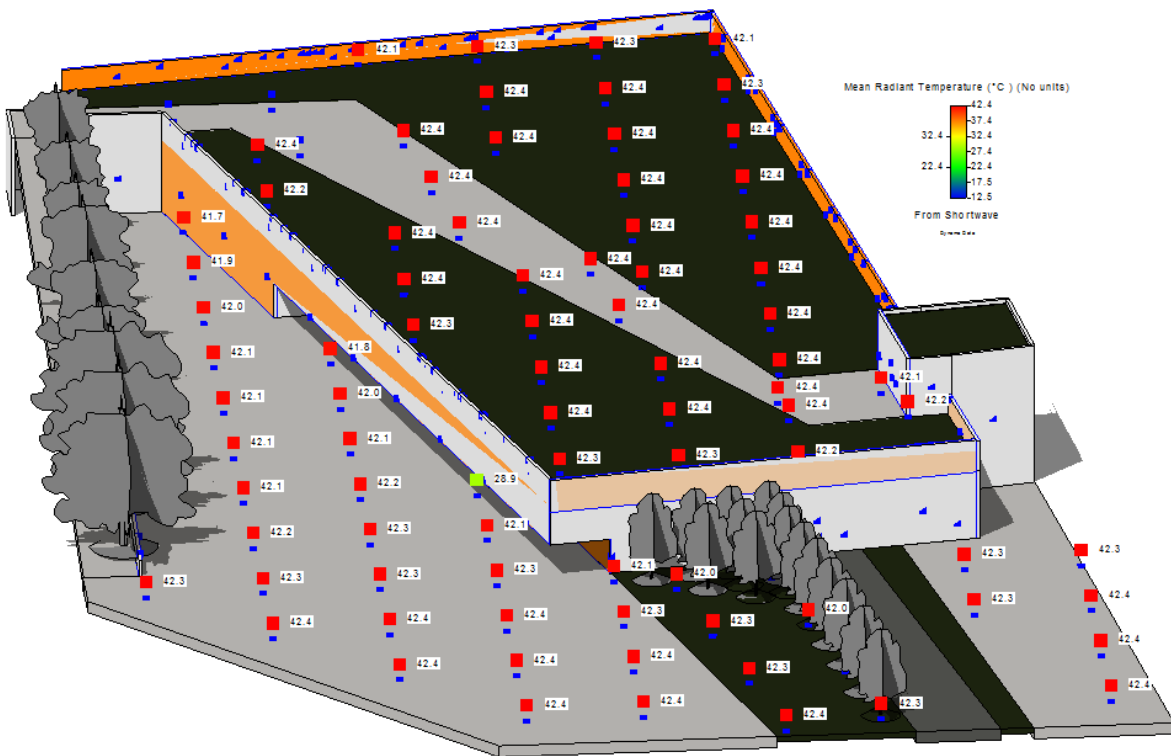


Figure 55. Influence of the Shortwave component over Mean Radiant Temperature

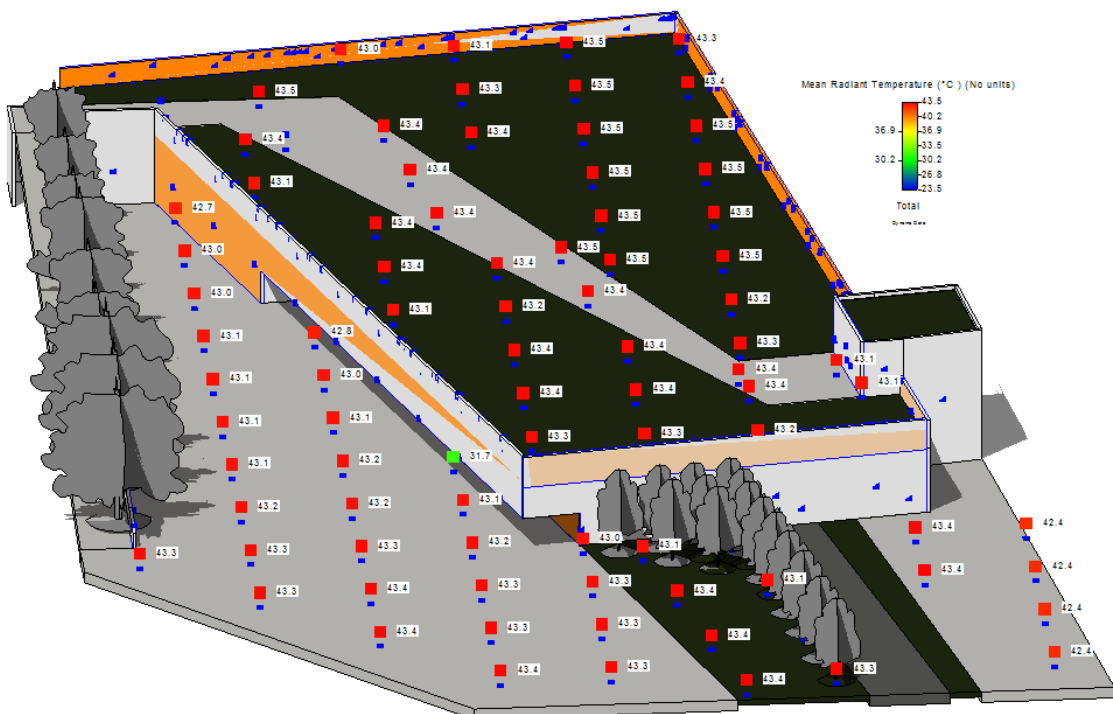


Figure 56. Total Mean Radiant Temperature.

Figure 56 represent the total mean radiant temperature calculated by the tool. Those are some hypothetical estimation the tool can make. They may differ significantly for the reality and some additional validations will be needed to verify the outcome and introduce changes if needed.

Due to the low capacity of points that can be studied for the Mean Radian Temperature the accuracy is extremely low and no legit results can be demonstrate and no conclusions can be made. It is to be divided in separate components in order to improve the workflow and show represents the theoretical results in the difference in the comfort of the space, which will appear in the final version in this work.

As shown above Surface Temperature has significant influence over the Mean Radiant Temperature so in the paragraph below it will be demonstrated how change in the material and colour can hypothetically affect the surface temperature and in consequences the comfort of the open space.

4.4.7 CONCLUSIONS

From the comparison of the values estimated by the tool and the values measured in reality, one can conclude that maximum differences range from +10 °C to -10 °C, with an average difference between the interval of $\pm 2^{\circ}$ C and $\pm 5^{\circ}$ C. The biggest difference found was in the vertical elements and in the shaded areas. This difference is due to some simplifications in the representation of the hourly change in the surface temperature. Further development of the tool is needed in order to restrict the error interval.

The objective of creating a functioning tool for thermal comfort within BIM environment was completed and the validation of the surface temperature component gave satisfying results. The tool can be used to study different scenarios of changes in the urban environment, and it can demonstrate how changes in the physical environment can lead to raise/fall in surface temperature and consequently to change in the environment temperature.

The tool shows correctly the difference between different materials the grass areas are much colder than the concert surfaces. It also represents the temperature difference in the shadow/sunlit components and the change in surface temperature during the course of the day.

The view factors modules can be individually used in order to understand the sky visibility from each point of the urban space. Higher values mean more exposure to sunlight while lower factors refer to enclosed areas. This part of the tool is quite heavy and time consuming to run with high precision, but also delimiting the accuracy of this component didn't influence significantly the final results.

The objective of creating a functioning tool for thermal comfort within BIM environment was completed and the validation of the surface temperature component gave satisfying results. The tool can be used to study different scenarios of changes in the urban environment, and it can demonstrate how changes in the physical environment can lead to raise/fall in surface temperature and consequently to change in the environment temperature.

4.5 Changes in the physical environment

The influence of the material and colour over the surface temperature will be discussed by over exaggeration of the studied component.

- What if all the space was painted black or white?
- What if we replace all the concrete surfaces with grass or with a high heat capacity material?
- What if we introduce more shading elements like trees?

These are all questions that can help planners and engineers designing more comfortable environment in open public spaces.

4.5.1 CHANGE IN MATERIALS AND COLOURS

In this paragraph three scenarios will be studied:

- all pavements are made of asphalt;
- initial material is preserved, but it is painted of *white*, forcing an exaggeration of albedo to 1, and;
- Introduction of more trees and green areas.

Table 6 shows the thermal properties of these new solutions (materials and colours) that will be used in the study.

Table 6. Thermal properties of the new materials [3-6].

| | Asphalt (<i>black</i>) | Painted pavement (<i>white</i>) | Green Area |
|------------------------------|--------------------------|-----------------------------------|------------|
| Albedo (0-1) | 0.10 | 1 | 0.25 |
| Density (kg/m ³) | 2400 | - | 1600 |
| Emissivity (0-1) | 0.96 | - | 0.96 |
| Heat Capacity (J/kgK) | 920 | - | 800 |
| Thermal Conductivity (W/mK) | 0.75 | - | 0.25 |

First Scenario: Asphalt Pavement

The objective of this scenario is to show that if all the pavements are made from black asphalt the temperature will rise.

Asphalt has a low albedo and thermal conductivity, which will predispose it to receive and trap heat, resulting in increasing surface temperature.

The tool shows a high increase in the surface temperature relatively to the normal scenario.

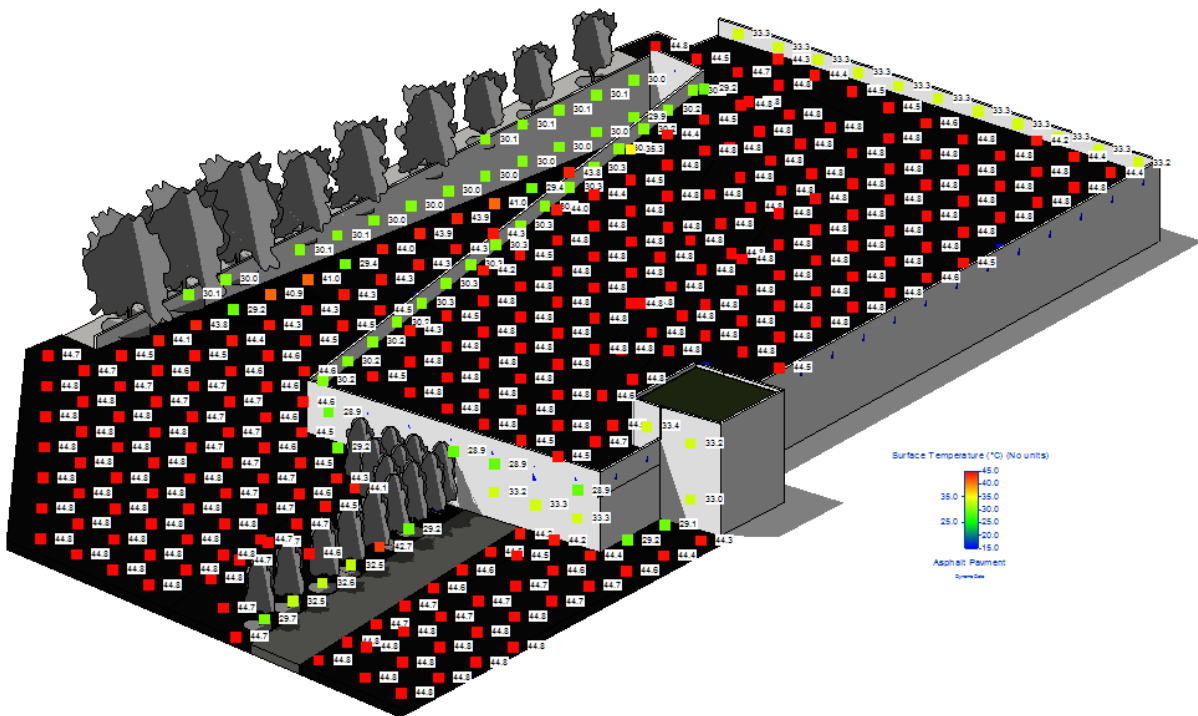


Figure 57. Increase in surface temperature as result of asphalt pavement.

Second Scenario: All pavements “painted” of white

In this hypothetical study, all surfaces of the model are “painted” white and the albedo is exaggerated to 1 in order to show visible changes in the temperature.

In this situation, all the solar radiation is reflected in the atmosphere and there is no possibility for heat storage, which lead to the low temperatures demonstrated in Figure 57. This scenario is overexaggerated in order to demonstrate that solar radiation is one of the main contributors for the surface temperature value.

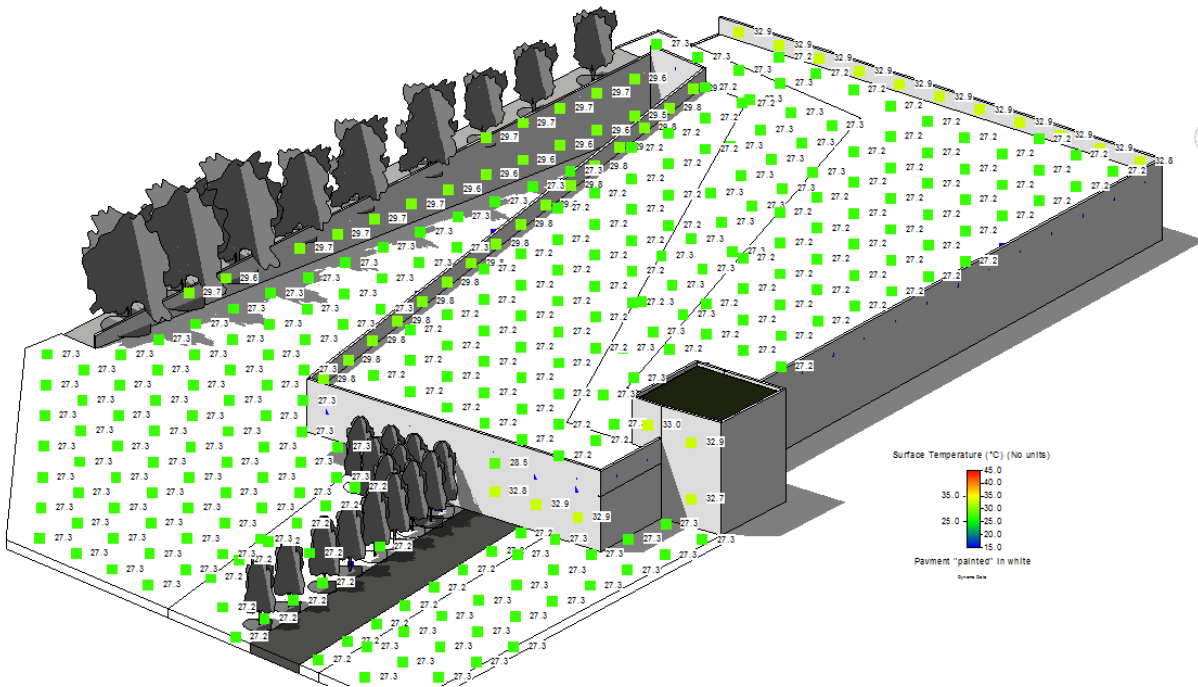


Figure 58. All pavement "painted" white.

Third Scenario: *Introducing more trees and green space.*

The objective is to see how tree shadows and green areas will reduce the surface temperature of the space.

The tool demonstrated, as expected, that introducing green areas can lower the surface temperature. The high temperature on the upper level can be explained by higher values of the sky view factor as it is an open space with no buildings in the closest surroundings and receives a bigger portion of the incoming solar radiation.

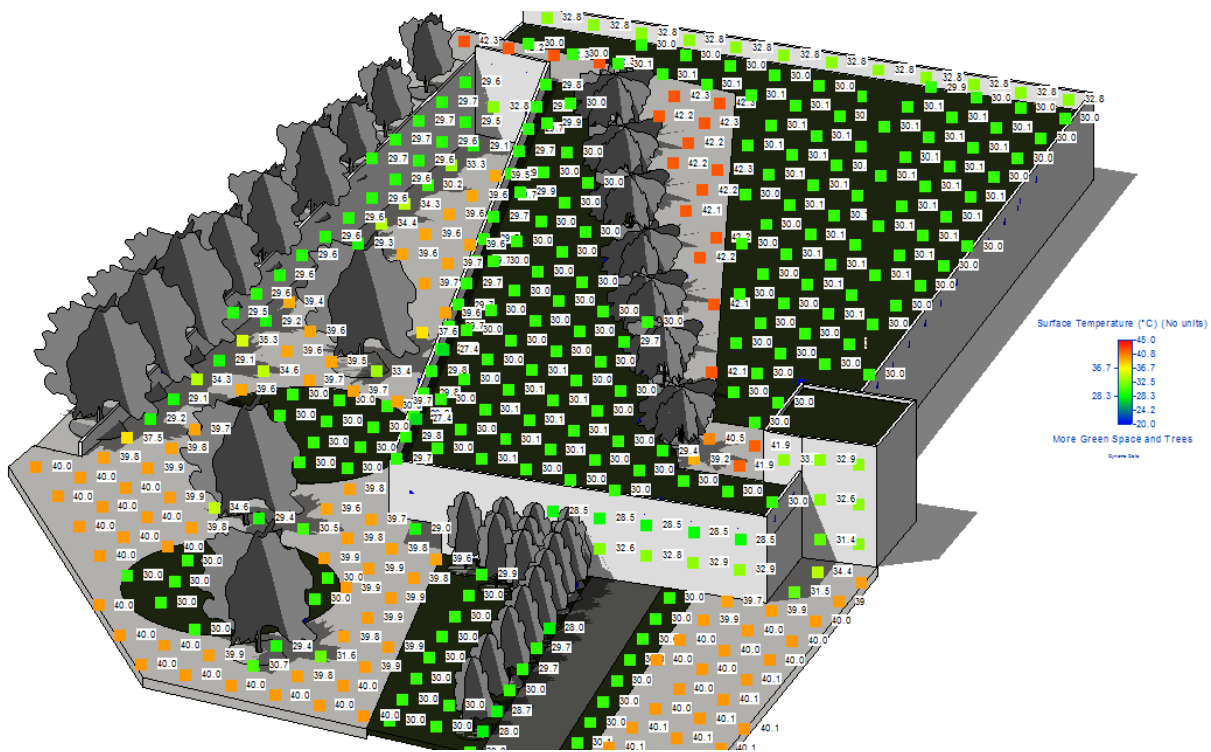


Figure 59. Surface Temperature when introducing more green space and trees.

Given the represented scenarios the tool executed correctly the expected theoretical changes in the environment. When the pavement is changed to asphalt the temperature increases when all pavement is painted white the surface temperature falls. In the 3rd example, the changes are more obvious in the introduction of more green spaces and trees. As mean radiant temperature is based on the surface temperature, lowering surface temperature will result in more comfortable space and avoid accumulation of heat in open spaces and allows the planner to study the changes in the micro climate before implementing the design.

5

CONCLUSIONS

5.1 Final Reflection

In the final chapter of this thesis, one can conclude that the initial objectives set for this work were achieved.

When exploring the concepts of GIS and BIM, it was concluded that both of them could be used for urban planning, although there is little or no present interoperability between them.

CIM methodology is still the only theoretical approach and there have been only a few examples of its practical application. Major companies are taking the first steps into and investing in creating CIM models capable of representing the urban environment. New viewpoints for urban design are created by giving the possibilities to look at the city environment from a different angle and reducing the energy waste in the city function.

It was concluded that there are few tools for estimation of thermal comfort of public space. Most of the existing programs don't have 3D geometry capabilities and the ones that have use CAD-based models with no semantic data attached. There are difficulties in the representation of half-shaded surfaces and attribution of the thermal parameters to the corresponding elements.

Even though BIM is a relatively new methodology to represent materials, surfaces and quantities in a project, using 3D visualization, it was not intended for urban planning purposes. This dissertation proved that is possible to do so, with some adaptation, and with that intention was developed a tool that can support the decision-making process.

The developed tool covered most of the flaws that existing programs have and establish new possibilities for the future development of this methodology. By using Dynamo capabilities, it was possible to create a tool for estimating view factors, surface temperature and mean radiant temperature by using. Using Revit, a 3D model of Trindade Metro Station was created, and the tool was tested on it.

From the two main components surface temperature and mean radiant temperature, it was only possible to validate the first one due to equipment availability. Then, the results were compared. Between measurements of real surface temperature around the Station, taken on hot summer day with no clouds, and the estimated results from the model, simulating conditions predisposing for high surface temperature, it was concluded that the tool represents correctly the hourly change of temperature and the difference between the surface, with an average error between 2 °C to 3 °C. Higher difference values are register due to the comparing the tool outcome to mean measured surface temperature which results in imprecision in the vertical and shaded elements.

The absolute maximum error was around 10°C and it was found on the vertical components (walls) of the model, but it has been expected due to simplifications in the energy balance equation and the solution to this anomaly will be left for future works.

Difficulties were found in the accuracy of the view factors and in consequence in the mean radiant temperature due to the tool being too “heavy” to run the analyses. The process is too fully automated, it requires manually selecting the surfaces for the desired study, exporting data from Revit’s Insight Solar Analysis and importing them again in Dynamo workflow.

It was possible to analyze different scenarios by changing the material and the color of the surface. The tool demonstrates correctly raise in surface temperature when the pavement is made of asphalt and reduction in surface temperature when the floor is painted white. An alternative scenario with more green areas and trees was created to demonstrate decrease in temperature in shaded and non-build areas. It can be also concluded that surface temperature is the main factor conditioning mean radiant temperature and in consequence thermal comfort.

This tool can be used as decision-making tool for comfort study of public space giving the possibilities for planners to see how build environment can contribute to the urban microclimate giving the possibilities to interfere before the implementation of the project. Although this tool is only a proof of concept it can be considered as future possibilities for integrating AEC industry and city planning for creating a sustainable urban environment.

5.2 Future developments

Although the development of the tool has reached satisfactory level or the conclusion of this work, it is far from finished. Changes must be made to improve the tool workflow and making in “lighter” to run. Another future objective will be to separate the Floor and Wall element to two categories: one that have air on both sides and one that have air on the one side and soil on the other giving the possibility to represent better the heat exchange.

The tool methodology involves some “manual” work mainly in exporting, formatting and importing the excel files. This process can be automated with the help of programming.

The view factors involved in the process will also need refinement, especially the view factor between person and surface. In this work is considered that the person receives energy only from the four main directions. As a human body receives heat from all directions and all surfaces a similar method as in the Sky View Factor must be created and applied.

Surface temperature calculations must be improved in order to include heat exchange between the surface that can increase the accuracy of the results.

Validation of the mean radiant component is to be expected for verifying if the tool represents the reality correctly and in order to proceed to thermal comfort calculation.

Finally, integration between GIS and BIM file formats is needed for a more accurate representation of the existing reality. The Revit coordinate system does not correspond to the standard GIS coordinate system which can lead to confusion when pinpointing the location of the model.

AAAAAC aa^

REFERENCES

1. Campbell-Dollaghan, K. *A Brief History of Buildings That Melt Things*. 2013 [cited 2018 25.06]; Available from: <https://gizmodo.com/a-brief-history-of-buildings-that-melt-things-1247657178>.
2. Stadler, A. and T.H. Kolbe. *Spatio-semantic coherence in the integration of 3D city models*. in *Proceedings of the 5th International ISPRS Symposium on Spatial Data Quality ISSDQ 2007 in Enschede, The Netherlands, 13-15 June 2007*. 2007.
3. de Laat, R. and L. Van Berlo, *Integration of BIM and GIS: The development of the CityGML GeoBIM extension*, in *Advances in 3D geo-information sciences*. 2011, Springer. p. 211-225.
4. Benner, J., A. Geiger, and K. Leinemann. *Flexible generation of semantic 3D building models*. in *Proceedings of the 1st international workshop on next generation 3D city models, Bonn*. 2005.
5. El-Mekawy, M., *Integrating BIM and GIS for 3D city modelling: The case of IFC and CityGML*. 2010, KTH.
6. Hernández-Moreno, S., *Current technologies applied to urban sustainable development*. Theoretical and Empirical Researches in Urban Management, 2009. **4**(4 (13)): p. 125-140.
7. Chourabi, H., et al. *Understanding smart cities: An integrative framework*. in *System Science (HICSS), 2012 45th Hawaii International Conference on*. 2012. IEEE.
8. Gupta, P., et al. *Geographical information system in transportation planning*. in *map Asia conference*. 2003.
9. Marble, D.F., *The potential methodological impact of geographic information systems on the social sciences*. Interpreting space: GIS and archaeology, 1990: p. 9-21.
10. Berry, J.K., *Fundamental operations in computer-assisted map analysis*. International journal of geographical information system, 1987. **1**(2): p. 119-136.
11. Hopkins, L.D., *Methods for generating land suitability maps: a comparative evaluation*. Journal of the American Institute of Planners, 1977. **43**(4): p. 386-400.
12. Institute, R.T.P., *Geographic Information Systems: a planner's introductory guide prepared by the Institute's GIS Panel* 1992, The Royal Town Planning Institute . London,.
13. Su, D.Z., *GIS-based urban modelling: practices, problems, and prospects*. International Journal of Geographical Information Science, 1998. **12**(7): p. 651-671.
14. YEh, A.G., *Urban planning and GIS*.
15. GIS, G. *Limitations or Challenges of GIS*. 2018 [cited 2018 15.05]; Available from: <http://grindgis.com/remote-sensing/limitations-or-challenges-of-gis>.
16. Eastman, C., *An Outline of the Building Description System. Research Report No. 50*. 1974.
17. Van Nederveen, G. and F. Tolman, *Modelling multiple views on buildings*. Automation in Construction, 1992. **1**(3): p. 215-224.
18. Bergin, M.S., *A brief history of BIM*. Archdaily, 2012. **7**: p. 12.
19. Eastman, C.M., et al., *BIM handbook: A guide to building information modeling for owners, managers, designers, engineers and contractors*. 2011: John Wiley & Sons.
20. Howell, I. and B. Batcheler, *Building information modeling two years later—huge potential, some success and several limitations*. The Laiserin Letter, 2005. **22**(4).
21. Isikdag, U., et al., *Building information models: a review on storage and exchange mechanisms*. Bringing ITC Knowledge to Work, 2007.
22. BIMFORUM., *Level of Development Specification: For Building Information Models*. 2017.

23. AIA, *AIA Contract Document G202-2013, Building Information Modeling Protocol Form* 2013.
24. TC184, I., SC4, " *ISO 16739: 2013 Industry Foundation Classes (IFC) for data sharing in the construction and facility management industries,*". International Organization for Standardization (ISO), 2013.
25. Isikdag, U. and S. Zlatanova, *A SWOT analysis on the implementation of Building Information Models within the Geospatial Environment*. Urban and Regional data Management, UDMS Annuals, 2009: p. 15-30.
26. DynamoPrimer. *What is Dynamo?* 2018 [cited 2018 21.06.]; Available from: http://dynamoprimer.com/en/01_Introduction/1-2_what_is_dynamo.html.
27. Cheryl A. O'Neill , T.G.U. and T.G.a.P. Radoslav Brandersky , Inc. *BIM and Smarter Cities The use of BIM for Planning*. 2014; Available from: https://bimforum.org/wp-content/uploads/2014/04/TGP_Boston-BIMForum-Final.pdf.
28. Isikdag, U., J. Underwood, and G. Aouad, *An investigation into the applicability of building information models in geospatial environment in support of site selection and fire response management processes*. *Advanced engineering informatics*, 2008. **22**(4): p. 504-519.
29. Hamilton, A., et al., *Urban information model for city planning*. *Journal of Information Technology in Construction (ITCon)*, 2005. **10**(6): p. 55-67.
30. Xu, X., et al., *From building information modeling to city information modeling*. *Journal of Information Technology in Construction (ITCon)*, 2014. **19**: p. 292-307.
31. BIMLERN. *IFC*. 2017 [cited 2018 18.06]; Available from: http://bimlearn.org/ifc-%DA%86%DB%8C%D8%B3%D8%AA-%D8%9F/ifc_discipline_and_merged_models/.
32. Kaiser, E.J., D.R. Godschalk, and F.S. Chapin, *Urban land use planning*. Vol. 4. 1995: University of Illinois Press Urbana, IL.
33. AECbytes. *City Information Modeling* 2016 [cited 2018 20.06]; Available from: <http://aecbytes.com/feature/2016/CityInformationModeling.html>.
34. Stavric, M., et al., *From 3D building information modeling towards 5D city information modeling*. *3D Issues in Urban and Environmental Systems*. Bologna, Italy: Società editrice ESCULAPIO, COST, 2012.
35. Choei, N.-Y. and S.-H. Jeon, *Procedural Modeling of a Residential Site Using the Interoperability between the GIS and CityEngine: An Adaptation of the Radburn Type Cul-de-sac Roadsystem and Housing*. *GSTF Journal of Engineering Technology (JET)*, 2016. **3**(4): p. 4.
36. ESRI. *Esri CityEngine*. 2018 [cited 2018 19.06]; Available from: <http://www.esri.com/software/cityengine/features>.
37. ESRI. *Industries-GIS, Urban Planning and Architecture*. 2018 [cited 2018 20.06]; Available from: <http://www.esri.com/software/cityengine/industries>.
38. ESRI. *The CityEngine Features*. 2018 [cited 2018 19.06]; Available from: <https://cehelp.esri.com/help/index.jsp?topic=/com.procedural.cityengine.help/html/quickstart/overview.html>.
39. Bentley. *Bentley Products*. 2018 [cited 2018 16.06]; Available from: <https://bentley.com/en>.
40. Bentley. *Bentley® Geo Web Publisher™: Easily Author and Deploy Web GIS Applications*. 2010 [cited 2018 15.06]; Available from: <https://www.bentley.com/-/media/91F548F2F68142F3BC7F384D5F03EE26.ashx>.
41. Bentley. *Singapore Land Authority*. 2015 [cited 2018 17.06]; Available from: https://www.bentley.com/en/project-profiles/singapore_land_authority_3d_mapping.
42. Satterthwaite, D. *Climate change and urbanization: Effects and implications for urban governance*. in *United Nations Expert Group meeting on population distribution, urbanization, internal migration and development*. 2008. DESA New York.
43. Karl, T.R. and K.E. Trenberth, *Modern global climate change*. *science*, 2003. **302**(5651): p. 1719-1723.

44. Kalnay, E. and M. Cai, *Impact of urbanization and land-use change on climate*. *microscope*, 1991. **352**: p. 600-603.
45. McCarthy, J.J., et al., *Climate change 2001: impacts, adaptation, and vulnerability: contribution of Working Group II to the third assessment report of the Intergovernmental Panel on Climate Change*. Vol. 2. 2001: Cambridge University Press.
46. Haines, A., et al., *Climate change and human health: impacts, vulnerability and public health*. *Public health*, 2006. **120**(7): p. 585-596.
47. Habitat, U., *Cities and climate change: Global report on human settlements 2011*. London: Earthscan, 2011.
48. Tanner, T., et al., *Urban governance for adaptation: assessing climate change resilience in ten Asian cities*. *IDS Working Papers*, 2009. **2009**(315): p. 01-47.
49. Ali-Toudert, F. and H. Mayer, *Numerical study on the effects of aspect ratio and orientation of an urban street canyon on outdoor thermal comfort in hot and dry climate*. *Building and environment*, 2006. **41**(2): p. 94-108.
50. Shishegar, N., *Street Design and Urban Microclimate: Analyzing the Effects of Street Geometry and Orientation on Airflow and Solar Access in Urban Canyons*. *Journal of clean energy technologies*, 2013. **1**(1).
51. Givoni, B., *Climate considerations in building and urban design*. 1998: John Wiley & Sons.
52. Bourbia, F. and F. Boucheriba, *Impact of street design on urban microclimate for semi arid climate (Constantine)*. *Renewable Energy*, 2010. **35**(2): p. 343-347.
53. Nakata, C., L.C.L. Souza, and D.S. Rodrigues. *A GIS extension model to calculate urban heat island intensity based on urban geometry*. in *The 14th International Conference on Computers in Urban Planning and Urban Management*. 2015. Joseph Ferreira, Jr. and Robert Goodspeed.
54. Voogt, J. *How researchers measure urban heat islands*. in *United States Environmental Protection Agency (EPA), State and Local Climate and Energy Program, Heat Island Effect, Urban Heat Island Webcasts and Conference Calls*. 2007.
55. Rizwan, A.M., L.Y. Dennis, and L. Chunho, *A review on the generation, determination and mitigation of Urban Heat Island*. *Journal of Environmental Sciences*, 2008. **20**(1): p. 120-128.
56. Oke, T.R., *The distinction between canopy and boundary-layer urban heat islands*. *Atmosphere*, 1976. **14**(4): p. 268-277.
57. Erell, E., D. Pearlmutter, and T. Williamson, *Urban microclimate: designing the spaces between buildings*. 2012: Routledge.
58. Oke, T., *The urban energy balance*.
59. Cleugh, H. and T. Oke, *Suburban-rural energy balance comparisons in summer for Vancouver, BC*. *Boundary-Layer Meteorology*, 1986. **36**(4): p. 351-369.
60. Cleugh, H. and S. Grimmond, *Urban climates and global climate change*. *The Future of the World's Climate (Second Edition)*, 2011: p. 47-76.
61. Hafner, J. and S.Q. Kidder, *Urban heat island modeling in conjunction with satellite-derived surface/soil parameters*. *Journal of applied meteorology*, 1999. **38**(4): p. 448-465.
62. Kondoh, A. and J. Nishiyama, *Changes in hydrological cycle due to urbanization in the suburb of Tokyo Metropolitan Area, Japan*. *Advances in Space Research*, 2000. **26**(7): p. 1173-1176.
63. Voogt, J.A. and C. Grimmond, *Modeling surface sensible heat flux using surface radiative temperatures in a simple urban area*. *Journal of Applied Meteorology*, 2000. **39**(10): p. 1679-1699.
64. Lemonsu, A. and V. Masson, *Simulation of a summer urban breeze over Paris*. *Boundary-Layer Meteorology*, 2002. **104**(3): p. 463-490.
65. Huang, H., R. Ooka, and S. Kato, *Urban thermal environment measurements and numerical simulation for an actual complex urban area covering a large district heating and cooling system in summer*. *Atmospheric Environment*, 2005. **39**(34): p. 6362-6375.

66. Kato, S. and Y. Yamaguchi, *Analysis of urban heat-island effect using ASTER and ETM+ Data: Separation of anthropogenic heat discharge and natural heat radiation from sensible heat flux*. Remote Sensing of Environment, 2005. **99**(1-2): p. 44-54.
67. Ashie, Y., V.T. Ca, and T. Asaeda, *Building canopy model for the analysis of urban climate*. Journal of wind engineering and industrial aerodynamics, 1999. **81**(1-3): p. 237-248.
68. Giridharan, R., et al., *Urban design factors influencing heat island intensity in high-rise high-density environments of Hong Kong*. Building and Environment, 2007. **42**(10): p. 3669-3684.
69. Kolokotroni, M. and R. Giridharan, *Urban heat island intensity in London: An investigation of the impact of physical characteristics on changes in outdoor air temperature during summer*. Solar energy, 2008. **82**(11): p. 986-998.
70. Wong, N.H. and S.K. Jusuf, *GIS-based greenery evaluation on campus master plan*. Landscape and urban planning, 2008. **84**(2): p. 166-182.
71. Taha, H., et al., *Residential cooling loads and the urban heat island—the effects of albedo*. Building and environment, 1988. **23**(4): p. 271-283.
72. Prado, R.T.A. and F.L. Ferreira, *Measurement of albedo and analysis of its influence the surface temperature of building roof materials*. Energy and Buildings, 2005. **37**(4): p. 295-300.
73. Oke, T.R., *Canyon geometry and the nocturnal urban heat island: comparison of scale model and field observations*. International Journal of Climatology, 1981. **1**(3): p. 237-254.
74. Solarairheating. *Intro to solar heating*. [cited 2018 25.05]; Available from: <http://solarairheating.org/intro-to-solar-heating/>.
75. Taylor, B. and P. Guthrie. *The first line of defence: Passive design at an urban scale*. in *Proceedings of Conference: Air Conditioning and the Low Carbon Cooling Challenge, Cumberland Lodge, Windsor, UK*. 2008.
76. Santamouris, M., et al., *Thermal and air flow characteristics in a deep pedestrian canyon under hot weather conditions*. Atmospheric Environment, 1999. **33**(27): p. 4503-4521.
77. Peterson, J.T. *The climate of cities: a survey of recent literature*. in *National Air Pollution Control Administration Publication No. AP-59*. 1969. Citeseer.
78. Taha, H., D. Sailor, and H. Akbari, *High-albedo materials for reducing building cooling energy use*. 1992.
79. Pigeon, G., et al., *Anthropogenic heat release in an old European agglomeration (Toulouse, France)*. International Journal of Climatology, 2007. **27**(14): p. 1969-1981.
80. Urano, A., T. Ichinose, and K. Hanaki, *Thermal environment simulation for three dimensional replacement of urban activity*. Journal of Wind Engineering and Industrial Aerodynamics, 1999. **81**(1-3): p. 197-210.
81. Gómez, F., J. Jabaloyes, and E. Vano, *Green zones in the future of urban planning*. Journal of urban planning and development, 2004. **130**(2): p. 94-100.
82. Iso, E., *7730: 2005*. Ergonomics of the thermal environment-Analytical determination and interpretation of thermal comfort using calculation of the PMV and PPD indices and local thermal comfort criteria, 2005.
83. Maruani, T. and I. Amit-Cohen, *Open space planning models: A review of approaches and methods*. Landscape and urban planning, 2007. **81**(1-2): p. 1-13.
84. Givoni, B., et al., *Outdoor comfort research issues*. Energy and buildings, 2003. **35**(1): p. 77-86.
85. Ali-Toudert, F. and H. Mayer, *Thermal comfort in an east–west oriented street canyon in Freiburg (Germany) under hot summer conditions*. Theoretical and Applied Climatology, 2007. **87**(1-4): p. 223-237.
86. Pickup, J. and R. de Dear. *An outdoor thermal comfort index (OUT_SET*)-part I-the model and its assumptions*. in *Biometeorology and urban climatology at the turn of the millenium. Selected papers from the Conference ICB-ICUC*. 2000.

87. Johansson, E. and R. Emmanuel, *The influence of urban design on outdoor thermal comfort in the hot, humid city of Colombo, Sri Lanka*. International journal of biometeorology, 2006. **51**(2): p. 119-133.
88. Lin, T.-P., A. Matzarakis, and R.-L. Hwang, *Shading effect on long-term outdoor thermal comfort*. Building and Environment, 2010. **45**: p. 213-221.
89. Hwang, R.-L., T.-P. Lin, and A. Matzarakis, *Seasonal effects of urban street shading on long-term outdoor thermal comfort*. Building and Environment, 2011. **46**(4): p. 863-870.
90. Chen, L. and E. Ng, *Outdoor thermal comfort and outdoor activities: A review of research in the past decade*. Cities, 2012. **29**: p. 118-125.
91. Gulyás, Á., J. Unger, and A. Matzarakis, *Assessment of the microclimatic and human comfort conditions in a complex urban environment: modelling and measurements*. Building and Environment, 2006. **41**(12): p. 1713-1722.
92. ISO, I., *7726, Ergonomics of the thermal environment, instruments for measuring physical quantities*. Geneva: International Standard Organization, 1998.
93. ASHRAE, A., *Standard 55-2010: Thermal Environmental Conditions for Human Occupancy. 2010*. American Society of heating, Refrigerating and Airconditioning Engineers: Atlanta.
94. Nikolopoulou, M., *Designing open spaces in the urban environment: a bioclimatic approach*. 2004: Centre for Renewable Energy Sources, EESD, FP5.
95. Chu, Y.-C., M.-F. Hsu, and C.-M. Hsieh, *A Field Assessment on Natural Ventilation and Thermal Comfort of Historical District—A Case of the Wugoushui Settlement in Taiwan*. Journal of Earth Science and Engineering, 2015. **5**: p. 463-472.
96. Ahmed, K.S., *Comfort in urban spaces: defining the boundaries of outdoor thermal comfort for the tropical urban environments*. Energy and Buildings, 2003. **35**(1): p. 103-110.
97. Oke, T., *Boundary Layer Climates*. Vol. 5. 1987: Psychology Press.
98. Handbook, A., *Fundamentals*. American Society of Heating, Refrigerating and Air Conditioning Engineers, Atlanta, 2001. **111**.
99. Gaitani, N., G. Mihalakakou, and M. Santamouris, *On the use of bioclimatic architecture principles in order to improve thermal comfort conditions in outdoor spaces*. Building and Environment, 2007. **42**(1): p. 317-324.
100. ISO, B., *8996: 2004 Ergonomics of the thermal environment—determination of metabolic rate*. BSI, London, 2004.
101. Landsberg, L., et al., *Do the obese have lower body temperatures? A new look at a forgotten variable in energy balance*. Transactions of the American Clinical and Climatological Association, 2009. **120**: p. 287.
102. Havenith, G., I. Holmér, and K. Parsons, *Personal factors in thermal comfort assessment: clothing properties and metabolic heat production*. Energy and buildings, 2002. **34**(6): p. 581-591.
103. 9920, I., *Ergonomics of the thermal environment in Estimation of thermal insulation and water vapour resistance of a clothing ensemble*. 2007.
104. Clark, R. and O.G. Edholm, *Man and his thermal environment*. 1985: Edward Arnold.
105. Nikolopoulou, M. and S. Lykoudis, *Thermal comfort in outdoor urban spaces: analysis across different European countries*. Building and Environment, 2006. **41**(11): p. 1455-1470.
106. Nagano, K. and T. Horikoshi, *New index indicating the universal and separate effects on human comfort under outdoor and non-uniform thermal conditions*. Energy and Buildings, 2011. **43**(7): p. 1694-1701.
107. Fanger, P., *Thermal comfort: analysis and applications in environmental engineering*. 1982.
108. Ismail, A., et al., *Thermal comfort assessment and optimization of environmental factors by using Taguchi method*. American Journal of Applied Sciences, 2009. **6**(9): p. 1731-1741.
109. Cheng, V., et al., *Outdoor thermal comfort study in a sub-tropical climate: a longitudinal study based in Hong Kong*. International Journal of Biometeorology, 2012. **56**(1): p. 43-56.

110. Nikolopoulou, M., N. Baker, and K. Steemers, *Thermal comfort in outdoor urban spaces: understanding the human parameter*. Solar energy, 2001. **70**(3): p. 227-235.
111. Thorsson, S., M. Lindqvist, and S. Lindqvist, *Thermal bioclimatic conditions and patterns of behaviour in an urban park in Göteborg, Sweden*. International Journal of Biometeorology, 2004. **48**(3): p. 149-156.
112. Höppe, P., *Heat balance modelling*. Experientia, 1993. **49**(9): p. 741.
113. Höppe, P., *The physiological equivalent temperature—a universal index for the biometeorological assessment of the thermal environment*. International journal of Biometeorology, 1999. **43**(2): p. 71-75.
114. VDI, V., *3787, Part I: Environmental Meteorology, Methods for the Human Biometeorological Evaluation of Climate and Air Quality for the Urban and Regional Planning at Regional Level. Part I: Climate*. Part I: Climate. Beuth, Berlin, 1998.
115. Thorsson, S., et al., *Different methods for estimating the mean radiant temperature in an outdoor urban setting*. International journal of climatology, 2007. **27**(14): p. 1983-1993.
116. Huang, J., J. Cedeño-Laurent, and J. Spengler, *CityComfort+: A Simulation-Based Method for Predicting Mean Radiant Temperature in Dense Urban Areas*. Building and Environment, 2014.
117. Toudert, F.A., *Dependence of outdoor thermal comfort on street design in hot and dry climate*. 2005: Meteorologisches Institut der Universität Freiburg.
118. Kántor, N. and J. Unger, *The most problematic variable in the course of human-biometeorological comfort assessment—the mean radiant temperature*. Open Geosciences, 2011. **3**(1): p. 90-100.
119. Bergman, T.L., et al., *Fundamentals of heat and mass transfer*. 2011: John Wiley & Sons.
120. Martinez, I., *Radiative View Factors*. 1995-2018.
121. Brasebin, M., et al., *Measuring the impact of 3D data geometric modeling on spatial analysis: Illustration with Skyview factor*. Usage, Usability, and Utility of 3D City Models—European COST Action TU0801, 2012: p. 02001.
122. Unger, J., *Connection between urban heat island and sky view factor approximated by a software tool on a 3D urban database*. International Journal of Environment and Pollution, 2008. **36**(1-3): p. 59-80.
123. Lindberg, F., B. Holmer, and S. Thorsson, *SOLWEIG 1.0—Modelling spatial variations of 3D radiant fluxes and mean radiant temperature in complex urban settings*. International journal of biometeorology, 2008. **52**(7): p. 697-713.
124. Rakha, T., P. Zhand, and C. Reinhart, *A Framework for Outdoor Mean Radiant Temperature Simulation: Towards Spatially Resolved Thermal Comfort Mapping in Urban Spaces*.
125. Zacharias, J., T. Stathopoulos, and H. Wu, *Microclimate and downtown open space activity*. Environment and Behavior, 2001. **33**(2): p. 296-315.
126. Kikegawa, Y., et al., *Impacts of city-block-scale countermeasures against urban heat-island phenomena upon a building's energy-consumption for air-conditioning*. Applied Energy, 2006. **83**(6): p. 649-668.
127. Shashua-Bar, L., D. Pearlmutter, and E. Erell, *The influence of trees and grass on outdoor thermal comfort in a hot-arid environment*. International Journal of Climatology, 2011. **31**(10): p. 1498-1506.
128. Müller, N., W. Kuttler, and A.-B. Barlag, *Counteracting urban climate change: adaptation measures and their effect on thermal comfort*. Theoretical and Applied Climatology, 2014. **1**(115): p. 243-257.
129. Memon, R.A., D.Y. Leung, and L. Chunho, *A review on the generation, determination and mitigation of Urban Heat Island*. Journal of Environmental Sciences, 2008. **1**: p. 020.
130. Kolokotroni, M., I. Giannitsaris, and R. Watkins, *The effect of the London urban heat island on building summer cooling demand and night ventilation strategies*. Solar Energy, 2006. **80**(4): p. 383-392.

131. Autodesk. *Solar Radiation Metrics Part-1*. Apr 27 2018 [cited 2018 19.06]; Available from: <https://knowledge.autodesk.com/support/revit-products/learn-explore/caas/simplecontent/content/solar-radiation-metrics-part-1.html>.
132. Autodesk. *Project Parameters*. 2018 [cited 2018 25.06]; Available from: <https://knowledge.autodesk.com/support/revit-products/getting-started/caas/CloudHelp/cloudhelp/2016/ENU/Revit-Model/files/GUID-24033B80-62D4-4E04-AC15-FA8A6194A64F-htm.html>.
133. An, N., S. Hemmati, and Y.-J. Cui, *Assessment of the methods for determining net radiation at different time-scales of meteorological variables*. Journal of Rock Mechanics and Geotechnical Engineering, 2017. **9**(2): p. 239-246.
134. OMEGA. *Emissivity of Common Materials*. [cited 2018 25.06]; Available from: <https://www.omega.com/literature/transactions/volume1/emissivityb.html>.
135. McEvoy, A., et al., *Practical handbook of photovoltaics: fundamentals and applications*. 2003: Elsevier.
136. Wikipedia. *List of thermal conductivities*. [cited 2018 25.06].
137. Protimeter. *Protimeter MMS2*. 2018 [cited 2018 18.07]; Available from: <https://www.amphenol-sensors.com/microsites/protimeter/MMS2>.
138. Wikipedia. *Quadratic Function*. 2018 [cited 2018 05.03]; Available from: https://en.wikipedia.org/wiki/Quartic_function.

ANNEXES

ANNEX A

ANEXO A DYNAMO CODE

In this attachment the Dynamo code behind the tool will be explained. The code is divided in four modules:

- *Initial Data*: where the tool will acquire the basic inputs;
- *View Factors*: Sky View Factor and View Factor between person and surface used for calculation of the heat exchange;
- *Surface Temperature* for calculating the hourly change in surface temperature; and finally
- Mean Radiant Temperature calculation section.

A.1 Initial Data

The structure of the initial data involves three parts as shown in Figure 4:

- Importing Solar Analysis (in blue);
- Parameters extraction from initial data (green on top); and
- Separation of the Floor and Wall elements (light green on bottom).

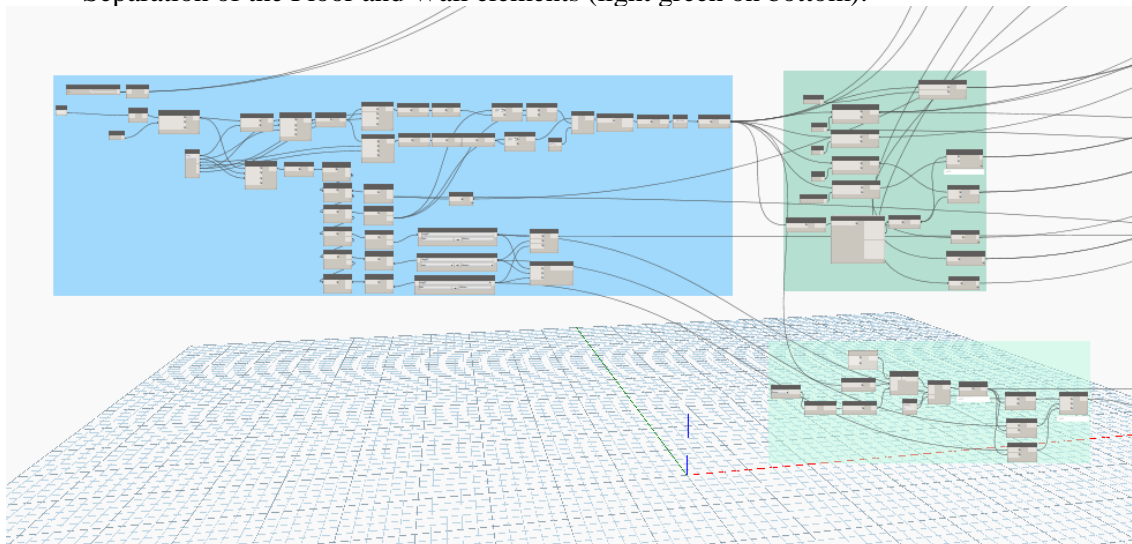


Figure A. 1. Initial Data structure.

A.1.1 IMPORTING SOLAR ANALYSIS RESULTS

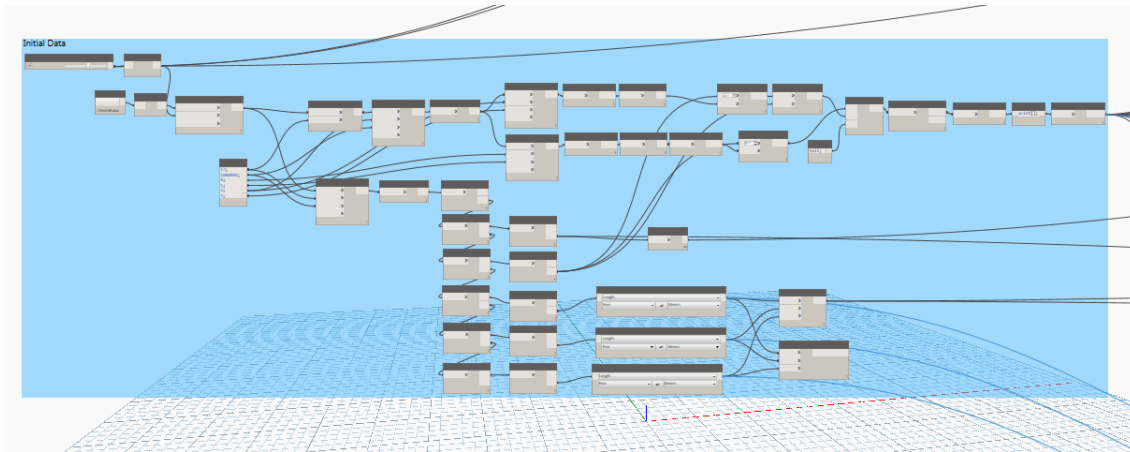


Figure A. 2. Node group for importing Solar Analysis Results.

The tool workflow begins with extracting, from the Excel file, information about the solar radiation and the related X, Y, Z coordinates for each analytical point. *Analytical point* is a unit containing information about the physical characteristic of a given point in the space. It may belong to a surface or be suspended in the air. In this work analytical points structured in grids will be used to describe the interaction between urban surfaces.

From the Excel file a list is imported by numbers for each frame. For example, values from 9:00-11:00 are assigned to the number 1, from 11:00-12:00 to number 2 and so on. For each frame the surface received heat and used it to calculate the temperature for the time frame and recorded the heating in the surface that will serve as beginning point for the next time frame. This allows the correct transferring of heat from the first time interval to the second, from the second to the third etc.

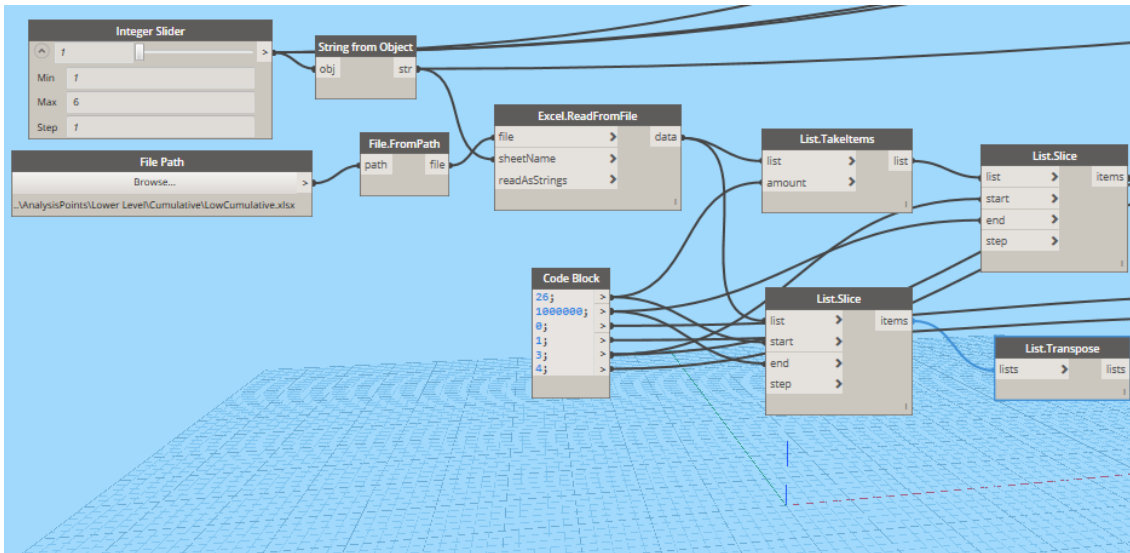


Figure A. 3. Extraction of data from excel file.

The information in Excel includes three parts with:

- *general information* about the data of the analysis, surface area, study time and location.
- information about the category, average insolation, element ID and total surface area, and;
- information about the solar radiation and coordinates.

| A | B | C | D | E | F | G | H | I | J | K | L | M | N |
|----------------------|--------------------|----------------|------------------|------------------|----------------------|---------------|------------------|--------------|-----------------|-------------|----------|--------|----------------------|
| Source | Date | Time | Model | Type | Study Average Inzolt | Total Study S | Total Study In | Study Date F | Study Time Flar | Longitud | Latitude | Unit | |
| Revit 2016 | 21/07/2018 | | 14:04 | Trinidadsdc1.rvt | Cumulati | 553.18036397 | 10476.144 | 5735197.4 | 15/07/2018,1 | 13:00,14:00 | -8.603 | 41.152 | Wh/m ² A' |
| Analysis Surface | Parent object type | Category | Parent object ID | Average | Surface Area | Total Surface | Inzolation Value | | | | | | |
| 1254917600 | Wall | Walls | 304233 | 299.27 | 2121.856328 | 635002.38 | | | | | | | |
| 1250343840 | Wall | Walls | 305854 | 312.57 | 3823.000102 | 1194358.1 | | | | | | | |
| 1250339600 | Wall | Walls | 306274 | 35.178 | 3850.433254 | 366477.27 | | | | | | | |
| 1250337360 | Wall | Walls | 306674 | 341.36 | 502.1377322 | 171409.51 | | | | | | | |
| 1250331040 | Wall | Walls | 311290 | 83.663 | 1905.588328 | 153427.18 | | | | | | | |
| 1217139056 | Floor | Floors | 312523 | 663.73 | 33500.38858 | 26217632 | | | | | | | |
| 1216661520 | Floor | Floors | 312842 | 625.31 | 6423.718157 | 4020578.4 | | | | | | | |
| 1217135776 | Wall | Walls | 312364 | 294.06 | 531.0933013 | 173814.16 | | | | | | | |
| 1250334480 | Wall | Walls | 314336 | 323.31 | 340.4338118 | 309714.46 | | | | | | | |
| 1217806720 | Wall | Walls | 316518 | 112.25 | 182.1508574 | 20447.052 | | | | | | | |
| 1217808480 | Wall | Walls | 316588 | 354.51 | 186.6856012 | 66181.59 | | | | | | | |
| 1217675408 | Floor | Floors | 328576 | 747.88 | 34801.29722 | 26027110 | | | | | | | |
| 1217137456 | Floor | Floors | 328736 | 712.36 | 8610.886393 | 6139254.9 | | | | | | | |
| 1217810240 | Wall | Walls | 333397 | 345.41 | 1122.274054 | 387644.56 | | | | | | | |
| 1217811520 | Wall | Walls | 334254 | 292.23 | 2172.432077 | 634850.57 | | | | | | | |
| 1217813840 | Wall | Walls | 334349 | 283.32 | 237.3209934 | 84235.743 | | | | | | | |
| 1217815520 | Wall | Walls | 334477 | 104.32 | 1109.806236 | 116442.28 | | | | | | | |
| 1217815840 | Wall | Walls | 334477 | ### | 116.3364505 | -0.0003892 | | | | | | | |
| 1217817320 | Wall | Walls | 334739 | 110.68 | 2154.343937 | 238438.36 | | | | | | | |
| 1217818000 | Wall | Walls | 334739 | 320.35 | 2155.584858 | 630533.54 | | | | | | | |
| 1217820080 | Wall | Walls | 335014 | 107.23 | 130.4335581 | 20432.133 | | | | | | | |
| Analysis point index | Inzolation value | Parent surface | point x | point y | point z | normal x | normal y | normal z | | | | | |
| 1 | 307.5461426 | 1254917600 | 116139.657 | 234566 | 15.58527403 | 0.1500441 | -0.3886793 | 0 | | | | | |
| 2 | 180.355957 | 1254917600 | 116156.349 | 234566 | 15.58527403 | 0.1500441 | -0.3886793 | 0 | | | | | |
| 3 | 296.6645203 | 1254917600 | 116173.041 | 234571 | 15.58527403 | 0.1500441 | -0.3886793 | 0 | | | | | |
| 4 | 331.4502258 | 1254917600 | 116189.7331 | 234573 | 15.58527403 | 0.1500441 | -0.3886793 | 0 | | | | | |
| 5 | 338.2103271 | 1254917600 | 116206.4251 | 234576 | 15.58527403 | 0.1500441 | -0.3886793 | 0 | | | | | |
| 6 | 341.3765863 | 1254917600 | 116223.1171 | 234579 | 15.58527403 | 0.1500441 | -0.3886793 | 0 | | | | | |
| 7 | 325.3838806 | 1250343840 | 116111.7375 | 234571 | 16.405484 | -0.3530278 | -0.3028827 | 0 | | | | | |
| 8 | 324.1086426 | 1250343840 | 116106.5784 | 234587 | 16.405484 | -0.3530278 | -0.3028827 | 0 | | | | | |
| 9 | 321.3973858 | 1250343840 | 116101.4192 | 234604 | 16.405484 | -0.3530278 | -0.3028827 | 0 | | | | | |
| 10 | 319.5127563 | 1250343840 | 116036.2601 | 234620 | 16.405484 | -0.3530278 | -0.3028827 | 0 | | | | | |

1st

2nd

3rd

Figure A. 4. Excel file produced by Solar Analysis.

The information in the first part is not needed or useful so it was not considered.

The information of the second part allows relating the analytical surface containing the analytical points with the element ID to obtain the needed element parameters needed for the calculation of the surface temperature like albedo, emissivity, density, heat capacity and thermal conductivity. One needs this step because the third part have no information about the element ID. This algorithm assigns *Parent object ID* when Analysis Surface in part 2 is equal to Parent surface in part 3.

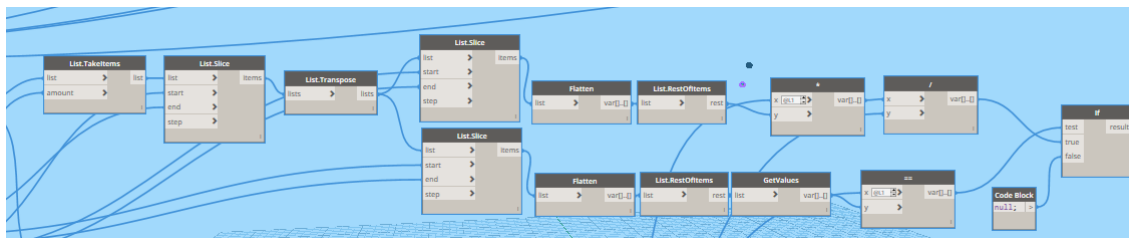


Figure A. 5. Attributing element ID to analytical points

The information from the third part is deconstructed into separated lists containing the solar radiation value and X, Y, Z coordinates. As Insight Solar Analysis export the coordinates in *feet* they must be transfer to *meters* in order for this tool to work in standard international units.

From X, Y and Z values points and coordinate system are formed.

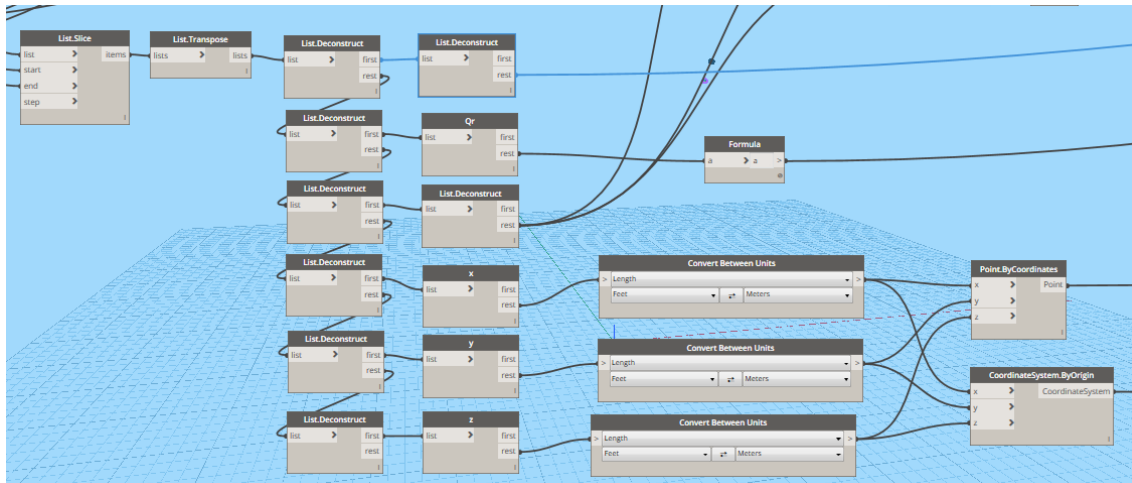


Figure A. 6. Separating information of analytical point into solar radiation with corresponding X, Y, Z values.

The result of this node group is:

- list of solar radiation values;
- list of coordinates for each value;
- list of element ID for each analytical point, and;
- corresponding number analytical point.

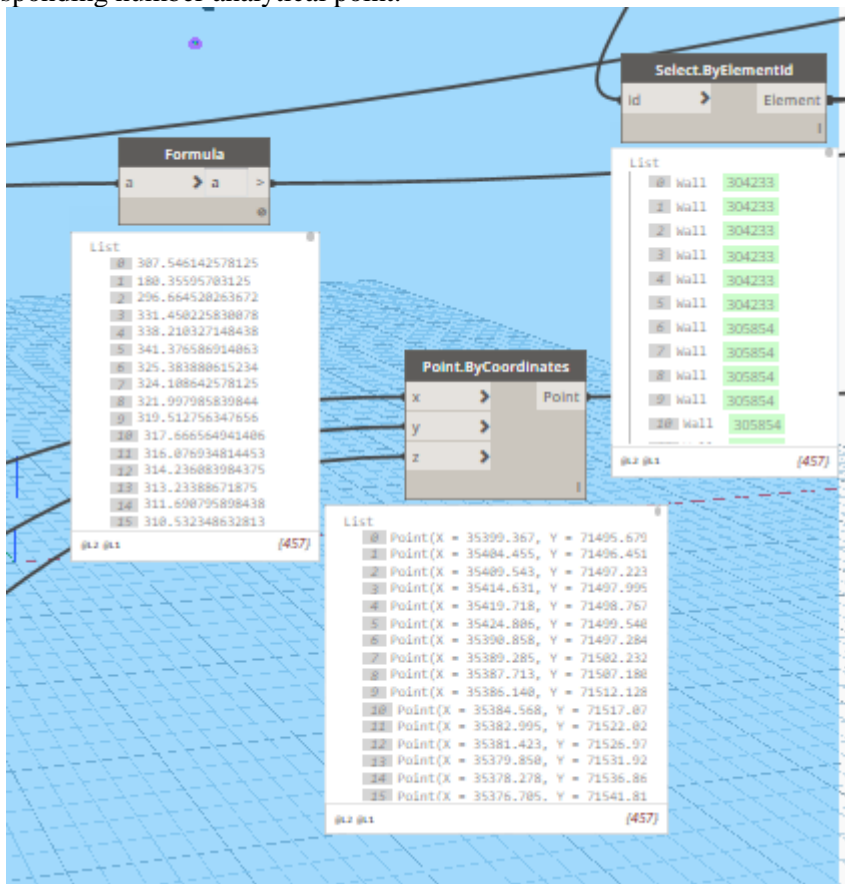


Figure A. 7. End result of the data extraction from the excel file.

A.1.2 PARAMETERS EXTRACTION FROM INITIAL DATA

From the Element ID parameters like emissivity and albedo can be extracted using *Element.GetParameterValueByName* node. It requires information input about the element and the name of the needed parameter and returns a numerical value for each analytical point. After the extraction the values are used as needed in the formulas as shown in Figure A. 8.

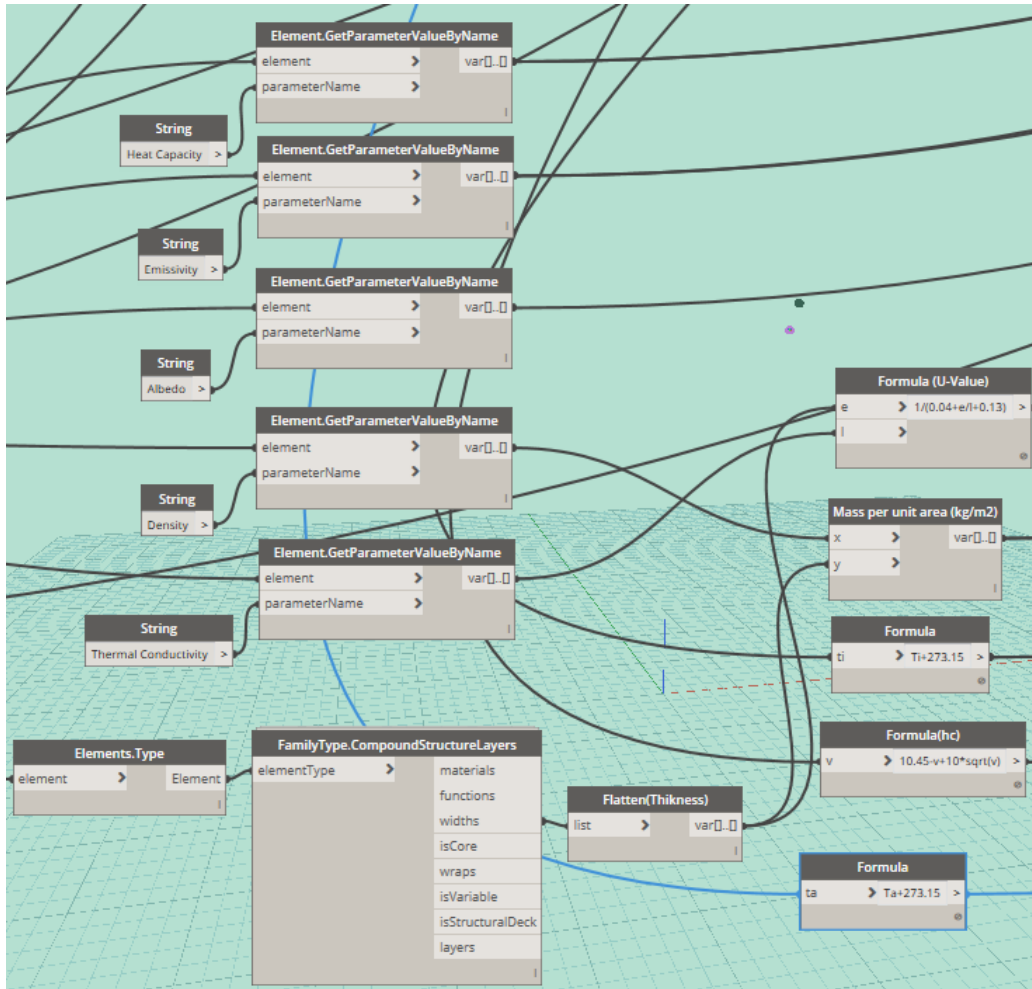


Figure A. 8. Getting the thermal parameters for each analytical point.

A.1.3 SEPARATION OF WALL AND FLOOR ELEMENTS

Mean Radiant Temperature is calculated on a surface parallel to the floor and height of 1,5m above the ground- average person core height. It is necessary to separated the Walls from Floors in order to obtain the point where human body can be placed in the space- Floors and the points form which will receive heat – Walls and Floors.

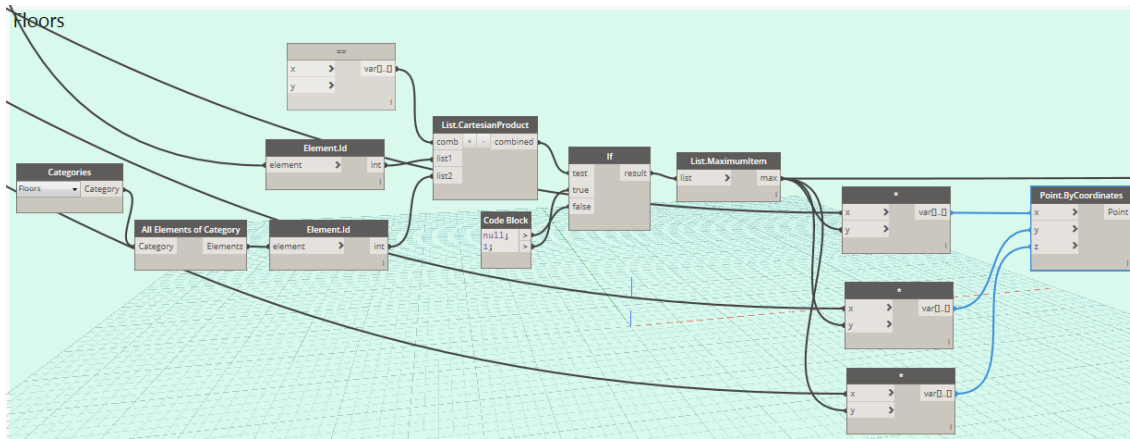


Figure A. 9. Separation of the Floors and Walls elements.

A.2 Sky View Factor

This section gives explanation about the node groups for the calculation of the Sky View Factor (SVF).

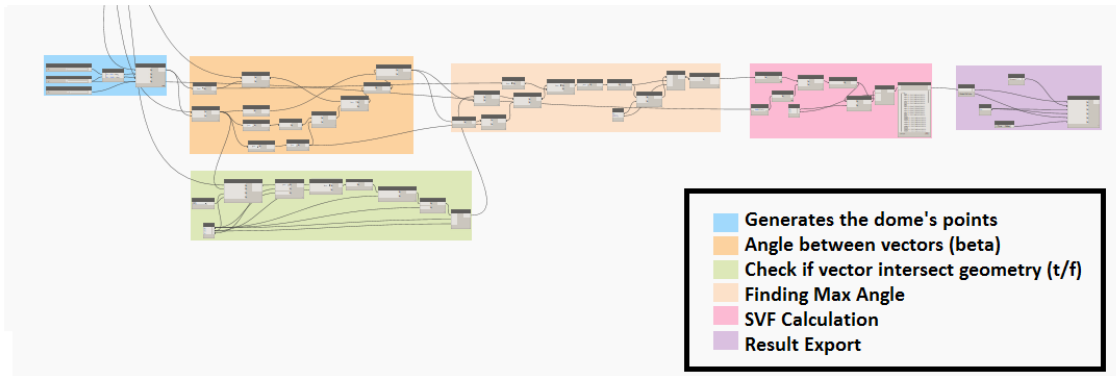


Figure A. 10. Node groups for SVF.

A.2.1 GENERATING DOME AROUND EACH ANALYTICAL POINT

Point.BySphericalCoordinates node is used to generate a dome with a given number of points. After this in the file “cs”, the coordinate system from Initial Data is connected to generate and create this dome around each analytical point.

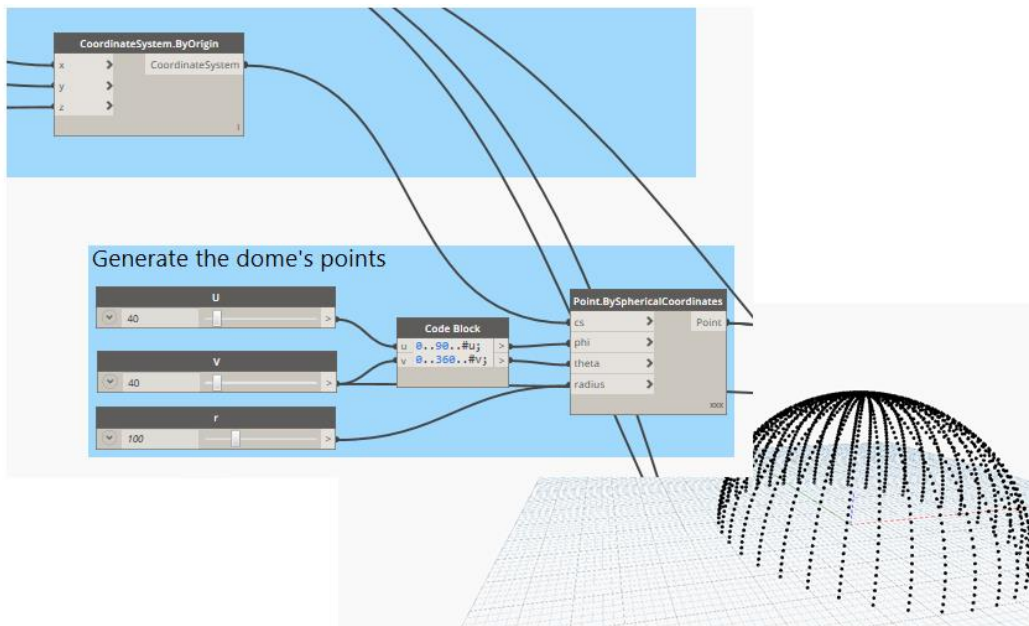


Figure A. 11. Generating dome's points.

A.2.2 DEFINING ANGLE BETWEEN VECTORS

Vectors are created from the centre analytical point to each point of the dome. The angle between vectors in the X, Y plane and every other vector above is calculated.

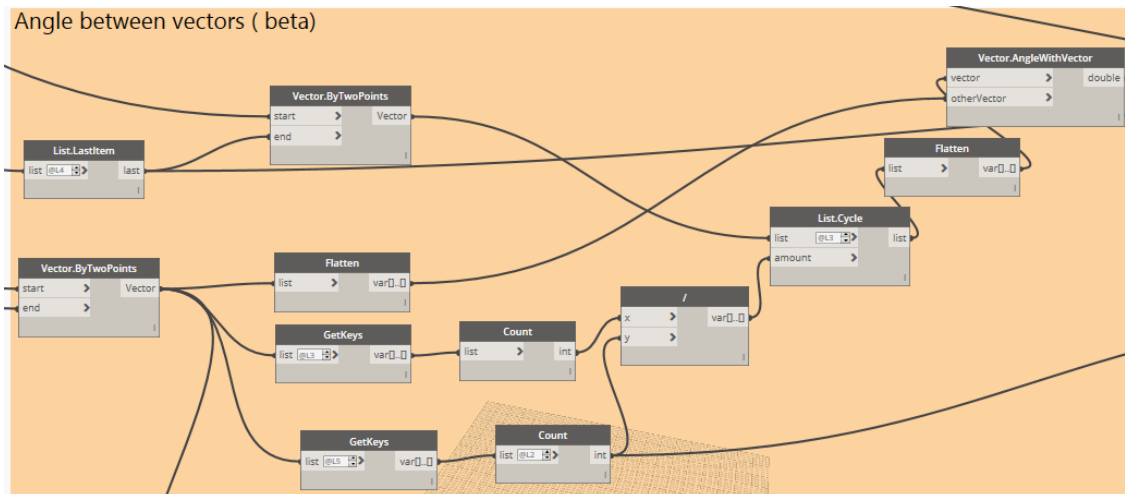


Figure A. 12. Finding the angle between vectors.

A.2.3 CHECK IF VECTORS INTERSECT GEOMETRY

With the help of the *RayBounce.ByOriginDirection* node, one verifies if the vectors origin-point intersect any surface and records the result as true or false.

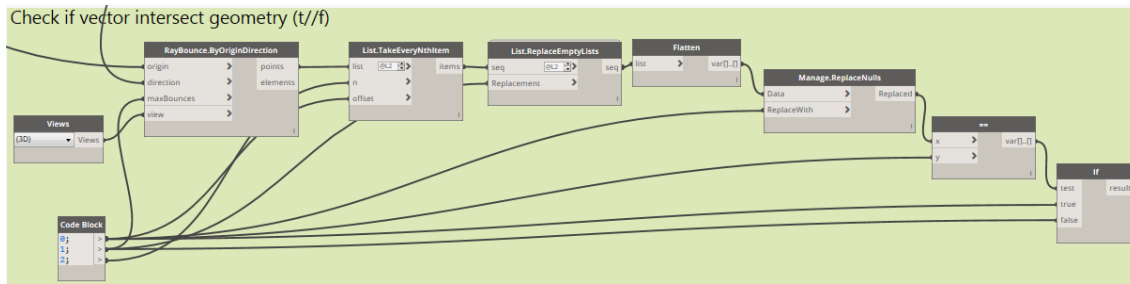


Figure A. 13. Check if vectors intersects with geometry.

A.2.4 FINDING MAXIMUM VALUE OF ANGLE

With the results from the previous two steps the highest intersecting vector and its angle with the base vector is selected and recorded in order to simulate the highest point of the urban surface that obstruct the view to the sky from a given observation point.

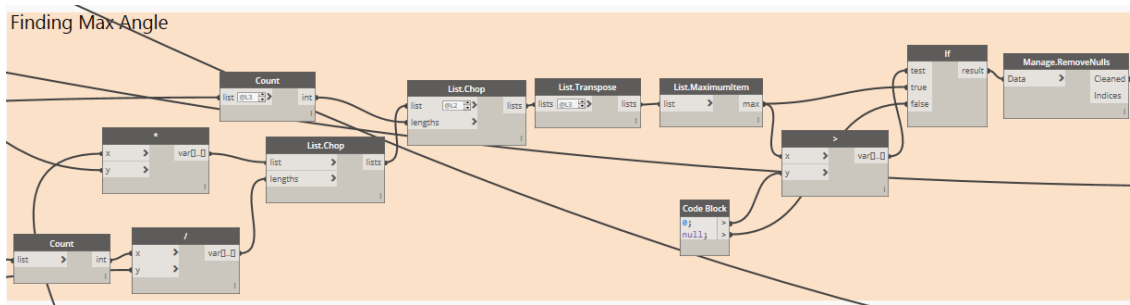


Figure A. 14. Finding maximum angle for SVF calculation.

A.2.5 CALCULATION OF SKY VIEW FACTOR

The Sky View Factor Calculation involves multiplying the quadrate of the sinus of the highest angle by the number of the dome’s horizontal divisions. These values are summed and the null values corresponding to “no angle of intersection” or clear sky are changed to the value 1.

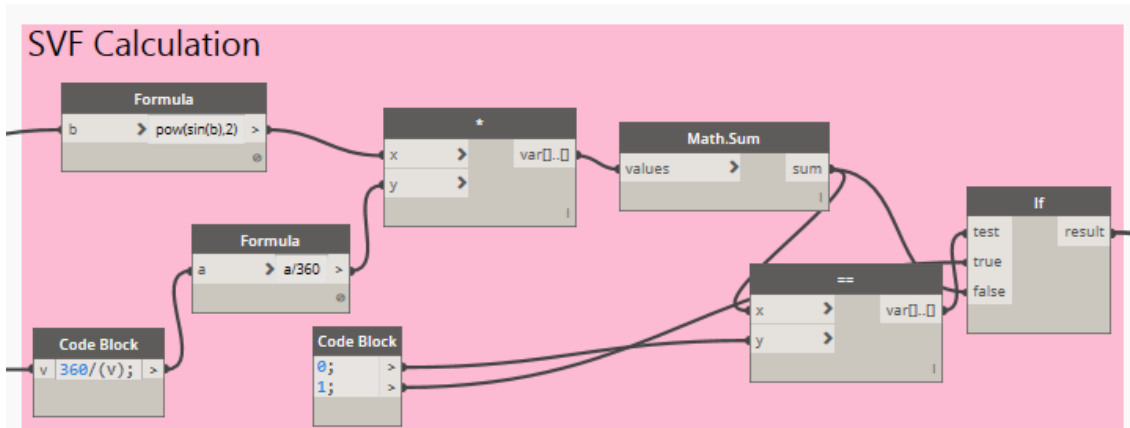


Figure A. 15. Calculation of the Sky View Factor.

A.2.6 RESULT EXPORT

Finally, the result is exported in excel file that will be used in the calculation of the Surface Temperature.

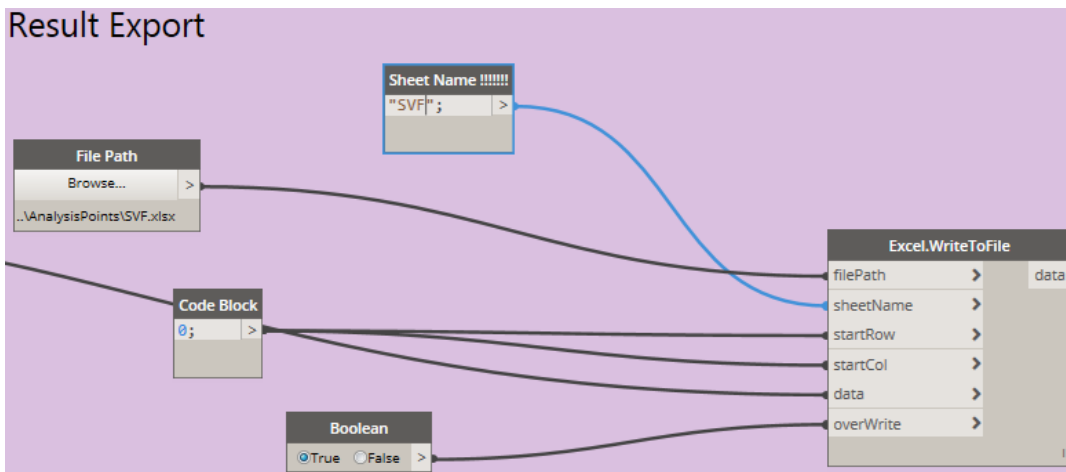


Figure A. 16. Exporting the results of the SVF calculation to excel file.

A.3 Surface Temperature

A.3.1 ENVIRONMENTAL PARAMETERS

The tool need information about the weather conditions in order to run. These can be constants or in this case the measured air temperature and humidity in the interval from 9:00 to 17:00. The information is recorded on two separate Excel Sheet with the flowing data:

Table A. 1 Measured Air Temperature and Humidity recorded at the case study location.

| index | Time frame | Air Temperature Sheet (°C) | Humidity Sheet (%) |
|-------|-------------|----------------------------|--------------------|
| 1 | 9:00-11:00 | 24.2 | 71.4 |
| 2 | 11:00-12:00 | 25.6 | 65.6 |
| 3 | 12:00-13:00 | 30 | 61.2 |
| 4 | 13:00-14:00 | 31.4 | 58.5 |
| 5 | 14:00-15:00 | 30.5 | 57.8 |
| 6 | 15:00-17:00 | 30.7 | 57.3 |

Excel.ReadFromFile is used to pull out the information. The output is divided in six separate lists and node Flatten must be used to obtain only one list with these six values. Then the node *List.GetItemAtIndex* is used to obtain only one value for the desired time frame, whose corresponding index is the same as the one used in Initial Data group. There are also some constant values that can be in the Other Parameters group that are needed to run the tool it includes information about wind speed, level of cloudiness and *Tinical* and *Tinternal* are respectively the initial temperature of the surface and the internal soil/air temperature.

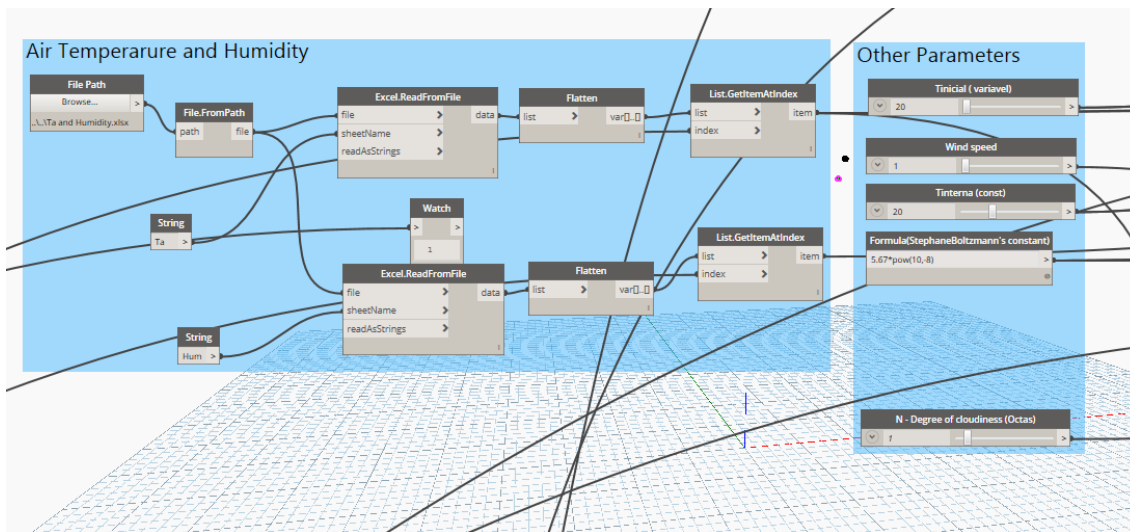


Figure A. 17. Node group for extracting air temperature humidity and other basic meteorological parameters.

A.3.2 INTERNAL TEMPERATURE

T_{internal} is considered constant for all time frame with the difference that the soil temperature is slightly colder than the air temperature. The purpose of this node group is to separate the Floors elements from the Walls and assign slightly different Internal Temperature for the Floors. This node is still to be developed as it assumes that a Wall has air on both sided and the Floor elements lay on soil which is not always the case.

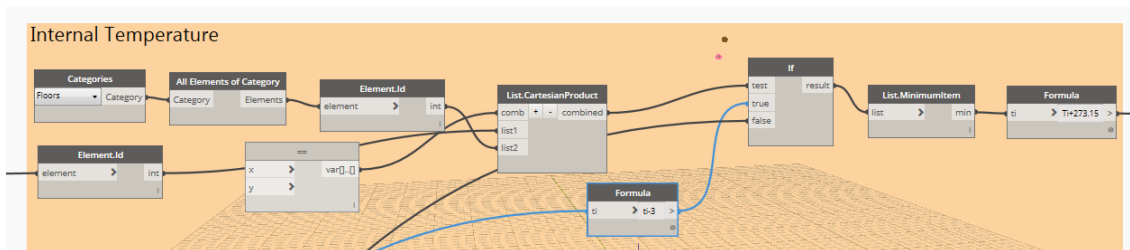


Figure A. 18. Internal Temperature node group

A.3.3 INITIAL TEMPERATURE

In the first time frame *T_{initial}* is equal to given value and for each following time frame is equal to the output of the previous time frame. As it will be show in the last paragraph of this section the *Surface Temperature* output is recorded in “Results” file with number from 1 to 6 for each interval. When the time interval in Initial data is set to 1 it means that there is still no information for the Initial Temperature and estimated value must be given from *Other Parameters* node group. The *If* node verifies if the value of the time frame in Initial Data is equal to 1. If it is true, the value form Other Parameters group is taken if not the value from the result file is used at index Initial Data time frame -1. For example, in the 2nd time frame we will have the data from the first. So, this node will take the information from “Results” file at index 2-1=1.

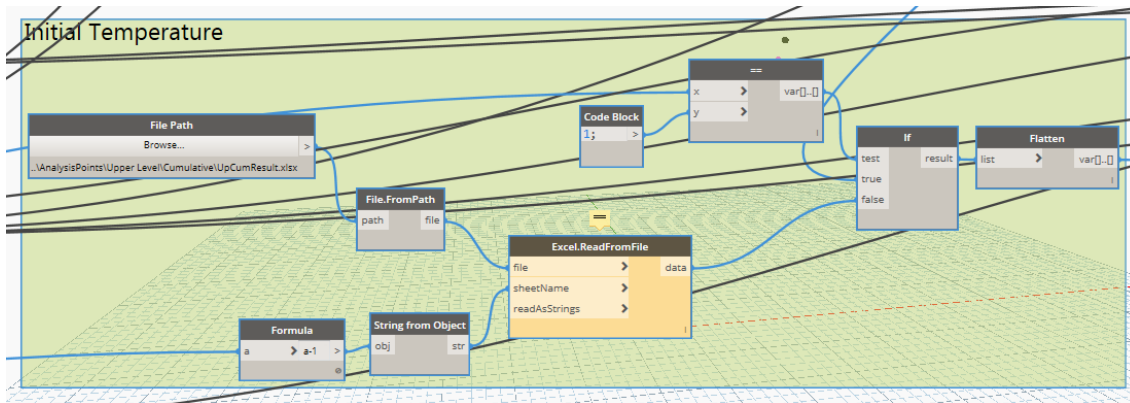


Figure A. 19. Initial temperature node group.

Note that in the 1st time frame there is no Sheet corresponding to the name 1-1=0 and this is why the *Excel.ReadFromFile* node is activated only in the second time frame from Initial Data.

A.3.4 IMPORTING SVF

In this node group the data obtained in the Sky View Factor paragraph is imported and flattened in order to be used directly in formulas.

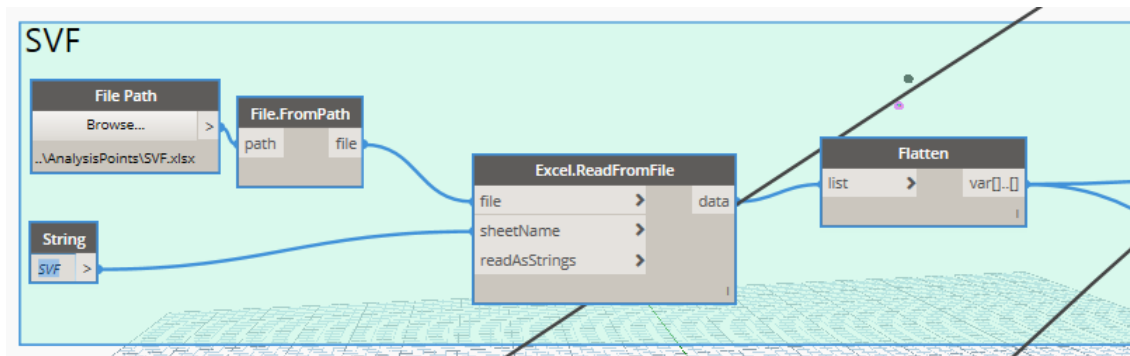


Figure A. 20. Importing SVF from excel file.

A.3.5 CALCULATING SURFACE TEMPERATURE

The calculation of the Surface Temperature is done by imputing the previously obtained parameters in formulas.

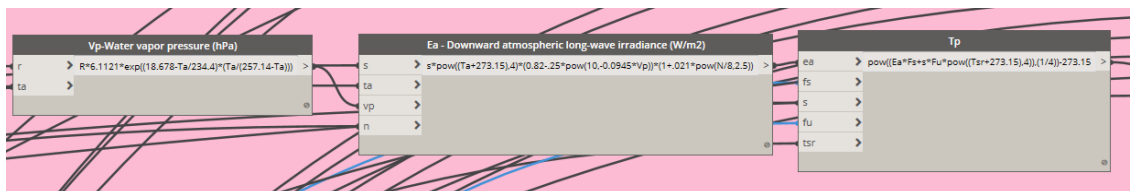


Figure A. 21. Calculations of Surface Temperature.

Dynamo does not possess a mathematical solver so, solution for incognita of 4th root equation it was created. It has the format of $AX^4 + BX + C=0$ as show on the figure below.

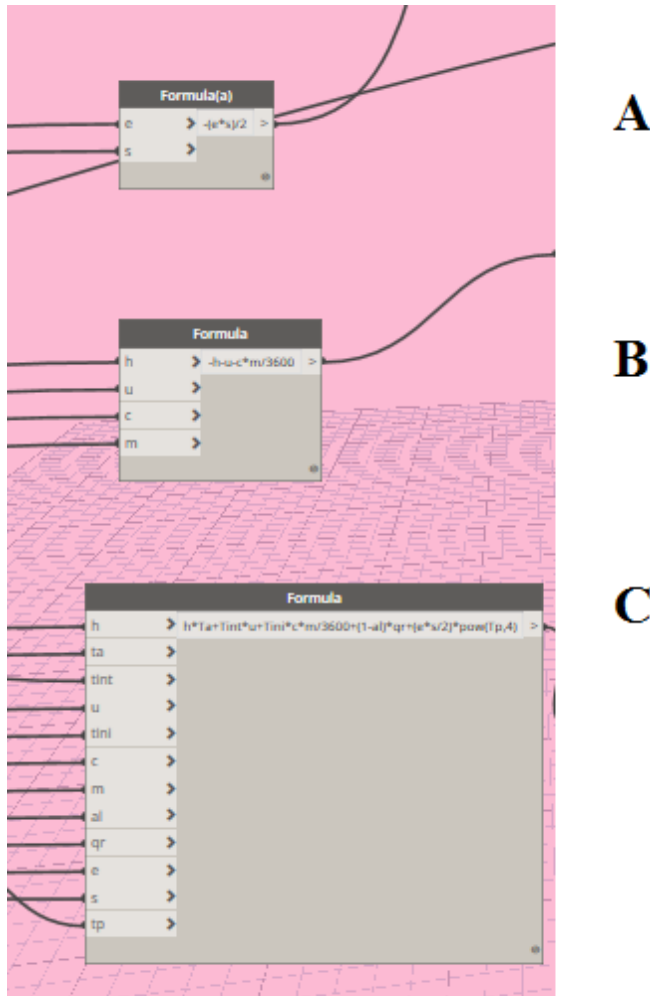


Figure A. 22. Calculating constants for quadratic function.

After the values of A, B and C were obtained they were included in the solution for the quadratic function equation using the formulas found in [138]. There are 4 possible outputs but only one is usable. The other 3 are or negative or non-real numbers.

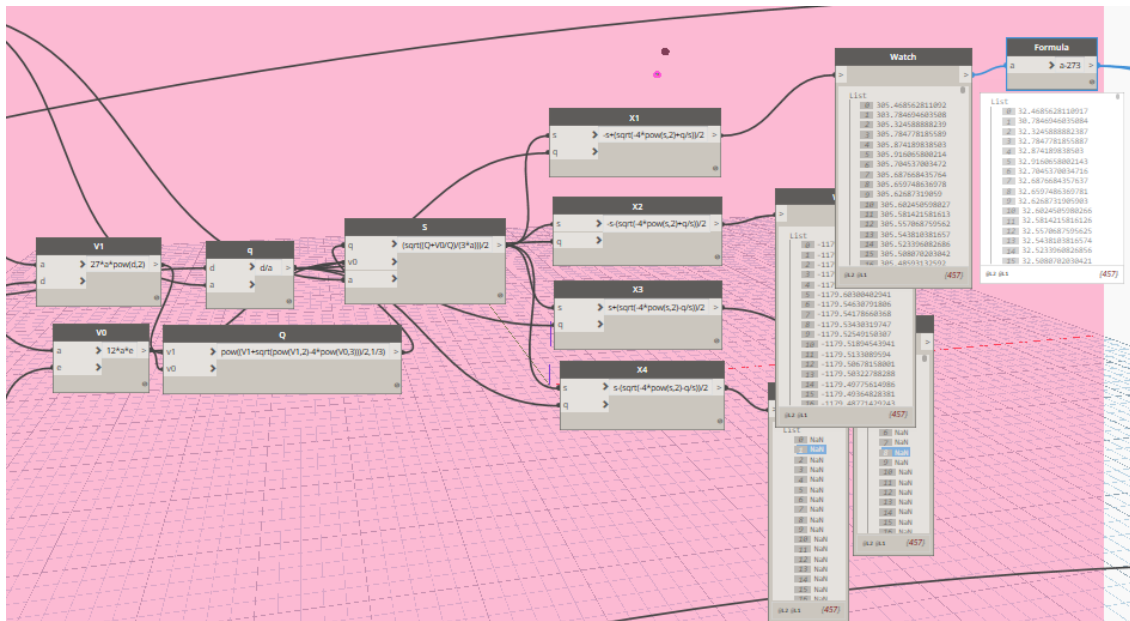


Figure A. 23. Calculation of the quadratic function.

A.3.6 RESULTS OUTPUT

The result of Surface Temperature node groups is recorded in excel file according to the number of the time frame. The data exported is the result data from the Calculation of the Surface Temperature node group. Those results are used for Initial Temperature for the next time frame.

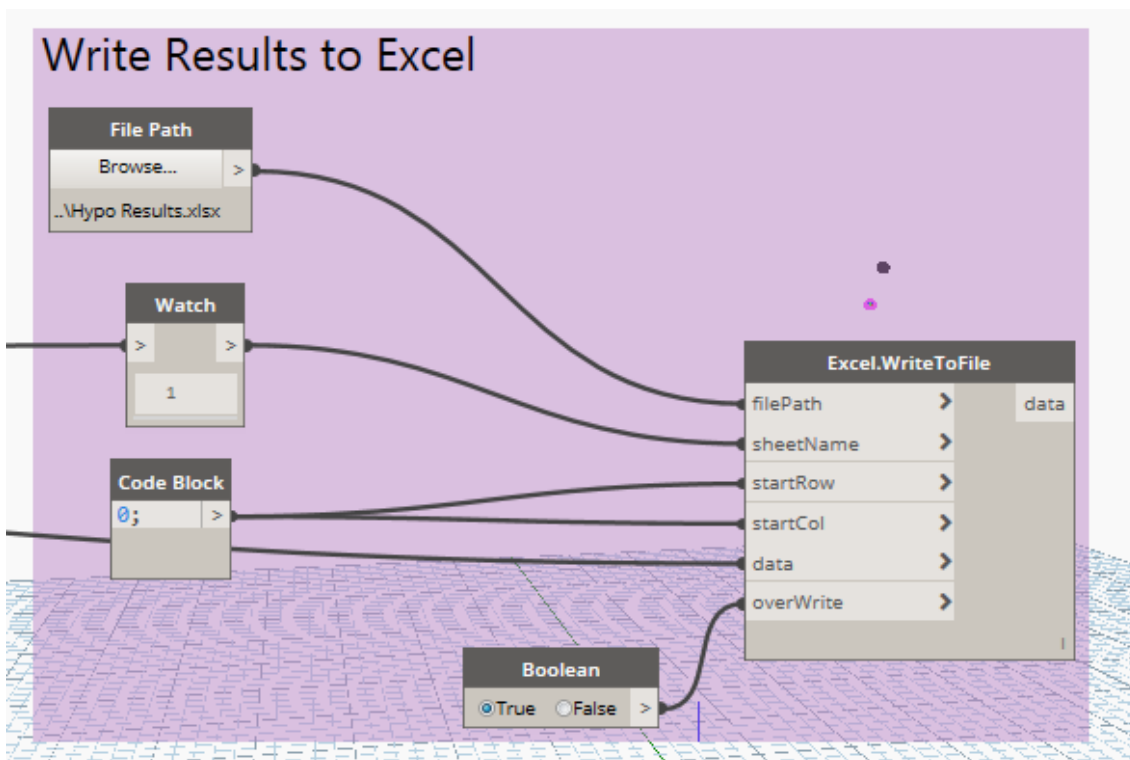


Figure A. 24. Surface Temperature result output.

A.4 View Factor Surface to Person

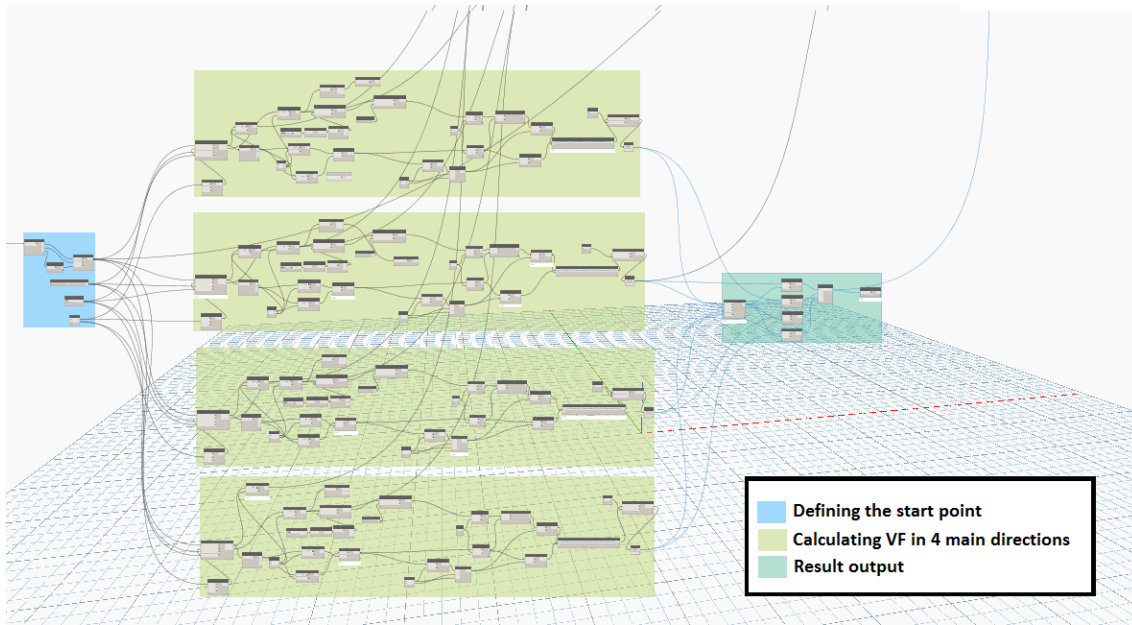


Figure A. 25. Node groups for calculating View Factors between Person and Surface.

A.4.1 DEFINING STARTING POINT

In this point analytical point of the Floors elements are shifted 1,5m of the ground to simulate the average person core height. Additional constants are place hear that will be used in next step.

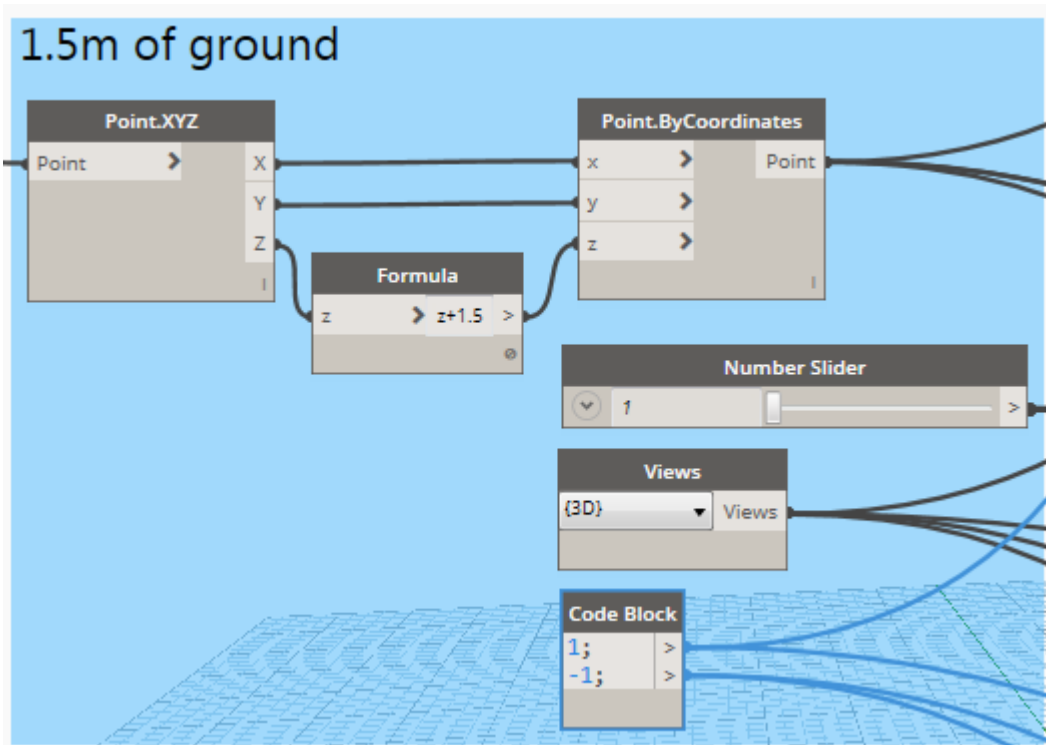


Figure A. 26. Defining the starting points.

A.4.2 CALCULATING VIEW FACTOR IN 4 MAIN DIRECTIONS

4 node groups are used to simulate the ray tracing for each of the 4 main directions: front, back, left and right. A *RayBounce.ByOriginDirection* node is used to register if the vectors in this direction are intersecting any surface and if yes it registers the point of intersection and the element ID.

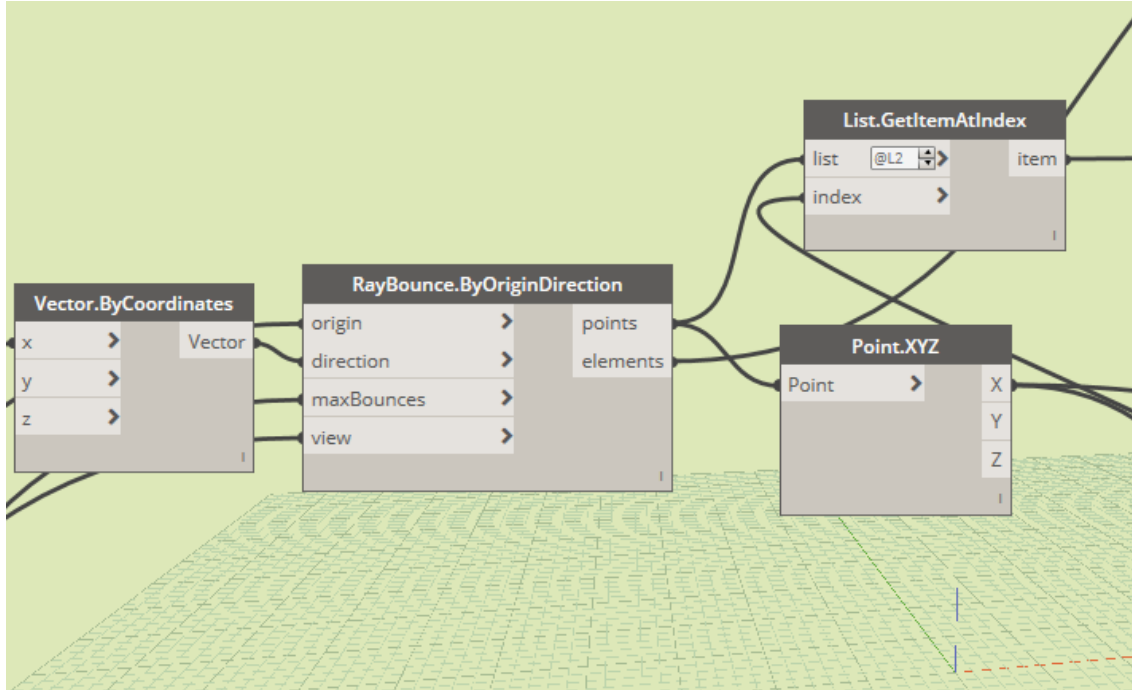


Figure A. 27. Finding if vectors intersect with any geometry.

The figure below shows the process of finding the distance of the point of origin to the point of intersection that will be used for the view factor calculation.

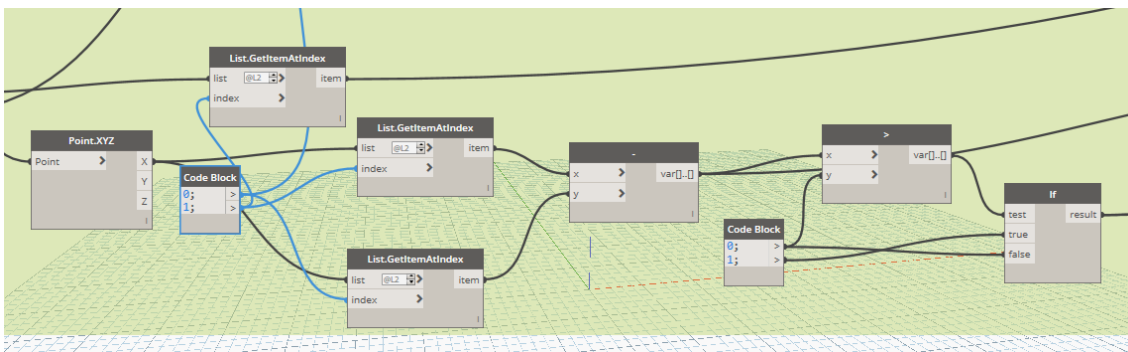


Figure A. 28. Calculating minimum distance between analytical and intersection points.

From the element ID the height of the wall is extracted in order to see the area of influence of the surface energy radiation.

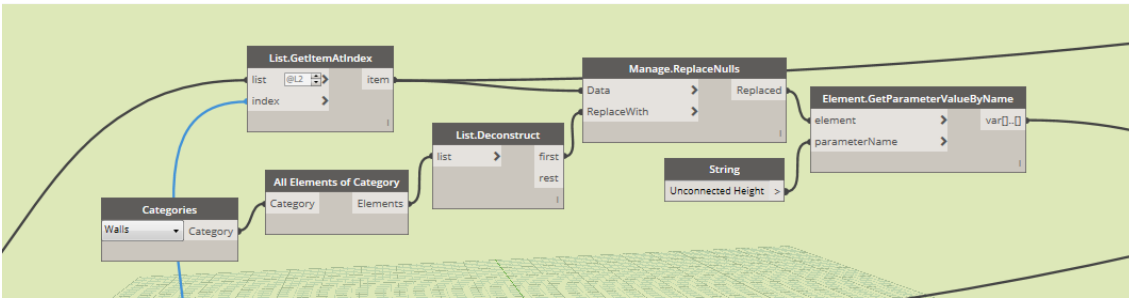


Figure A. 29. Extraction of wall height.

On the figure below the calculation of the View Factor are made using the corresponding formulas.

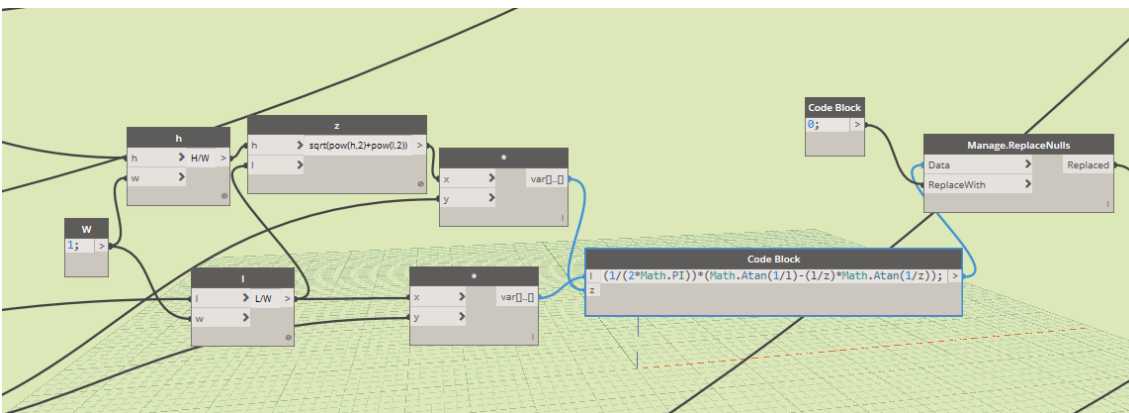


Figure A. 30. Calculating the View Factor.

This node group repeats 4 time for each of the following vectors: (x=1, y=0); (x=0, y=1); (x=-1, y=0); (x=0, y=-1);

A.4.3 RESULT

The result is 4 values for each analytical point the sum of which has to be 0.8 which is standard value for heat exchange from the surrounding walls. The other 0.2 come from upcoming heat radiation from the floor and down coming radiation from ceilings.

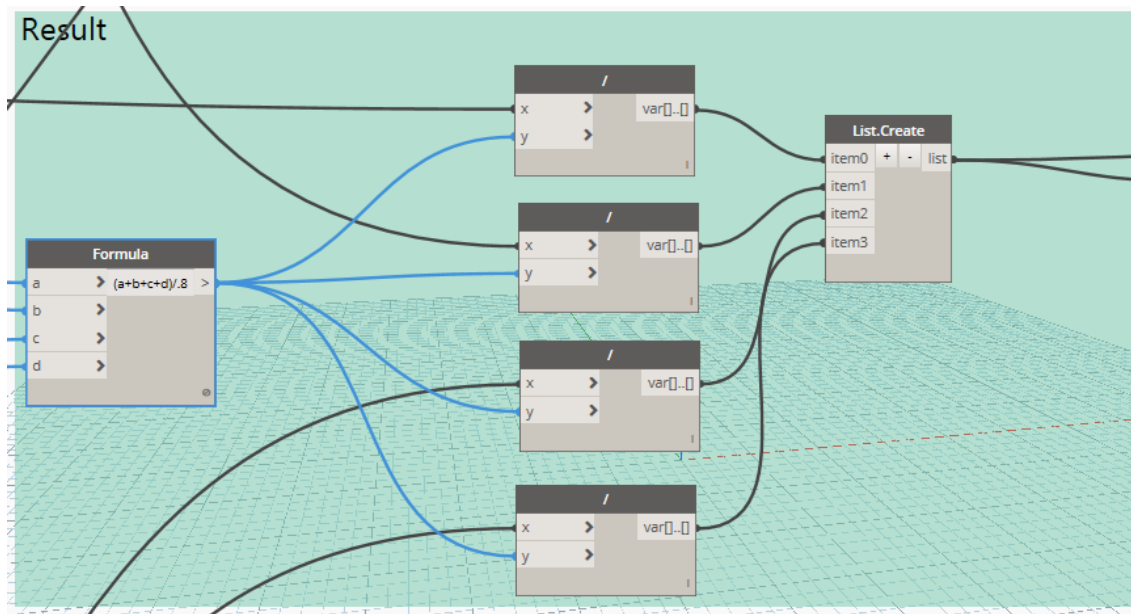


Figure A.31. Results of the View Factor calculation.

A.5 Mean Radiant Temperature

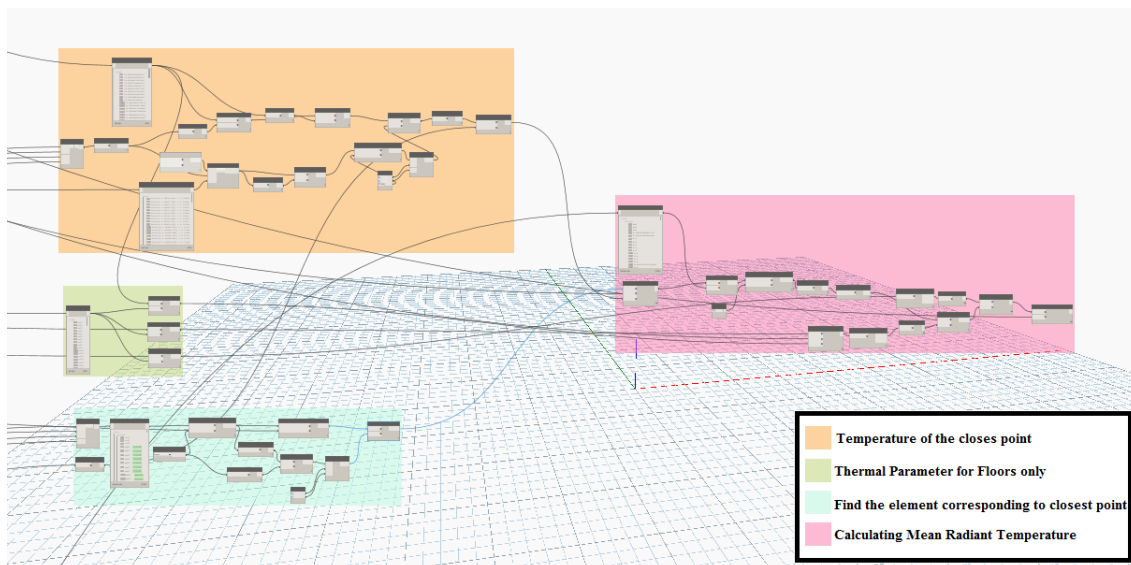


Figure A.32. Node group for calculating Mean Radiant Temperature.

A.5.1 FINDING TEMPERATURE OF CLOSEST POINT

As the view factor intersection points are not the same with the wall analytical points there is need to find the closet wall analytical point to the intersection point and register the temperature value. This is made by creating using the *List.CartesianProduct* node that calculates the distance between each analytical and intersection point. The minimum distance is considered the closes point and the its temperature value is taken and attributed to the intersection point.

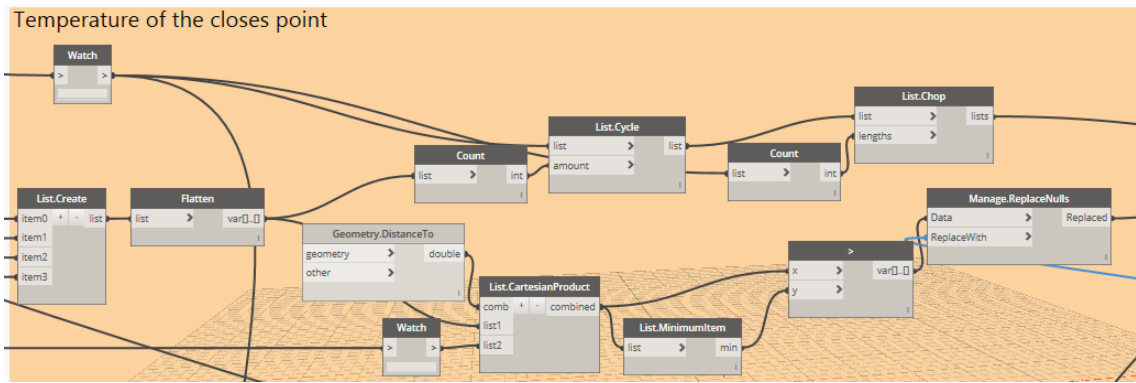


Figure A. 33. Finding the temperature of the closes wall analytical point.

A.5.2 THERMAL PARAMETERS FROM FLOORS ONLY

This node group provide thermal parameter only for the floor elements by multiplying the complete lists of thermal parameters to the position of the floor elements obtained in the Initial Data section. If there is floor the value is multiplied by 1 and if it is another element it is multiplied by 0.

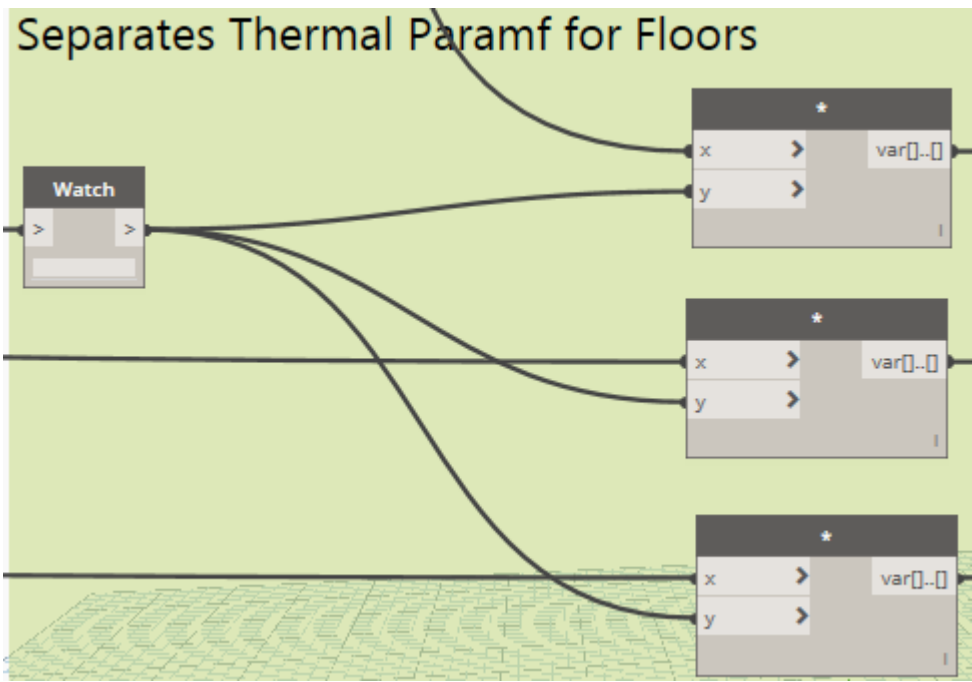


Figure A. 34. Separating thermal parameter for floors only.

A.5.3 FINDING THE ELEMENT CORRESPONDING TO THE CLOSEST POINT

This node group extract the emissivity for each element of the corresponding intersection point.

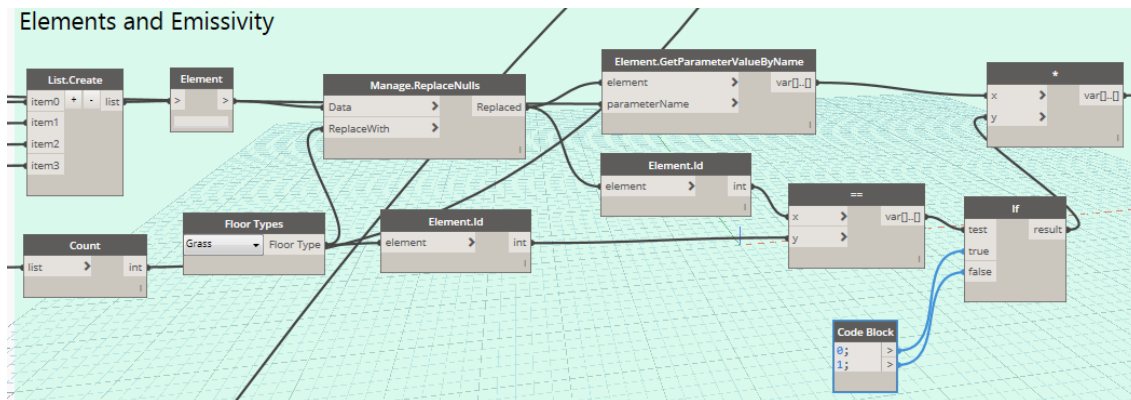


Figure A. 35. Removing information about the element of the corresponding intersection point.

A.5.4 CALCULATING MEAN RADIANT TEMPERATURE

The calculation of the Mean Radian Temperature is made by using the corresponding formulas and the values obtained from the previous paragraphs. It multiplies the surface temperature in each of the 4 direction to the corresponding View Factor and the elements emissivity. Adding the upcoming heat radiation from the floor elements. In this node is made the combination of the effects of the shortwave and longwave radiation which result in the final value of the Mean Radian Temperature for each analytical floor point.

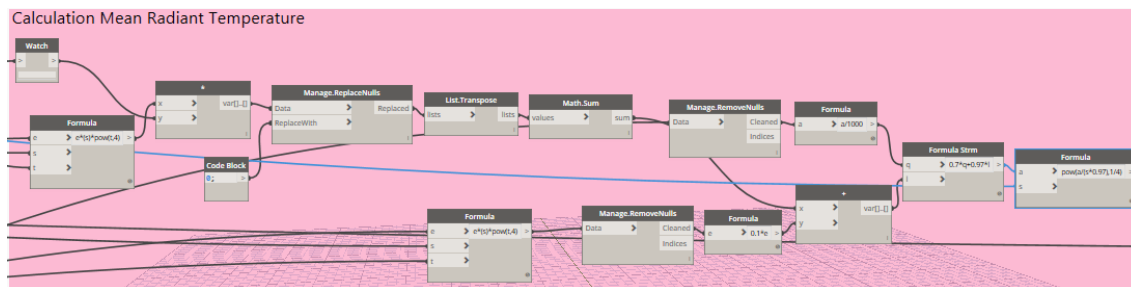


Figure A. 36. Calculation of the Mean Radiant Temperature.

ANNEX B

MEASUREMENT RESULTS

This annex reports the results of the measurement for the surface temperature. The values were taken on the 15.07.2018, between 9:00 to 17:00. To represent the hourly change of the surface temperature, in each measurement point, were registered six values. For some of the points, in which it was impossible to measure the surface temperature, due to limitation of the equipment or the presence of physical barriers, the referring results were left in blank.

A.1 Around the elevator on the upper floor of Trindade Metro Station

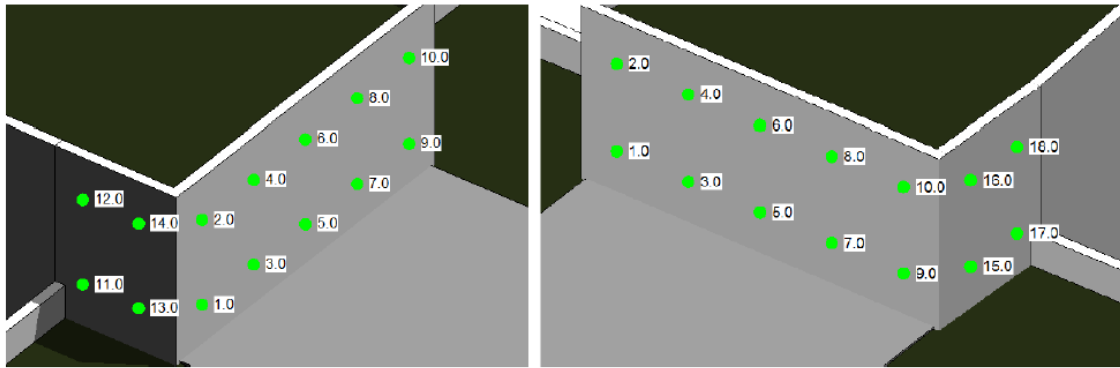


Figure B. 1 Walls around the elevator of Trindade Station in Porto, Portugal.

Table B. 1. Measured values of the surface temperature (°C) in the walls around the elevator of Trindade Station in Porto, Portugal: 15th July 2018

| | 9:00-11:00 | 11:00-12:00 | 12:00-13:00 | 13:00-14:00 | 14:00-15:00 | 15:00-17:00 |
|----|------------|-------------|-------------|-------------|-------------|-------------|
| 1 | | | | | | |
| 2 | 21.2 | 20.4 | 20.9 | 21.2 | 23.7 | 29.1 |
| 3 | | | | | | |
| 4 | 22 | 21.6 | 20.8 | 21.1 | 23.9 | 29 |
| 5 | | | | | | |
| 6 | 21.7 | 23.8 | 20.6 | 21.4 | 24.1 | 28.6 |
| 7 | | | | | | |
| 8 | 21.7 | 20.1 | 20.4 | 21.3 | 24.2 | 29.1 |
| 9 | | | | | | |
| 10 | 21 | 20.1 | 20.6 | 21.3 | 23.8 | 27.4 |
| 11 | | | | | | |
| 12 | 21.1 | 20.6 | 18.6 | 17.9 | 20 | 19.8 |
| 13 | | | | | | |
| 14 | 21.1 | 20 | 18.8 | 18.4 | 20.4 | 20.1 |
| 15 | | | | | | |
| 16 | 21.9 | 22.3 | 28.5 | 26.4 | 24.5 | 24.5 |
| 17 | | | | | | |
| 18 | 22 | 22.1 | 27 | 26.9 | 26.7 | 25 |

Category: Walls
 Elements ID: 312964; 316518; 316588

Total Area: 86 m²
 Grid Size: +/- 4 m

A.2 Upper level floor of Trindade Metro Station

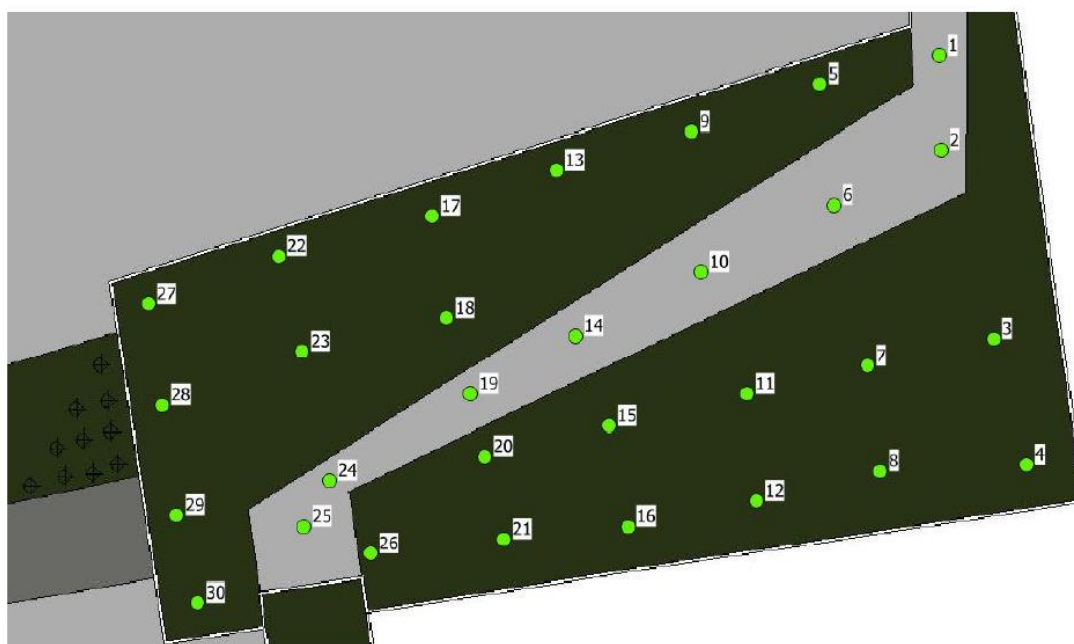


Figure B. 2. Upper level floor of Trindade Station in Porto, Portugal.

Table B. 2. Measured values of the surface temperature ($^{\circ}\text{C}$) on the floor of the upper level of Trindade Station in Porto, Portugal: 15th July 2018

| | 9:00-11:00 | 11:00-12:00 | 12:00-13:00 | 13:00-14:00 | 14:00-15:00 | 15:00-17:00 |
|----|------------|-------------|-------------|-------------|-------------|-------------|
| 1 | 24 | 25.1 | 36.9 | 38.8 | 39.8 | 41.3 |
| 2 | 26.4 | 25.4 | 37.8 | 39.5 | 43.9 | 44.6 |
| 3 | 19.9 | 20.3 | 23.9 | 22 | 24.5 | 27.6 |
| 4 | 20.5 | 20.1 | 25.3 | 21.4 | 21.6 | 26.3 |
| 5 | 21.4 | 21.5 | 28.1 | 26.9 | 27.4 | 29.3 |
| 6 | 23.8 | 24.6 | 34.7 | 40.6 | 42.9 | 40.7 |
| 7 | 20.8 | 21.3 | 23.8 | 27.3 | 29 | 27.8 |
| 8 | 19.3 | 20.1 | 27.8 | 22 | 23.9 | 29 |
| 9 | 21.5 | 22.4 | 22.6 | 23.5 | 26.4 | 27.9 |
| 10 | 26.8 | 27.1 | 38.4 | 39.4 | 44.2 | 44.6 |
| 11 | 24.4 | 23.4 | 21.3 | 20.6 | 23.6 | 26.1 |
| 12 | 24.3 | 22.1 | 21.6 | 21.8 | 28.1 | 25.4 |
| 13 | 20.8 | 21.3 | 24.4 | 28.4 | 25.5 | 26.3 |
| 14 | 24.8 | 25.4 | 37.5 | 43.3 | 43.3 | 43.4 |
| 15 | 24.3 | 22.1 | 23.1 | 28.3 | 24.7 | 25.1 |
| 16 | 22.9 | 23.1 | 23.3 | 27.6 | 24.6 | 26.7 |
| 17 | 19.8 | 20.5 | 26 | 26.6 | 24.4 | 25.3 |
| 18 | 19.2 | 20.4 | 26.7 | 28.6 | 27.9 | 26.1 |
| 19 | 22.2 | 23.6 | 34.4 | 41.3 | 41.1 | 42.1 |
| 20 | 20 | 21.5 | 22 | 26.1 | 21.8 | 24.3 |
| 21 | 18.8 | 20.1 | 24.6 | 24 | 21.4 | 25.4 |
| 22 | 18.1 | 22.1 | 22 | 24.4 | 27.2 | 26.2 |
| 23 | 21.5 | 23.1 | 22 | 26.7 | 28.5 | 24.5 |
| 24 | 21.7 | 21.8 | 34.6 | 37.1 | 39.6 | 42.1 |
| 25 | 20.9 | 21.7 | 34.1 | 36.1 | 40.5 | 43.5 |
| 26 | 17.3 | 18.3 | 18.5 | 18.6 | 20.2 | 21.3 |
| 27 | 21.5 | 20.1 | 21.8 | 22.6 | 22.6 | 24.8 |

| | | | | | | |
|-----------|------|------|------|------|------|------|
| 28 | 22.2 | 22.3 | 25 | 25.4 | 27.6 | 26.1 |
| 29 | 21.9 | 20.1 | 22 | 24.2 | 22.6 | 24.8 |
| 30 | 18.8 | 20.4 | 23.7 | 23.8 | 25.1 | 26.3 |

Category: Floors
Elements ID: 328576; 328736

Total Area: 4033 m²
Grid Size: +/- 10 m

A.3 Surrounding walls on the upper level of Trindade Metro Station

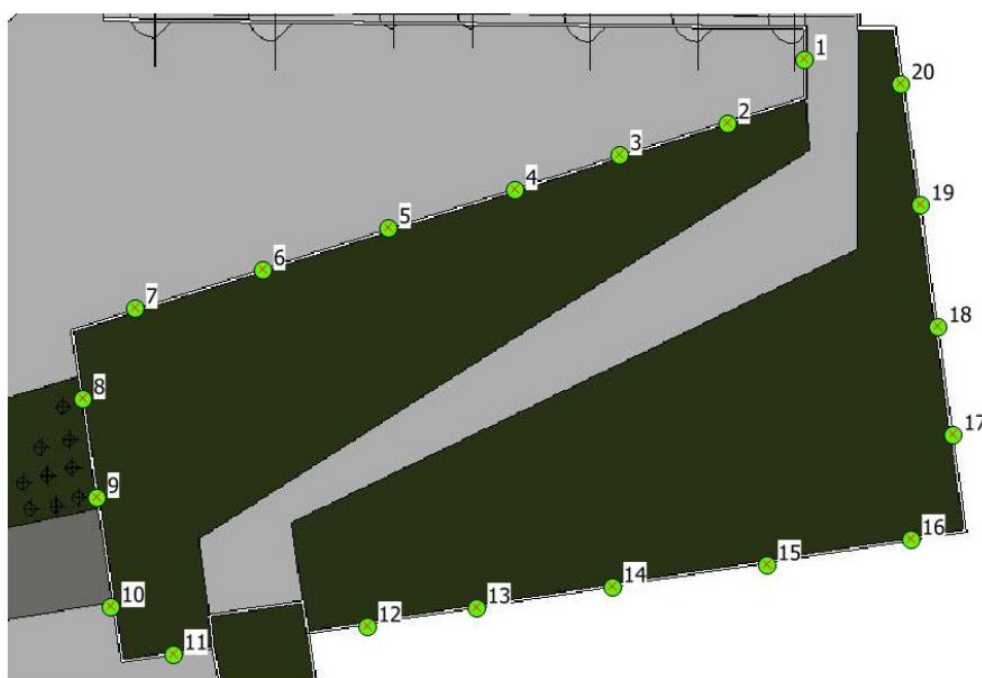


Table B. 3. Measured values of the surface temperature (°C) on the walls of the upper level of Trindade Station in Porto, Portugal: 15th July 2018.9:00-11:00

| | | 11:00-12:00 | 12:00-13:00 | 13:00-14:00 | 14:00-15:00 | 15:00-17:00 |
|----|------|-------------|-------------|-------------|-------------|-------------|
| 1 | 22 | 22.6 | 23.3 | 22 | 26.4 | 27.9 |
| 2 | 25.7 | 28.1 | 30.3 | 23.8 | 24.4 | 26.2 |
| 3 | 27.8 | 29.6 | 32.6 | 25.6 | 25.4 | 26.9 |
| 4 | 31.7 | 30.6 | 31.5 | 24.8 | 26.6 | 27 |
| 5 | 31.8 | 32.7 | 34.8 | 26.3 | 24.9 | 25.2 |
| 6 | 29.3 | 31.4 | 35.3 | 26.5 | 22 | 23.4 |
| 7 | 27.7 | 33 | 37.5 | 27.2 | 22 | 23.2 |
| 8 | 22.2 | 25.6 | 28.4 | 22.2 | 22.7 | 23.1 |
| 9 | 21.1 | 26.1 | 27 | 24 | 22.4 | 22.4 |
| 10 | 21 | 21.8 | 25.4 | 23.3 | 21.1 | 22.6 |
| 11 | 18.5 | 19.6 | 23.2 | 25.1 | 26.3 | 31.8 |
| 12 | 17.6 | 17.8 | 17.2 | 16.9 | 21.4 | 27.6 |
| 13 | 18.2 | 18.6 | 20.3 | 21.9 | 27 | 32.7 |
| 14 | 17.8 | 17.6 | 18.4 | 23.8 | 28.7 | 33.5 |
| 15 | 16.3 | 16.4 | 18.2 | 22 | 28.4 | 32.5 |
| 16 | 16.3 | 16.9 | 18.5 | 22 | 32 | 34.6 |
| 17 | 20.5 | 22.1 | 24.3 | 25.9 | 28.6 | 28.9 |
| 18 | 22 | 26.3 | 27.8 | 27.9 | 27.8 | 28.4 |
| 19 | 22.2 | 25.6 | 27.3 | 30 | 31.3 | 32 |
| 20 | 23.6 | 26.9 | 30.2 | 30.1 | 29.4 | 27.3 |

Category: Walls
 Elements ID: 303958; 304103; 304233; 305854;
 306674; 316117

Total Area: 254 m²
 Grid Size: +/- 10 m

A.4 Lower level floor of Trindade Metro Station

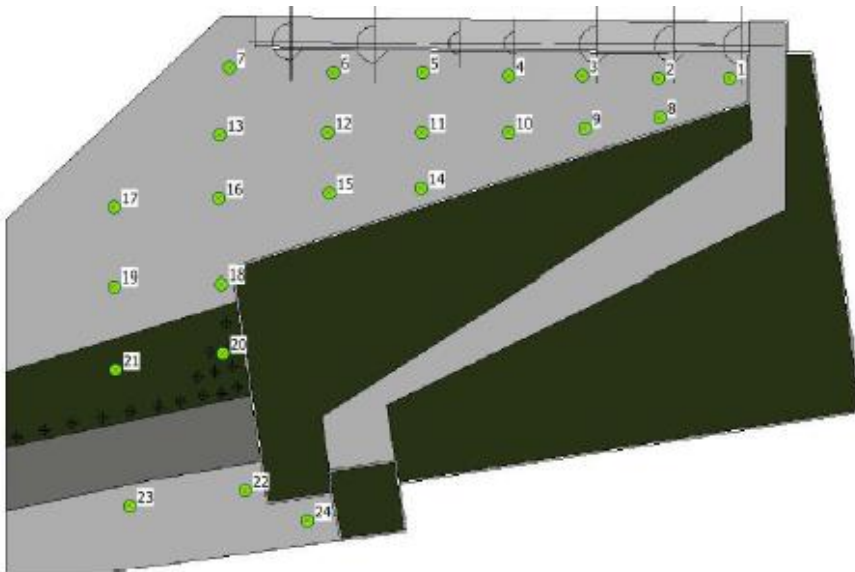


Figure B. 3. Lower level floor of Trindade Station in Porto, Portugal.

Table B. 4. Measured values of the surface temperature (°C) on the floor of the lower level of Trindade Station in Porto, Portugal: 15th July 2018.

| | 9:00-11:00 | 11:00-12:00 | 12:00-13:00 | 13:00-14:00 | 14:00-15:00 | 15:00-17:00 |
|----|------------|-------------|-------------|-------------|-------------|-------------|
| 1 | 19.6 | 21.6 | 28.4 | 42.3 | 39.9 | 31.6 |
| 2 | 25.4 | 31 | 33 | 32.9 | 31.2 | 26.4 |
| 3 | 27.3 | 33.4 | 31.5 | 36.1 | 32.1 | 26 |
| 4 | 26.5 | 32.1 | 33.9 | 42.6 | 28.1 | 24.3 |
| 5 | 27.1 | 32.5 | 33 | 40.1 | 28.5 | 27.6 |
| 6 | 25.4 | 33.7 | 35.5 | 42.1 | 29.6 | 27.4 |
| 7 | 26.3 | 33.4 | 33.5 | 36.1 | 29.7 | 26.8 |
| 8 | 20.1 | 21.3 | 35.4 | 37.8 | 38.7 | 25.3 |
| 9 | 19.6 | 21.5 | 33.9 | 38.6 | 37.5 | 36.5 |
| 10 | 18.4 | 21.3 | 33.6 | 39.2 | 36.1 | 34.2 |
| 11 | 24.6 | 28.3 | 33 | 43.1 | 40.1 | 28.2 |
| 12 | 25.1 | 28.9 | 40.9 | 42.3 | 41.5 | 37.1 |
| 13 | 26.5 | 33.7 | 36.2 | 40.1 | 42.1 | 38.3 |
| 14 | 19.6 | 21.9 | 34.5 | 38.1 | 40.1 | 42.8 |
| 15 | 20.4 | 22.7 | 35.4 | 3.1 | 42.1 | 45.7 |
| 16 | 22.7 | 29.1 | 36.2 | 39.9 | 41.9 | 46 |
| 17 | 26.8 | 32.4 | 35.8 | 40.1 | 41.6 | 44.3 |
| 18 | 22.9 | 28.5 | 36.4 | 38.2 | 45.2 | 43.5 |
| 19 | 26.3 | 29.6 | 36.7 | 41.4 | 40.8 | 42.1 |
| 20 | 18.1 | 18.8 | 18.3 | 18.3 | 26 | 27.3 |
| 21 | 22.3 | 25.4 | 23.8 | 20.1 | 25.4 | 26.1 |
| 22 | 23.4 | 28.9 | 37.6 | 38.5 | 40.2 | 43.1 |
| 23 | 23.9 | 28.5 | 38.7 | 38.9 | 43 | 45.6 |

Category: Floors
 Elements ID: 312523; 312842; 324493

Total Area: 4702 m²
 Grid Size: +/- 10 m

A.5 Sidewall near the elevator of Trindade Metro Station

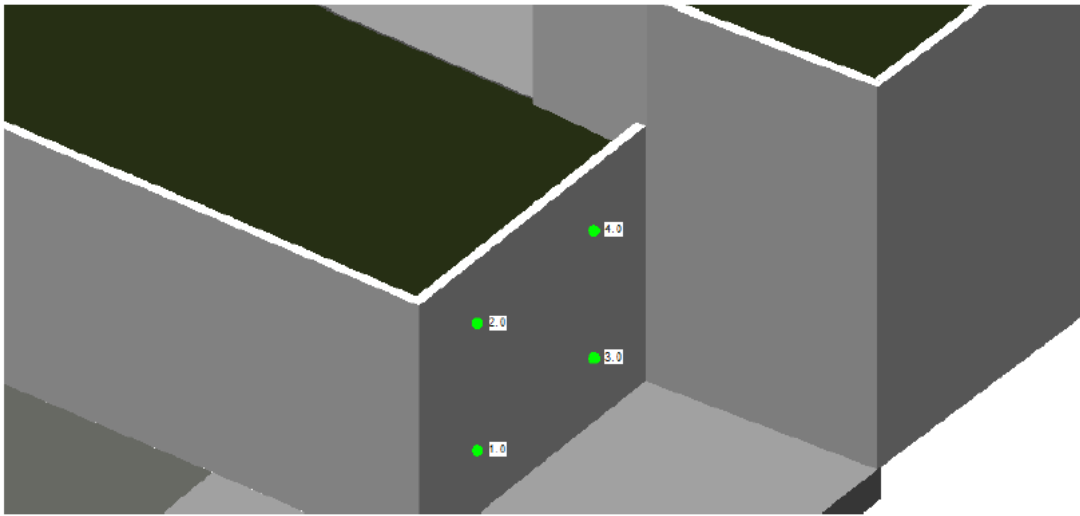


Figure B. 4. Sidewall near the elevator of Trindade Station in Porto, Portugal.

Table B. 5. Measured values of the surface temperature (°C) on the sidewall of the elevator on the lower level of Trindade Station in Porto, Portugal: 15th July 2018.

| | 9:00-11:00 | 11:00-12:00 | 12:00-13:00 | 13:00-14:00 | 14:00-15:00 | 15:00-17:00 |
|---|------------|-------------|-------------|-------------|-------------|-------------|
| 1 | | | | | | |
| 2 | | | | | | |
| 3 | 21.1 | 21.8 | 22.1 | 26.8 | 33.5 | 29.8 |
| 4 | 22.3 | 24.1 | 25.3 | 26.7 | 34.1 | 30.1 |

Category: Walls
Elements ID: 316117

Total Area: 82 m²
Grid Size: +/- 4 m

A.6 Sidewalk of Trindade Metro Station facing Rua de Camões

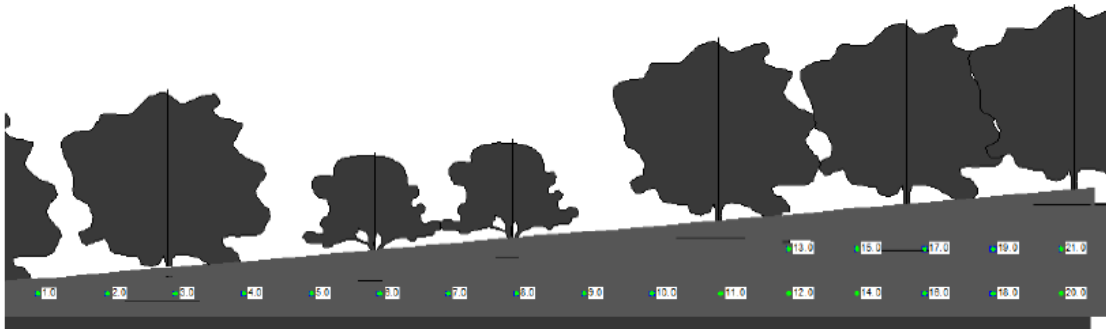


Figure B. 5. Sidewalk of Trindade Station facing Rua de Camões, Porto, Portugal

Table B. 6. Measured values of the surface temperature (°C) on the sidewalk of Trindade Station in Porto facing Rua da Camões, Portugal: 15th July 2018.

| | 9:00-11:00 | 11:00-12:00 | 12:00-13:00 | 13:00-14:00 | 14:00-15:00 | 15:00-17:00 |
|----|------------|-------------|-------------|-------------|-------------|-------------|
| 1 | 25.4 | 25.8 | 26.5 | 24.2 | 19.6 | 19.7 |
| 2 | 26.3 | 26.1 | 27.1 | 23.1 | 19.7 | 19.2 |
| 3 | 25.3 | 27.3 | 26.6 | 24.2 | 19.9 | 19.1 |
| 4 | 24.8 | 26.7 | 26.5 | 22.8 | 20.1 | 18.6 |
| 5 | 26.9 | 27.4 | 24.5 | 24 | 19.8 | 18.2 |
| 6 | | | | | | |
| 7 | | | | | | |
| 8 | | | | | | |
| 9 | 26.8 | 29.3 | 28.4 | 24 | 20.6 | 22.1 |
| 10 | 27 | 29.2 | 28.1 | 26.1 | 21.1 | 22.4 |
| 11 | 27.4 | 29.1 | 28.4 | 25.4 | 21.4 | 22.3 |
| 12 | 26.8 | 29.1 | 27.5 | 26 | 20.3 | 21.8 |
| 13 | | | | | | |
| 14 | 26.8 | 29.4 | 28.3 | 26 | 20.3 | 23.6 |
| 15 | | | | | | |
| 16 | 26.1 | 27.2 | 28.8 | 28.2 | 22 | 25.7 |
| 17 | | | | | | |
| 18 | 26.8 | 28.6 | 27.8 | 25.9 | 21.3 | 25.9 |
| 19 | | | | | | |
| 20 | | | | | | |
| 21 | 26.1 | 28.4 | 26.7 | 25.3 | 21.3 | 24.8 |

Category: Walls

Elements ID: 312964; 316518; 316588

Total Area: 356 m²

Grid Size: +/- 4 m

A.7 Sidewalk near the stairs in Trindade Metro Station



Figure B. 6. Sidewall near the stairs in Trindade Station, Porto, Portugal.

Table B. 7. Measured values of the surface temperature (°C) on the sidewall near the stairs of Trindade Station in Porto, Portugal: 15th July 2018.

| | 9:00-11:00 | 11:00-12:00 | 12:00-13:00 | 13:00-14:00 | 14:00-15:00 | 15:00-17:00 |
|---|------------|-------------|-------------|-------------|-------------|-------------|
| 1 | | | | | | |
| 2 | | | | | | |
| 3 | 26.3 | 28.4 | 28.7 | 20.9 | 21.6 | 21.3 |
| 4 | 24.6 | 29.1 | 29.1 | 30.3 | 21 | 22.4 |

Category: Walls
Elements ID: 306674

Total Area: 58 m²
Grid Size: +/- 4 m

A.8 Sidewalk perpendicular to the metro line in Trindade Metro Station

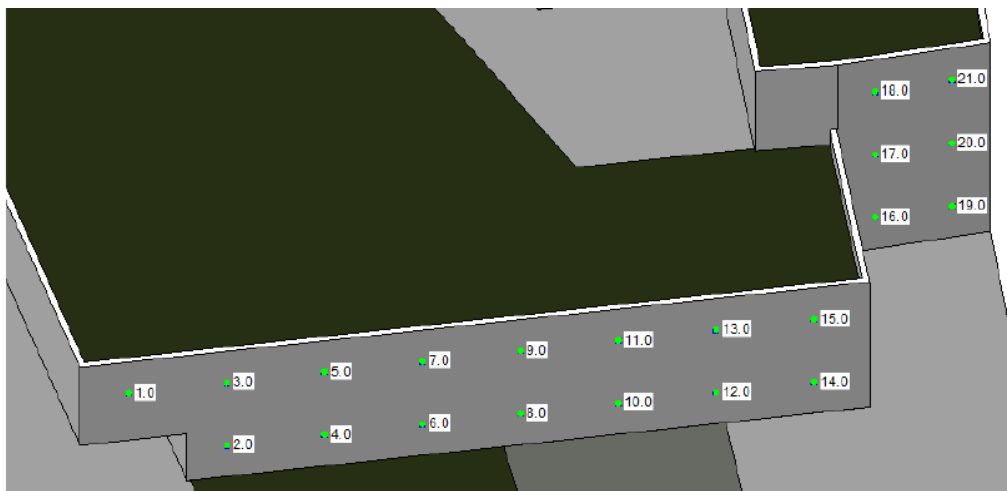


Figure B. 7. Sidewalk perpendicular to the metro line in Trindade Station, Porto, Portugal

Table B. 8. Measured values of the surface temperature (°C) on the sidewalk perpendicular to the metroline in Trindade Station, Porto, Portugal: 15th July 2018.

| | 9:00-11:00 | 11:00-12:00 | 12:00-13:00 | 13:00-14:00 | 14:00-15:00 | 15:00-17:00 |
|----|------------|-------------|-------------|-------------|-------------|-------------|
| 1 | 19.6 | 20.6 | 27.2 | 24.8 | 24.8 | 26.9 |
| 2 | 15.1 | 15.6 | 19.8 | 22.2 | 25.2 | 27.3 |
| 3 | 15.4 | 16 | 25.8 | 24.7 | 24.7 | 26.4 |
| 4 | | | | | | |
| 5 | | | | | | |
| 6 | | | | | | |
| 7 | | | | | | |
| 8 | | | | | | |
| 9 | | | | | | |
| 10 | | | | | | |
| 11 | | | | | | |
| 12 | | | | | | |
| 13 | 20.8 | 23.6 | 34.3 | 36.1 | 36.4 | 34.1 |
| 14 | | | | | | |
| 15 | 22.1 | 24.5 | 30.6 | 32.4 | 32.1 | 33.2 |
| 16 | | | | | | |
| 17 | | | | | | |
| 18 | | | | | | |
| 19 | | | | | | |
| 20 | | | | | | |
| 21 | | | | | | |

Category: Walls
Elements ID: 304233; 314336

Total Area: 358 m²
Grid Size: +/- 4 m

A.9 Central wall in Trindade Metro Station

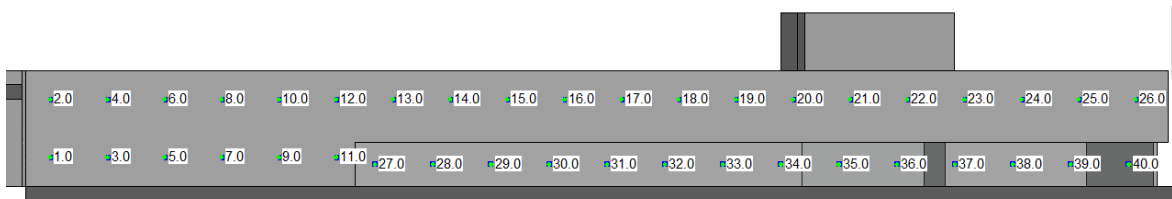


Figure B. 8. Central wall of Trindade Station, in Porto, Portugal

Table B. 9. Measured values of the surface temperature (°C) on the central wall in Trindade Station, Porto, Portugal: 15th July 2018.

| | 9:00-11:00 | 11:00-12:00 | 12:00-13:00 | 13:00-14:00 | 14:00-15:00 | 15:00-17:00 |
|----|------------|-------------|-------------|-------------|-------------|-------------|
| 1 | 19.6 | 20.7 | 22.2 | 26.7 | 33.2 | 39.2 |
| 2 | | | | | | |
| 3 | 20 | 21.7 | 21.9 | 26.3 | 32.8 | 40.1 |
| 4 | | | | | | |
| 5 | 20.3 | 21.3 | 21.5 | 26.4 | 34.9 | 41.2 |
| 6 | | | | | | |
| 7 | 20.6 | 21.4 | 21.6 | 26.2 | 34.7 | 39.7 |
| 8 | | | | | | |
| 9 | 20.1 | 20.9 | 21.9 | 25.4 | 34.6 | 37.7 |
| 10 | | | | | | |
| 11 | 19.7 | 20.1 | 20.2 | 23.2 | 34.7 | 38.4 |
| 12 | | | | | | |
| 13 | | | | | | |
| 14 | | | | | | |
| 15 | | | | | | |
| 16 | | | | | | |
| 17 | | | | | | |
| 18 | | | | | | |
| 19 | | | | | | |
| 20 | | | | | | |
| 21 | | | | | | |
| 22 | | | | | | |
| 23 | | | | | | |
| 24 | | | | | | |
| 25 | | | | | | |
| 26 | | | | | | |
| 27 | | | | | | |
| 28 | 16.6 | 17 | 18.6 | 17.9 | 17.6 | 18.5 |

| | | | | | | |
|----|------|------|------|------|------|------|
| 29 | 16.5 | 18.3 | 17.7 | 17.5 | 17.9 | 18.1 |
| 30 | 15.4 | 18.6 | 17.8 | 18.3 | 18.6 | 19 |
| 31 | 16.3 | 18.2 | 17.3 | 17.1 | 17 | 18.9 |
| 32 | 17.3 | 18.5 | 16.9 | 16.8 | 16.8 | 19.1 |
| 33 | 16 | 16.4 | 17.2 | 16.9 | 16.9 | 17.4 |
| 34 | 15.6 | 16.3 | 17.3 | 16.3 | 16.8 | 16.8 |
| 35 | 16.5 | 15.4 | 15.6 | 16.7 | 16.7 | 16.9 |
| 36 | 16.7 | 18.3 | 19.6 | 16.9 | 16.7 | 17.5 |
| 37 | 16.8 | 17.9 | 18.1 | 18.7 | 18.5 | 17.9 |
| 38 | 17.8 | 18.3 | 18.1 | 18.4 | 19 | 18.5 |
| 39 | 18.9 | 18.4 | 18.5 | 18.8 | 19.1 | 18.4 |
| 40 | 19.3 | 19.1 | 19 | 19.4 | 19 | 18.6 |

Category: Floors
 Elements ID: 312523; 312842; 324493

Total Area: 4702 m²
 Grid Size: +/- 10 m